Mohamed Khider University, Biskra

Faculty of Science and Technology

Department of Electrical Engineering

# MASTER'S THESIS

Science and Technology

Electrical Engineering

Renewable energy in electrical engineering

Ref: 2025

---

Presented and supported by:

BENBADI Rawdha

On: Monday 26 May 2025

## Optimization of a Photovoltaic pumping system

---

Jury:

| | | | |
|---|---|---|---|
| Pr. Rahoua Naaima | MCB | University of Biskra | Chairman |
| Pr.Derradji Belloum Karima | MAA | University of Biskra | Examiner |
| Pr. Tkouti Nacira | MCB | University of Biskra | Supervisor |

Academic year: 2024/2025

Mohamed Khider University, Biskra

Faculty of Science and Technology

Department of Electrical Engineering

# MASTER'S THESIS

Science and Technology

Electrical Engineering

Renewable energy in electrical engineering

Ref: 2025

---

On: Monday 26 June 2025

## Optimization of a Photovoltaic pumping system

Presented by:

BENBADI Rawdha

Favorable opinion of the supervisor:

Pr. TKOUTI Nacira

**Signature Favorable opinion of the Chairman of the Jury**

**Stamp and signature**

# Acknowledgments

First and foremost, we would like to thank our supervisor**, Pr. Tkouti Nacira**, for his guidance, knowledge, and assistance during our research journey.

We also thank **Mr. Bettahar Fares** for his assistance,

as well as our parents, siblings, and friends for their encouragement and support.

Finally, we salute the authors and researchers whose work has influenced our study,

and we sincerely thank everyone who has contributed in any way.

**إهـداء**

إلى من كانت دعواتها سرَّ بركتي، وحنانها مهدَ راحتي، وصبرها حصنَ ثباتي...
إلى أمي الحبيبة النبع الذي لا ينضب، والنور الذي لا يخبو...
يا من غرستِ في قلبي اليقين، ورافقتِ دربي بالدعاء، كنتِ وستبقين المعنى الأسمى لكل عطاء، ولكِ أُهدي ثمرة هذا الجهد خالصة من القلب، تقديرًا وعرفانًا.
وإلى أبي الكريم من علّمني أن الإصرار طريق النجاح، وأن التواضع رفعة، والعمل عبادة...
يا من كان حضورك دعامة الأمان، ودروسك في الحياة ركيزة اتكأتُ عليها في كل خطاي
لكَ كل الامتنان على ما غرسته فيّ من قيم ومبادئ لا تزول.
إلى إخوتي الأعزّاء، الذين كانوا لي خير سند:
إلى أخي رياض صاحب القلب الكبير والعقل الراجح...
كنتَ دومًا داعمًا بصمتك النبيل ومواقفك الثابتة.
إلى أختي مروى رفيقة الأيام الحلوة والمرة، يا من كنتِ لي أختًا وصديقة ونصفًا آخر يشبهني في كل شيء...
لكِ منّي محبة لا تنضب، وشكرًا على كل لحظة قرب.
وإلى أخي أنيس الروح الطيبة، والضحكة التي تخفف عن القلب عناء الأيام...
وجودك زادٌ جميل في حياتي.
وإلى صديقاتي المخلصات، من كنّ رفيقات الدرب، وشريكات الطموح، وأضواءً أنارت دربي:
إلى المهندسة فاطمة صديقة العقل والقلب، من كانت دعمها بلا حدود، وحضورها باعثًا على الطمأنينة والثقة.
إلى المهندسة إيمان عنوان الثبات والحكمة، ورفيقة الجهد والاجتهاد.
إلى المهندسة هناء صاحبة الفكر النيّر والروح الطيبة... كنتِ دائمًا حافزًا للمضي قدمًا.
إلى المهندسة صبرينة الصديقة الهادئة التي تمضي بصمت ولكن تترك أثرًا لا يُنسى

إلى منار الممرضة المهندسة، مزيج الرحمة والانضباط، صورة مشرقة للعطاء والتفاني

.إلى الدكتورة مروى عقل راجح، وروح صادقة... صحبتكِ كانت نعمة، وعلمكِ زاد

الى الدكتورة نسيمة مثال الرقيّ والتواضع والعلم الرفيع، كنتِ مصدر إلهام ودافعًا مستمرًا.
الى كوثر الشاعرة من جعلت للكلمة معنى، وللأدب طيفًا حيًّا... كنتِ إضافة نبيلة في مشواري.
وإلى كلّ من ساندني ولو بكلمةٍ طيبة، أو دعاءٍ خفي، أو ابتسامةٍ صغيرة
إلى كلّ من كان له في قلبي أثر، وإن لم يُذكر اسمه...
أنتم النور الذي لا يُرى، ولكن به تستنير الطرقات.

أهديكم هذا العمل المتواضع، ثمرة أعوامٍ من الجهد، وبصمةَ أملٍ كانت لتظلّ حلمًا لولا دعمكم.
فلكم مني جميعًا، كل التقدير والعرفان.

**Résumé**

Face aux défis croissants liés à l'approvisionnement en eau et en énergie dans les zones rurales et isolées, les systèmes de pompage d'eau photovoltaïques (PV) représentent une alternative durable et efficace aux systèmes conventionnels à combustibles fossiles. Ces systèmes subissent une instabilité et des oscillations de puissance dues aux variations du rayonnement solaire et de la température, ce qui éloigne leur fonctionnement du point de puissance maximale (MPP). Cette étude compare deux algorithmes MPPT : Perturb and Observe (P&O) et Conductance Incrémentale (INC). Les résultats de simulation montrent la supériorité de l'algorithme INC en termes de rapidité et de stabilité, avec une réduction significative des oscillations sous conditions environnementales changeantes. Cette étude démontre que l'algorithme INC améliore l'efficacité et la fiabilité des systèmes de pompage photovoltaïques.

**Mots-clés :** Systèmes de pompage photovoltaïques, suivi du point de puissance maximale, algorithme P&O, algorithme INC, stabilité du système

**Abstract**

Given the increasing challenges in providing water and energy to rural and remote areas, photovoltaic (PV) water pumping systems have become a sustainable and efficient alternative to conventional fossil fuel-based systems. These systems suffer from instability and power oscillations caused by variations in solar irradiance and temperature, leading to operation away from the Maximum Power Point (MPP). This study compares two MPPT algorithms: Perturb and Observe (P&O) and Incremental Conductance (INC). Simulation results demonstrate the superiority of the INC algorithm in tracking speed and system stability, significantly reducing oscillations under rapidly changing environmental conditions. This study highlights that the INC algorithm effectively improves the efficiency and reliability of PV water pumping systems.

**Keywords**: Photovoltaic water pumping systems, Maximum Power Point Tracking, P&O algorithm, INC algorithm, system stability.

ملخص

في مواجهة التحديات المتزايدة لإمدادات المياه والطاقة في المناطق الريفية والنائية، تمثل أنظمة ضخ المياه الكهروضوئية بديلاً مستداماً وفعالاً لأنظمة الوقود الأحفوري التقليدية. وتتعرض هذه الأنظمة لعدم الاستقرار وتذبذبات الطاقة بسبب الاختلافات في الإشعاع الشمسي ودرجة الحرارة، مما يبعد تشغيلها عن نقطة الطاقة القصوى .(MPP) تقارن هذه الدراسة بين خوارزميتين من خوارزميات :MPPT خوارزمية الاضطراب والمراقبة (P&O) وخوارزمية التوصيل التزايدي .(INC) تُظهر نتائج المحاكاة أن خوارزمية INC تتفوق من حيث السرعة والاستقرار، مع انخفاض كبير في التذبذبات في ظل الظروف البيئية المتغيرة. توضح هذه الدراسة أن خوارزمية INC تحسن من كفاءة وموثوقية أنظمة الضخ الكهروضوئية.

الكلمات المفتاحية: أنظمة الضخ الكهروضوئية، تتبع نقطة الطاقة القصوى، خوارزميةP&O ، خوارزميةINC ، استقرار النظام

# Table of Contents

# Table of Content

## List of Figures

# Liste of figures

# Liste of figures

## List of Tables

# General Introduction

## General introduction:

Recent decades have witnessed a growing trend towards renewable energy sources in the global energy landscape, driven by the imperatives of climate change, greenhouse gas abatement, and sustainable development. Among numerous renewables available, solar energy has attracted attention due to its abundance, cleanliness, and scope for decentralized use, particularly in rural and remote areas with high solar irradiance.[2]

One of the most feasible and practical applications of solar energy is the photovoltaic (PV) water pumping system, a cost-effective and clean solution to remote area water supply issues. [4]The system converts solar energy into electrical energy using PV panels, which is subsequently used to operate an electric motor to drive a water pump. They play a crucial role in increasing access to water for domestic, agricultural, and livestock use, thereby improving living standards and promoting socio-economic development in water-scarce regions.

However, the performance and operation of PV pumping systems significantly depend on different technical factors like accurate component modeling, system integration, and implementation of effective control and optimization strategies. One of the most vital techniques for ensuring increased energy conversion efficiency is Maximum Power Point Tracking (MPPT) algorithms that ensure that the PV array operates at its maximum power point under varying solar conditions.[3]

This research study is proposed to investigate, model, and optimize the performance of a stand-alone PV water pumping system with a focus on comparative evaluation of MPPT algorithms and their impact on overall system efficiency. The material of this thesis is organized in three main chapters:

Chapter One: is a comprehensive theoretical background of photovoltaic systems and water pumping technology. It provides the fundamental principles of solar energy conversion, the design and operation of PV systems, as well as the characteristics and types of electrical motors and hydraulic pumps most commonly used in water pumping systems.

Chapter Two: is committed to the mathematical modeling of the PV pumping system components. These include detailed dynamic models of the PV generator, DC-DC Boost converter, inverter, induction motor, and centrifugal pump. The

developed models are based on physical and electrical laws, allowing realistic simulation of system operation under varying operating conditions.

Chapter Three: provides the simulation and analysis of the system using MATLAB/Simulink. Two widely used MPPT algorithms Perturb and Observe (P&O) and Incremental Conductance (IncCond) were used to control the Boost converter. They were compared in terms of response time, stability, and overall energy efficiency. The simulation results provide an understanding of the suitability and efficiency of both algorithms for PV water pumping systems.

Through this work, we aim to contribute to the development of efficient and sustainable PV pumping systems, particularly for regions with limited access to conventional energy infrastructure. The findings of this study should guide better design and implementation practice, with the ultimate result of increased water accessibility and optimized energy use.

# Chapter I

# Principles of Photovoltaic Energy and Water Pumping Systems

## I.1 Introduction

This chapter provides an overview of the theoretical and technical foundations of photovoltaic (PV) systems and their integration into water pumping applications. It introduces basic solar energy concepts, including the photovoltaic effect, which enables the conversion of sunlight into electricity. The structure and operation of PV cells and systems are examined, along with their electrical characteristics and a brief history of technological development. The chapter highlights the advantages and limitations of different PV technologies. Finally, it focuses on PV water pumping systems as sustainable solutions for off-grid and rural areas, analyzing their components and control strategies

## I.2 Solar energy

Solar energy refers to the radiant light and heat emitted by the Sun, which can be harnessed using a range of technologies such as solar photovoltaics (PV), solar thermal collectors, and solar archi tecture to generate electricity, provide heating, and support sustainable energy systems .Solar ener gy is one of the most abundant and cleanest renewable energy sources available, offering signific ant potential to reduce greenhouse gas emissions and dependence on fossil fuels [9].

## I.3 Sunlight Energy

The Sun's core produces nuclear fusion reactions that produce heat and radiant light, which make up its energy. Numerous technologies, such as solar thermal systems for heating, photovoltaic (PV) systems for electricity generation, and solar architecture for passive solar design, are used to capture this energy [1]

## I.4 Sun

The main source of energy for Earth is the Sun, a G-type main-sequence star (G2V). It is a massive ball of plasma with a composition of mostly hydrogen (~74%) and helium (~24%) and heavier elements making up the remaining ~2%. The Sun's core, where nuclear fusion takes place, reaches temperatures of about 15 million, releasing a tremendous amount of energy outward through radiation and convection zones [2].

## I.5 Sun Characteristics [3]

- **Mass**: Approximately $1.989 \times 10^{30}$ kg.
- **Diameter**: About 1.39 million(km) fitting about 109 Earths side by side.
- **Volume:** Over 1.3 million Earths would fit inside it.

## I.6 Position of the sun relative to the Earth

In the celestial vault, the sun's position can be determined as a function of the observer's position on Earth and local time [4].

### I.6.1 Declination of the sun [37]

Cooper's equation below provides the angle's value in degrees, which is the angle formed by the course of the sun and the equatorial plane of the Earth:

$$\delta = 23.45 \circ \times \sin\left(\frac{360}{365}(jj - 81)\right) \quad \text{(I.1)}$$

- δ: is the declination in degrees.
- J: is the number of the day in the year for example:
- 1may 1june j= 61

### I.6.2 Geographical coordinates [5]

Three criteria are used by geographic coordinates to determine a point's location on the surface of the Earth:

a- **Latitude (φ):** which ranges from 0° at the Equator to ±90° at the poles, is the angle formed by the equatorial plane and the line that connects a location to the Earth's center.

b- **Longitude (λ**): The angle, from 0° to ±180°, east or west of the Prime Meridian (at Greenwich).

c- **altitude (h**): The vertical separation between a point on the surface of the Earth and mean sea level.

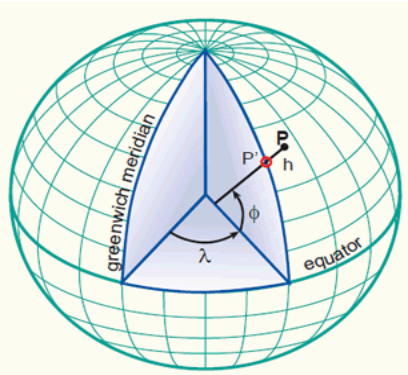


Figure(I.1):Geographical coordinates [6]

### I.6.3 Horizontal coordinates

Horizontal coordinates (altitude and azimuth) describe the position of a celestial object (like the sun) relative to an observer's local horizon.

This system is based on two main angles:

- **Altitude (h):** Angle above the horizon (0° at horizon to 90° at zenith).
- **Azimuth (A)**: Angle measured along the horizon, usually from North towards East (0° to 360°)

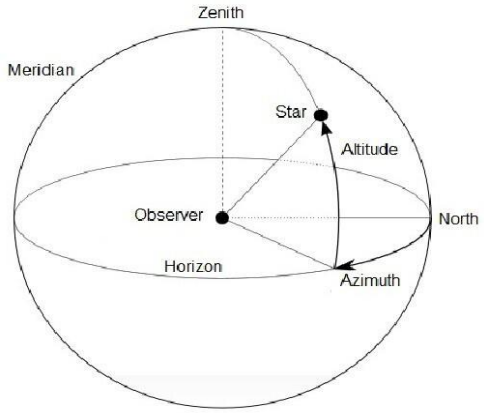


Figure (I.2): Horizontal coordinates [55]

## I.7 Solar Radiation

The amount of solar energy received per unit area is measured by a radiometric quantity called solar irradiance. According to the International System of Units, it can be expressed in either joules

per square meter (J/m2) or kilowatt-hours per square meter (kWh/m²). An albedometer or radiometer can be used to measure solar irradiance.

It is not to be confused with solar irradiance, which is a flux that is measured in W/m2, of which solar irradiance is the integral.

After accounting for atmospheric absorption and scattering, solar irradiance can be measured in orbit or on Earth's surface. The tilt of the sensor and the analysis spectrum of the measuring device determine the value that is measured [8].

### I.7.1 Components of solar radiation [8]

- **Direct Rayonnement**

It is the percentage of solar energy that reaches the earth directly, with a "Linear" (mineral deviation) path that is distinct at every moment.

The expression for radiation is as follows in the case of a horizontal plan:

$$I_h = I.\,Sin(h) \qquad \text{(I.2)}$$

I: direct radiation

h: height of the sun

- **Diffuse Rayonnement**

The term "diffus" refers to the radiation that emanates from all directions in the cosmos. This radiation is caused by the atmosphere's absorption and diffusion of solar energy, so as well as by reflecting on the nuages. Consequently, it makes up 20% of the total energy in the sky.

The energy received by the earth correlates with the maussade sky [8].

- **Radiation that is reflected**

Reflected radiation is the term used to describe solar radiation which is reflected by the earth or by objects on its surface.

This is influenced by the ground's albedo and can be important when the surface is very reflecting

(as next to a snowy surface or a water source) [8].

- **On a horizontal surface ( global radiation)**

**On horizontal surfaces**

To describes all solar radiation that reaches a planet's horizontal surface. As such, it encompasses both diffuse and vertical sun radiation.

**On inclined surfaces**

The total of the direct, diffuse, and reflected radiation on an inclined surface is known as overall radiation [8].

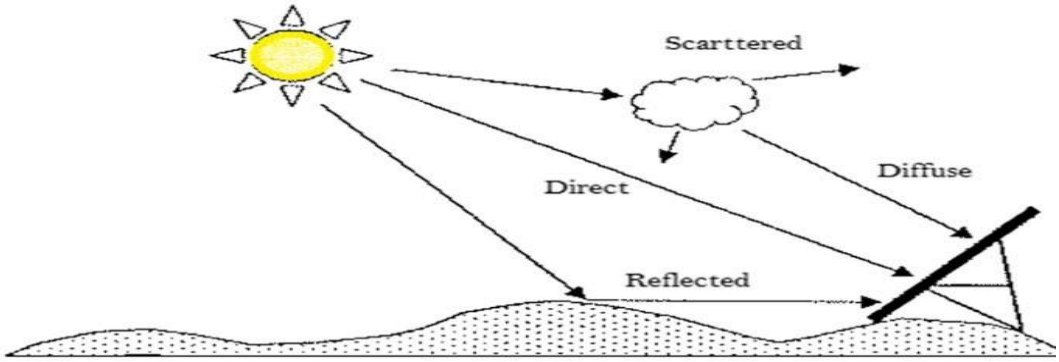


Figure (I.3) : solar radiation Components [22]

### I.7.2 Radiation spectrum

Photon waves, which are light particles, make up electromagnetic radiation (EMR). Both electrical and magnetic energy are present in these waves.Each photon's energy is directly proportional to its wavelength (λ), with the shorter the wavelength, the higher the photon's energy, as shown by the relationship below [27]:

$$E_{ph} = h \frac{C}{\lambda} \quad \text{(I.3)}$$

E(j) : Energy in Joul (j)

h (j.s) : Constante de Planck (*h*= 6,62607004 × 10 -34 m 2 kg / s)

c (m.s $^{-1}$) : Speed of light (c= 299 792 458 m / s)

λ (m) : Wavelength (often expressed in micrometers)

$\nu$ (Hz) = $\frac{c}{\lambda}$: Frequency.

The energy associated with this solar radiation breaks down roughly as follows[27]:

- -Ultraviolet UV 0.20 < l < 0.38 mm 6.4%.
- Visible 0.38 < l < 0.78 mm 48.0%.
- Infrared IR 0.78 < l < 10 mm 45.6%.

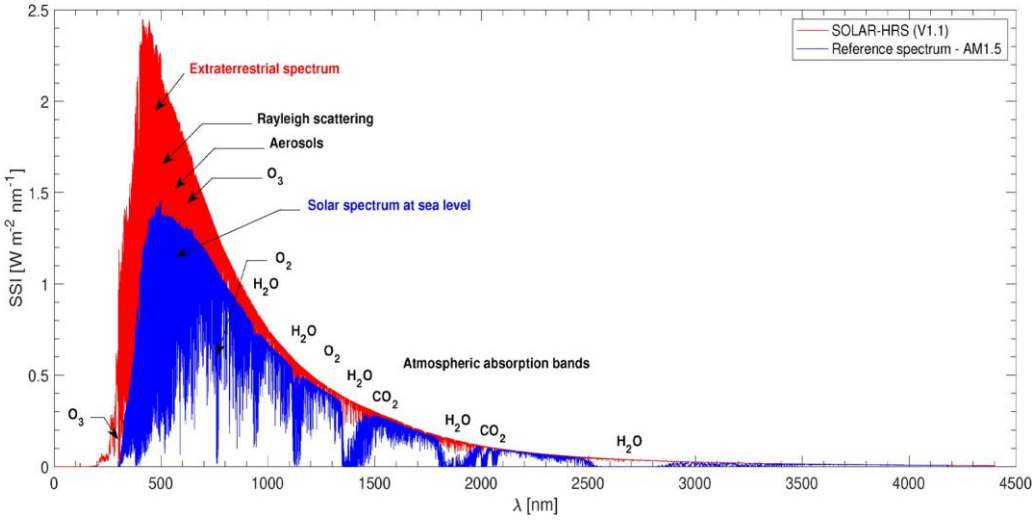


Figure (I.4) : Spectral analysis of solar radiation [27]

## I.8 The photovoltaic effect

The photovoltaic effect, which is the direct conversion of light into electricity when photons strike a cell, typically made of silicon, is the physical phenomenon upon which solar PV energy conversion is based. The latter is a semi-conductive electronic component that releases positively-charged "holes" and negatively-charged "electrons" when photons, the basic building blocks of light, are absorbed. An internal electric field separates these electrical charges, which are then gathered by a contact at the back and a grid at the front. Thus, the PV cell is a simple electrical generator [38] .

## I.9 Photovoltaic system

A photovoltaic system is a collection of parts that use solar energy to create electricity [33].

### I.9.1 The historique of photovoltaique system

**1839**: When Alexis Thérmoelectricity noticed that some materials generated an electric current when exposed to light, he made the initial discovery of the photovoltaic effect. This paved the way for further solar energy development [10].

**1873,** British engineer Willoughby Smith made one of the earliest real-world applications of the photoconductive phenomenon when he found that selenium could produce electricity when exposed to light [10].

**1883**: By applying a thin film of gold to selenium, Charles Fritts produced the first functional solar cell, which had an efficiency of roughly 1% [10].

**1954**: Bell Labs launches contemporary photovoltaic technology with the development of the first usable silicon solar cell, which has an efficiency of about 6% [11].

**1973**: Interest in solar power and other renewable energy sources rises as a result of the first oil crisis[12].

**]1985**: Commercial silicon solar cells become feasible for both home and commercial applications when their efficiency approach 15% [12].

**1990:** Using cadmium telluride, the NREL creates the first thin-film solar cell, paving the way for more affordable manufacturing techniques [13].

**1999**: Multi-junction solar cells are shown to achieve efficiencies of over 30% in laboratory experiments, opening the door for more sophisticated solar technology [13].

**2010:** With production prices drastically reduced, China becomes a major producer of solar panels [14].

**2020:** Significant developments in perovskite solar cells that point to possible efficiency of over 25% at reduced manufacturing costs [14].

### I.9.2 Photovoltaic cell

An electronic gadget called a photovoltaic cell converts solar radiation into electrical energy. It is composed of a finely processed semiconductor layer that converts solar energy into electrical energy. The word "photovoltaic" is a derivative of two words: "voltaic," which is taken from the name of Alessandro Volta, an Italian physicist who created the voltaic pile, an early form of an electric battery, and "photo," which is derived from the Greek word "phos," which means light.[15]

### I.9.3 Building a Photovoltaic Cell [15]

**a-P-N Junction**: A PV cell's fundamental structure includes a P-N (positive-negative) junction. By doping the silicon with particular impurities, this connection is produced. Positive charge carriers, or holes, are introduced by the material doping the P side, while negative charge carriers, or electrons, are introduced by the substance doping the N side.

**b- Absorption Layer:** This thin layer sits above the P-N junction and is known as the absorption layer. The capacity to absorb photons from sunlight depends on this layer. Electrons are energized by photons and emerge from their atomic bonds when they hit the absorption layer

c- **Metal Contacts**: To enable electron passage, metal contacts are positioned on the PV cell's top and bottom surfaces. The released electrons are captured by the metal contacts, which create an electrical circuit that allows them to be used as electrical power.

**d- Antireflection Coating**: An antireflection coating is frequently applied to the PV cell's surface to improve solar absorption. By reducing sunlight reflection, this coating makes it possible for more photons to enter the cell and aid in the production of energy.

**e- Encapsulation:** To shield photovoltaic cells from external elements like moisture and mechanical stress, they are frequently encased. Glass and transparent plastics are examples of encapsulation materials that offer a protective barrier while letting sunlight into the cell. **f- rear Surface Field**: To improve electron collecting and overall efficiency, more sophisticated PV cells may have a rear surface field.

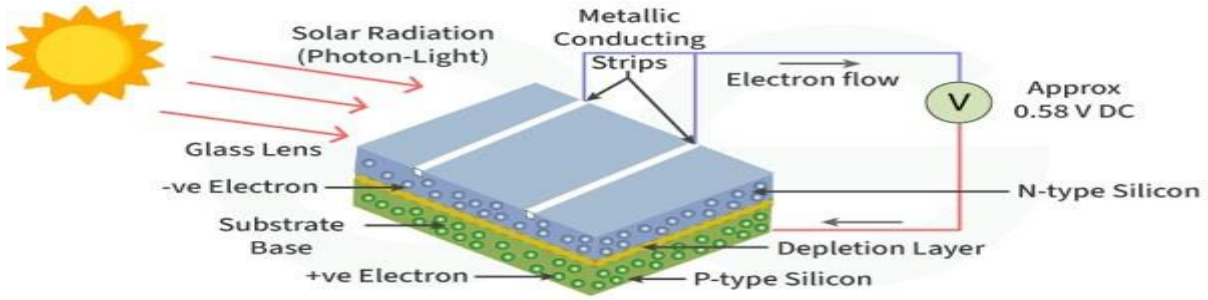


figure (I.5) : cell buillding [15]

Table I.1:comparaison beetwen Type of photovoltaic cell

| Technology | Monocrystalline Silicon[16] | Polycrystalline Silicon[17] | Amorphous Silicon[18] |
|---|---|---|---|
| Cell and Module |  | 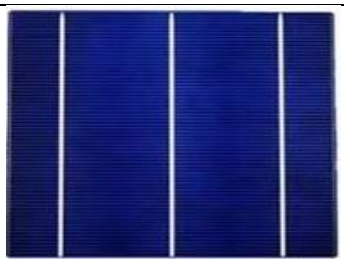 | 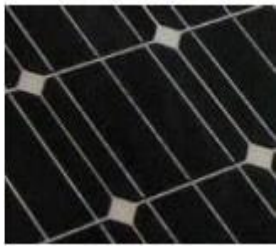 |
| Efficiency | 14% – 22% | 13% – 16% | 6% – 9% |
| Advantages | - High efficiency<br>- Space-efficient<br>- Long lifespan | - Lower cost<br>- Easier to produce<br>- Decent efficiency | - Works in low light<br>- Flexible<br>- Lightweight |
| Disadvantages | - More expensive<br>- Energy intensive to manufacture | - Lower efficiency than mono<br>- Less uniform appearance | - Shorter lifespan<br>- Rapid degradation<br>- Low efficiency |
| Applications | - High-performance residential and commercial systems<br>- Space applications | - Residential rooftops<br>- Off-grid systems | - Small devices (calculators, watches)<br>- Building-integrated PV |

### I.9.4 Photovoltaic cell association

- **In series**

The cells in a series grouping have the same current flowing through them, and the characteristic of the series grouping is obtained by summing the voltages. The following illustrates the feature that was obtained by joining identical cells in series **[8]**

$$V_{oc\,ns} = V_{oc} * N_s \quad (I.4)$$

$$I_{cc}\,N_s = I_{cc} \quad (I.5)$$

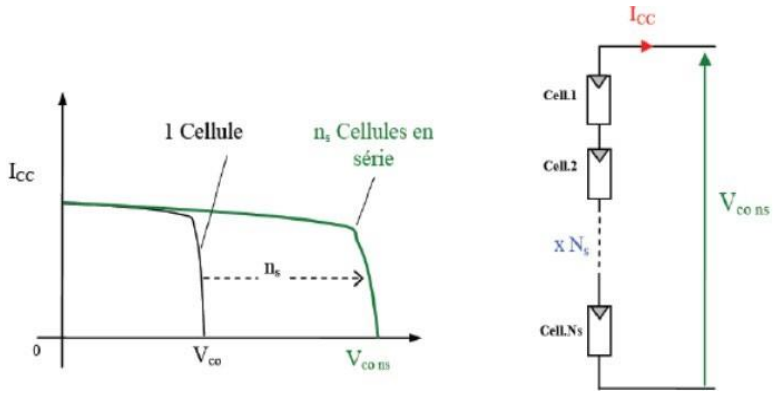


Figure(I.6) : Resulting characteristic of a grouping of ns cells in series [19]

$N_s$ :number of series cell

- **In parallel**

The traits of series and parallel cell groups are identical. By exposing all of the cells in a parallel cell group to the same voltage, the group characteristic can be calculated by adding up the currents at a specific voltage. The following illustrates the feature that was obtained by joining identical cells in parallel [8]:

$$V_{oc\,np} = V_{oc} \quad (I.6)$$

$$I_{cc\,np} = I_{cc} * N_P \quad (I.7)$$

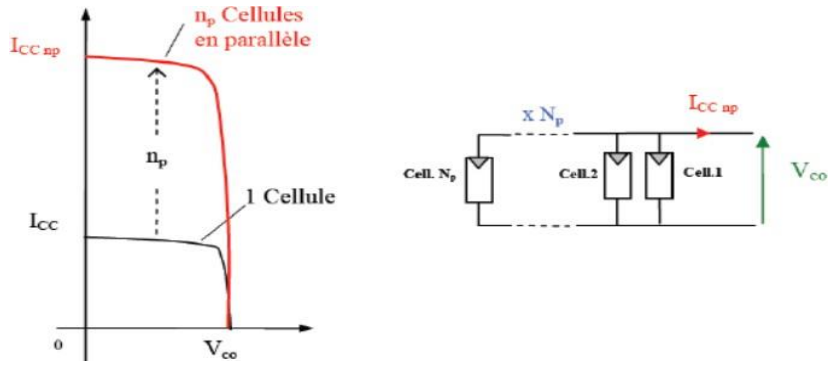


Figure(1-7) : Resulting characteristic of a grouping of n p cells in parallel [19]

$I_{cc}$ :shor circuit current

$V_{0c}$ :voltage of open circuit

$N_p$ : number of parallel cell

- **In Parallel/Series**

These cells are arranged in series or parallel to calculate the overall values for short-circuit current and total open-circuit voltage, as indicated in the equation below [8]:

$$I_{tcc} = N_p * I_{cc} \quad (I.8)$$

$$V_{toc} = N_p * V_{oc} \quad (I.9)$$

### I.9.5 The photovoltaic module

A module of solar cells is put together to provide greater power. Whereas a parallel connection raises current while preserving voltage, a series connection of many cells raises voltage for the same current. These cells are shielded from moisture by being encased in EVA (ethylene-vinyl-acetate) polyethylene. High-transmittance, mechanically strong tempered glass protects the front surface, while polyethylene protects the back Typically, a stiff anodized metal frame encircles the modules with mounting apertures. Each module has a junction box with two antiparallel diodes at the back. A module in the sun cannot discharge into a module in the shade thanks to these antiparallel diodes [20].

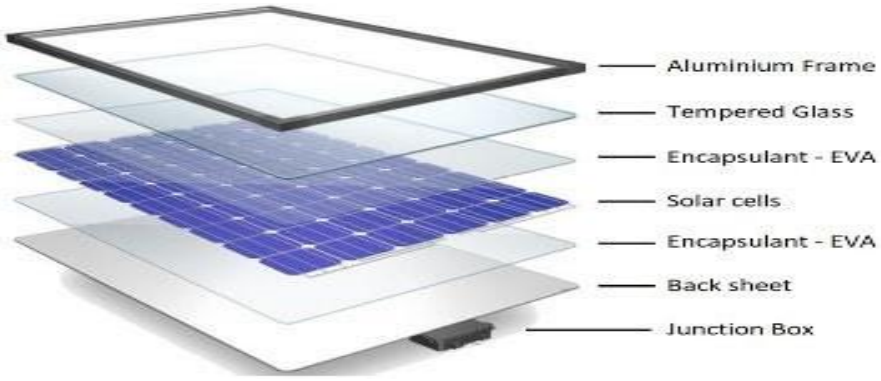


Figure (1-8):photovoltaique module Components [28].

### I.9.6 The photovoltaic generator

It is the instrument that transforms solar energy into electrical energy.

direct current. It is made up of several panels. The panel is composed of many modules that can be arranged in parallel, series, or hybrid configurations. The cells in the module are typically silicon-based and are arranged in rows, either in series, parallel, or hybrid configurations [20].

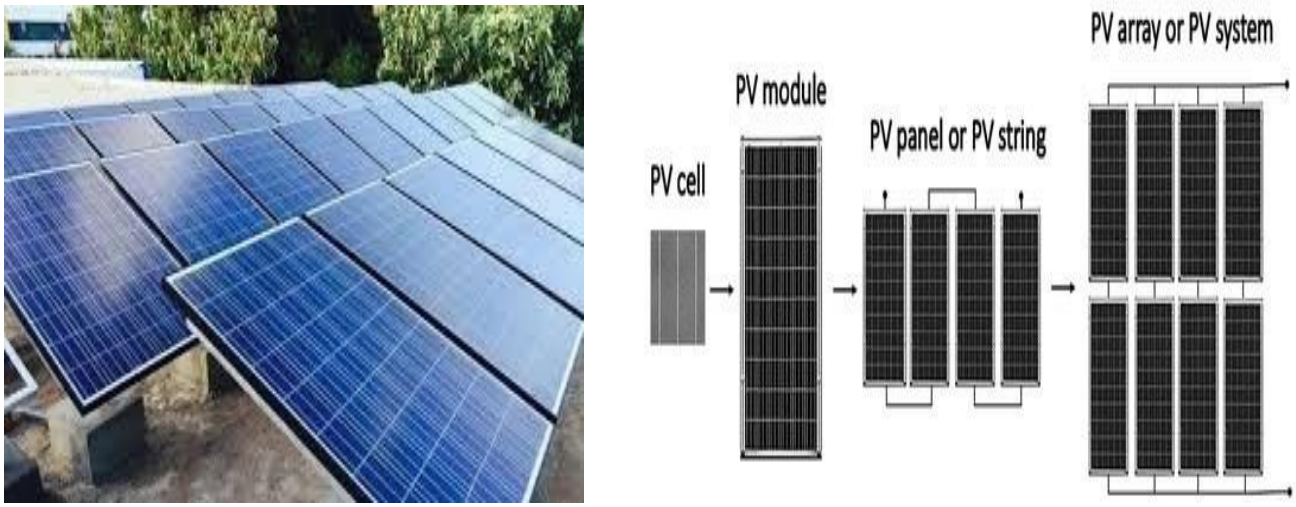


Figure(I.9): Photovoltaic generator [28]

### I.9.7 Electrical characteristics of a pv module

The (I-V) and (P-V) characteristics of a module :

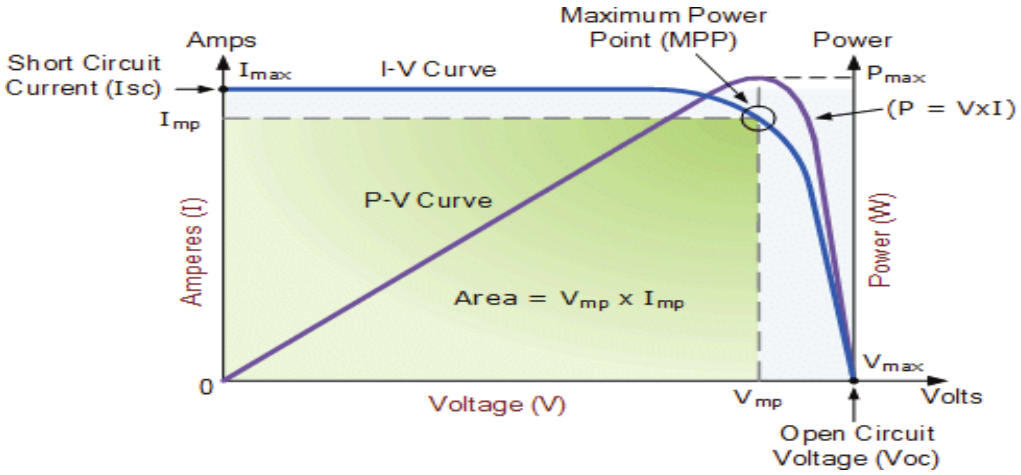


Figure(I.10) :the (I-V) and (P-V) characteristics[29]

The electric current available at a photovoltaic cell's terminals under fixed ambient operating conditions (temperature, air circulation speed, irradiance, etc.) is displayed in. A photovoltaic cell's I=f(U) characteristic is indicate in figure(I.10) [27].

- The open-circuit operating point, or no-load operating point (UCO=Uv): Uv when I=0 A
- For U = 0V, the short-circuit operating point is Icc
- The formula for the power supplied by the module is (P = U.I.) We can plot the curve (P = f(U)) and determine the power P for each point on the curve above. As seen in the above figure(08)
- The optimal maximum power Consequently, Pi would be equal to the open-circuit voltage (UCO = Uv) times the short-circuit current (ICC) [27].

  $P = P\ maxeideal = U_{C0}.\ I_{CC}$ (I.10)

The photovoltaic generator It is characterized by the following features [27] :

- **Peak power Pc**:
- The nominal power that the module delivers at standard conditions (1000 W/m² of illumination and 25°C). Peak watts (Wp) are the unit of measurement [25]

- **The current I :**supplied by the module as a function of the voltage at its terminals is represented by the I(V) characteristic [27].
- **No-load voltage Voc**: The voltage at the module terminals when there is no current flowing, for "full sun" lighting.
- **Current supplied by a short-circuited** : module for "full sun" illumination is known as the short-circuit current (Isc).
- **The point of maximum power :** or optimal operating point This depends on insolation. When peak power is at its highest in direct sunlight, this is the point at which the module delivers its maximum current Impp at its maximum voltage Vmpp [27].

  $Pmpp = Vmpp * Vmpp$ (I .11)
- **Efficiency** : is defined as the ratio of incident radiation power to optimal electrical power. The ratio of the maximum power output (Pmpp) to the power received by the module from solar radiation is known as energy efficiency. This efficiency can be expressed as follows, given (S) the module's surface area and (G) the irradiance:[27]

$$\eta = \frac{Pmpp}{G*S} \quad (I.12)$$

- **The forme factor : -**

  The ratio of the module's maximum power delivery to its optimum power (Pmpp) is known as the form factor [27]

  $$FF = \frac{Pmpp}{Voc*Isc} == \frac{Impp*Vmpp}{Voc*Isc} \quad (I.13)$$

### I.9.8 Protection of Photovoltaic generator

#### I.9.8.1 By by-pass diode: Hot-spot phenomenon

In this case, a local blockage that limits the current that the cellule may produce can be used to implant PV cells. The ombrées cells also experience an inverse tension change, changing from generator cells to receptor cells. A localized energy dissipation brought on by the opposite tension may even result in a hot spot that kills the cells. The derivation diodes are positioned in parallel, in the opposite direction as the solar cell, to get around this problem. This creates a sense of free . current and prevent the ombrées' cells from using energy [23].

### I.9.8.2 By non-return diode : against the current of return

It is always important to make sure that the tensions are equal when two sources of tension are connected in parallel since even a small change could destroy one of the PV generators due to a surge of intensity in one of the sources. In order to solve this issue, a simple A diode is connected in series with one or more PV panels to prevent current return in the event of a failure [23].

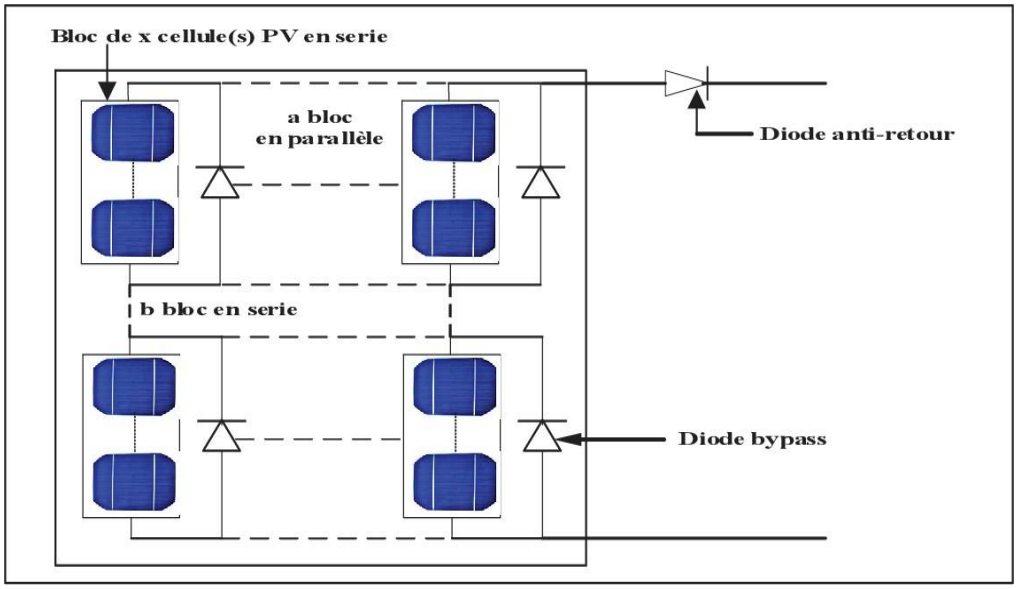


Figure(1- 11) :protection by by pass diode and non-return diode [28]

### I.9.9 Type of photovoltaique system

### I.9.9.1 On-Grid Solar System

Grid-tied, or on-grid, solar PV systems are those that are directly connected to the national grid. Among house and business owners, this type of solar PV system is the most popular. This kind of solution is ideal for people who wish to lower their energy costs and carbon footprint but are already linked to the grid [24].

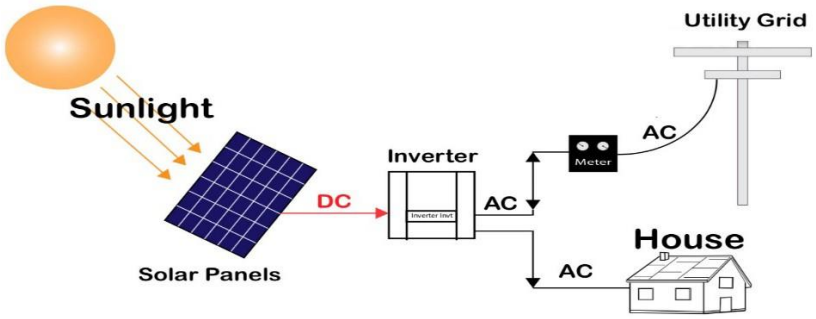


Figure (1-12) :on grid solar system [25]

### I.9.9.2-Hybrid Solar System

Batteries and solar panels are combined in hybrid solar systems to produce green energy. They enable for islanding during power outages and evening power use by storing excess energy in a home battery before sending it to the grid. In addition to being versatile and affordable, hybrid solar systems can be expanded at any moment. They have the benefit of charging batteries from inexpensive peak rates, but they are more costly than on-grid solutions. However, compared to grid-tied systems, they are less efficient since they have more components [24].

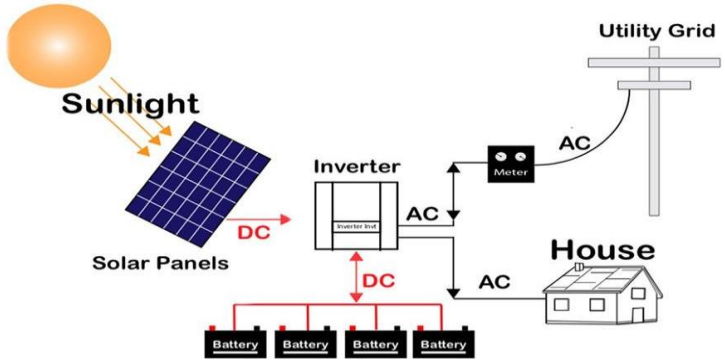


Figure (I-13): hybrid solar system [25]

### I.9.9.3 Off-grid solar system

For people who wish to be energy independent or who find it difficult to connect to the national grid, an off-grid solar system is perfect. Off-grid systems have the benefit of being energy self-

sufficient, supplying power even in remote areas, which is advantageous given the rising cost of energy. Compared to conventional grid-tied systems, they are more costly and require more components; however, because they are modular, they can be expanded to accommodate different energy requirements. Victron Energy off-grid solar systems are installed nationwide by Deege Solar [24]

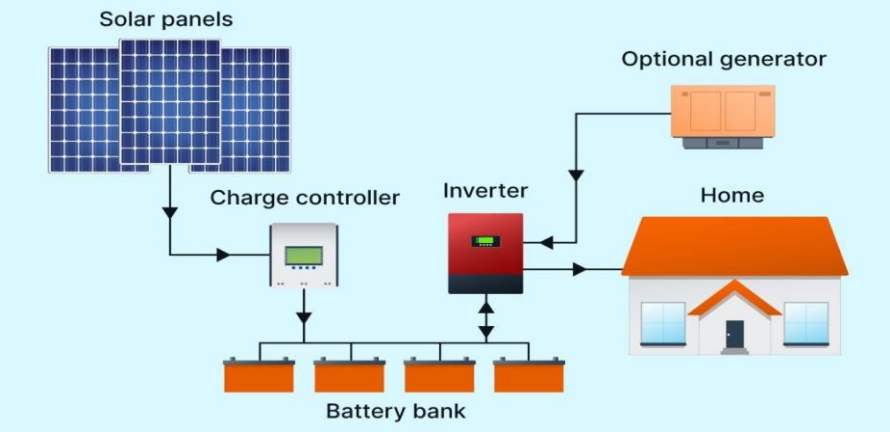


Figure (1-14): -Off-grid solar system [26]

### I.9.10 Advantages and disadvantages of PV energy

➢ **Advantages**

- Because there are no moving parts in the system, PV energy is dependable and renewable.
- PV panels' modular design makes them simple to install and flexible enough to meet a variety of energy requirements. Power applications ranging from milliwatts to hundreds of megawatts can be accommodated by system sizing.
- Because there is little maintenance involved and no need for fuel, transportation, or highly skilled workers, operating costs are extremely low.
- Because the final product is non-polluting and does not disturb the environment, PV technology is environmentally friendly [38].

➢ **Disadvantages**

- the production of PV modules is a sophisticated, expensive procedure.
- With a theoretical limit of 28% for a cell, a module's actual conversion efficiency is only about 10% to 15%.
- Only in remote locations with low energy demands can PV generators compete

- with diesel generators [38].

## I.10 Photovoltaic (PV) pumping systems

Photovoltaic (PV) pumping systems are solar-powered devices that use energy from photovoltaic panels to pump water directly from a source (like a well, river, or reservoir) by converting solar radiation into electrical energy that powers an electric motor connected to a water pump. PV pumping systems are especially well-suited for remote, off-grid locations where access to conventional electricity is limited or nonexistent. They are used for agricultural irrigation, livestock watering, and rural drinking water supply, and they provide a sustainable and eco-friendly substitute for diesel or grid-powered pumps [21].

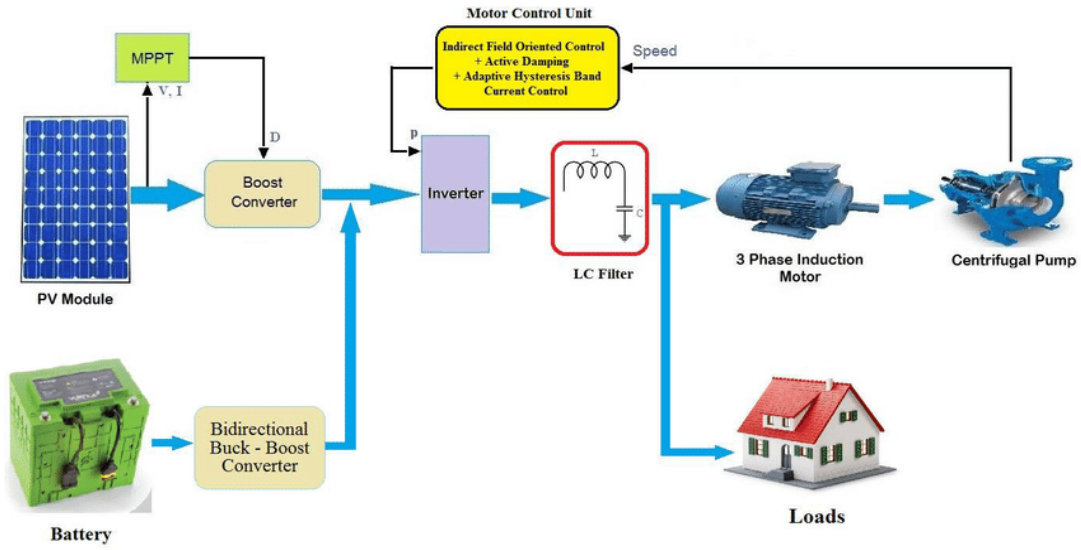


Figure(1-15): PV pumping system [30]

## I.11 Type of PV pumping

### I.11.1 pumping with the sun

The continuously variable power produced by the photovoltaic modules is directly utilized in this method. As a result, the pumping rate will change as the sun's ray intensity does [27].

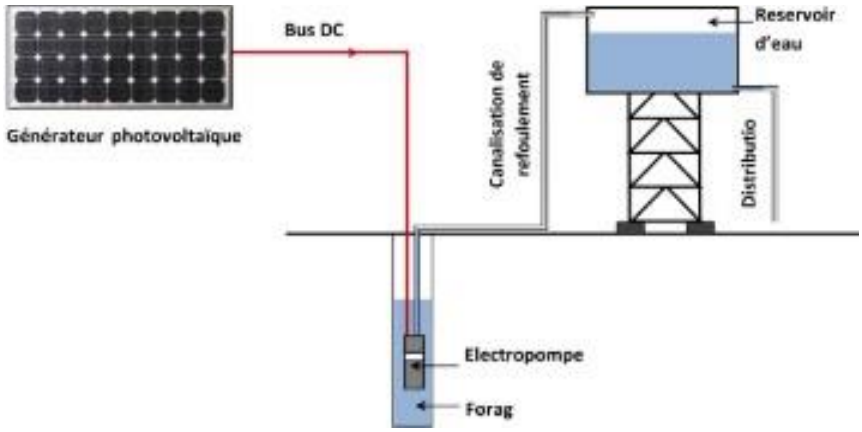


Figure(1-16) : Diagram of solar pumping [27]

### I.11.2 Pumping with energy storage

The technique involves energy storage, this time via batteries. These batteries store the energy produced by the photovoltaic cells during periods of sunshine, so that they can release this energy to pump water when required. The pumping rate can be set on demand, when users need it [27].

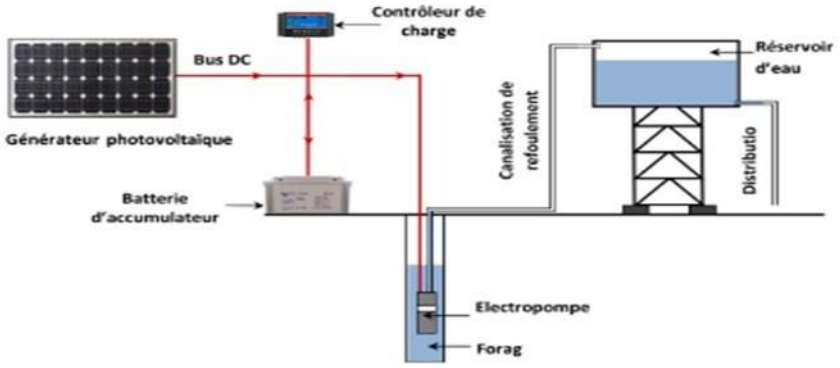


Figure (1-17): diagram of Pumping with energy storage [27]

## I.12 photovoltaic pumping system equipment

**I.12.1 Photovoltaic generator:** it is the important element in our system because is the source of electricity who feed the system.

### I.12.2 Power adapters

#### I.12.2.1 DC/DC converter

DC/DC converters are used to convert a fixed DC voltage into a variable DC voltage. High-frequency "chopping" is used to accomplish this energy conversion, and it is quite efficient. [31]

The converter is divided into two types:

**a-Buck converter**

The flyback chopper's basic circuit is depicted in Figure (1-18). The switch creates a rectangular voltage at the diode by connecting and disconnecting the circuit's input. A low-pass filter (LC) filters this voltage, resulting in a nearly DC voltage at the circuit's output. This kind of converter is typically used as a DC power supply in photovoltaic applications, where the output voltage is nearly constant but varies with temperature and sunshine. By regulating the switch's ON and OFF states ( and), the average output voltage can be changed [20].

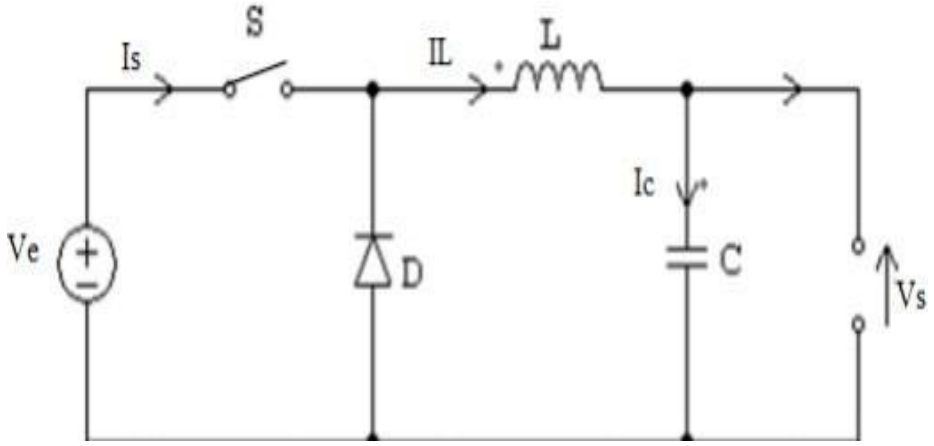


Figure (1-18) : schematic of Buck converter [31]

**b-Boost converter**

In photovoltaic applications, the step-up or step-down chopper is typically employed, particularly for battery charging. With the same parts as the step-down chopper but a different arrangement, the basic circuit of a step-up chopper is depicted in Figure (1.19). A variable duty cycle and a constant period are used to control switching states. The name comes from the fact that the average output voltage of this chopper is higher than the input

voltage. This structure needs a diode (spontaneous on/off) and a controlled switch (bipolar, MOS, IGBT, etc.) [20].

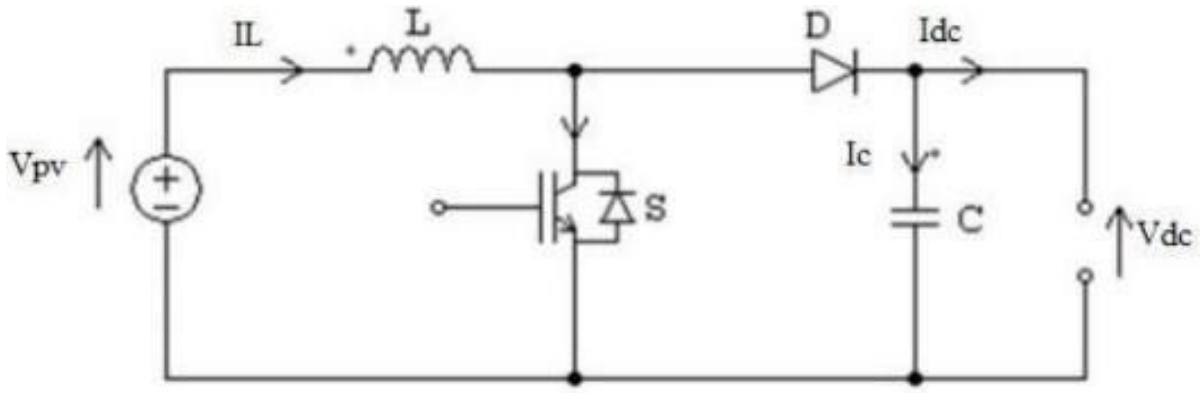


Figure (1-19): schematic of boost [31]

### I.12.2.2 converter controls

An efficient photovoltaic system's overall design is challenging by nature. On the source side, a solar generator's power output fluctuates significantly based on temperature, illumination, and load behavior fluctuation based on consumption, all of which are frequently unpredictable. Indeed, extractable electricity fluctuates in these shifting circumstances. It is feasible: this is how Maximum Power Point Tracking, or MPPT, got its start. Unlike fixed-voltage regulation, the MPPT (Maximum Power Point Tracking) approach uses a search algorithm to predict the power curve's maximum without interfering with the photovoltaic panel's regular functioning. Active power control forces the derivative of power with respect to time to zero in order to obtain maximum power point [20].

In order to attain maximum power on the current/voltage characteristic, MPPT searches for the reference value rather than relying on a preset one. When it comes to cutting costs and increasing efficiency, MPPT is crucial. When correctly tuned, MPPT can collect more than 97% of solar electricity. There are several MPPT systems now on the market, including traditional and

contemporary) for tracking a photovoltaic system's maximum power operating point, comprising [20].

**a- Perturbation and observation method (P&O)**

The P&O MPPT algorithm is a hill climbing approach where the PV system's operating voltage is affected by changes in voltage (dv), which are carried out in accordance with changes in power (dp), so that the two quantities' variations must be in the same direction. Due to significant output voltage oscillations at the MPPT, this method's disadvantage is that it causes the array terminal voltage to fluctuate with each MPPT cycle, which reduces the PV system's power. Moreover, it occasionally misses the MPPT [34].

**b- Incremental conductance (IC) method**

The second approach regulates PV system voltage according to the voltage corresponding to maximum power, based on instantaneous conductance (dI/dV) and conductance (I/V). Checking the positive or negative variation of dP/dV, respectively, increases or decreases the PV system voltage. to monitor the voltage corresponding to the maximum power. The advantages of the INC algorithm include excellent stability and precise system control in the face of abrupt changes in atmospheric conditions [34].

**c- Fuzzy logic (FL) method**

Multiple possible truth values can be processed through a single variable using fuzzy logic, a method of variable processing. In order to arrive at a variety of accurate conclusions, fuzzy logic uses heuristics and an open, imprecise spectrum of data to solve problems. Fuzzy logic is intended to solve issues by taking into account all relevant data and selecting the optimal course of action based on the input [35].

### I.12.2.3 The DC/AC inverter

The inverter's job is to convert the photovoltaic generator's direct current into either single-phase or three-phase alternating current. Typically made up of electronic switches like IGBTs (power transistors), inverters are bridge structures.

For fixed input and output characteristics, they are very effective. However, their variable nature and high cost.

The use of AC motors for solar pumping has long been disregarded due to the general lack of solar radiation and pump torque.

Generally speaking, pumping inverters are made with variable frequency (f) to accommodate changes in the speed at which the pump rotates. The AC voltage (U) to frequency (U/f) ratio is constant in this instance. The alternating current's frequency and sunlight intensity are directly correlated.

Adapting the operating point (current-voltage) to the generator is the inverter's second function. Managing and safeguarding the installation is its third [20].

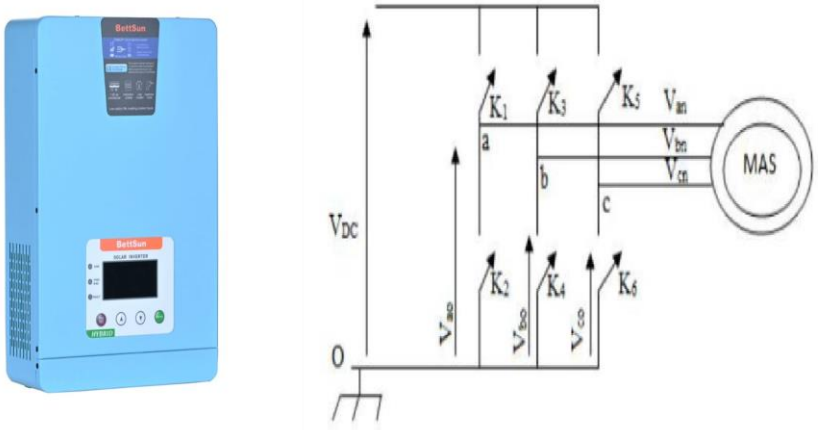


Figure (I.20): inverter schematic

### I.12.2.4 inverter control

Several strategies can be used to control voltage inverters. Which control strategy is used depends on the kind of load that needs to be managed, the power range, the inverter's semiconductors, and how easy it is to implement the algorithm. The control signal will be at the frequency of the intended output voltage, they are driven at full wave at low frequencies, and the DC source needs to be tunable (with a chopper or thyristor rectifier). They are managed by pulse-width modulation at high frequencies. This latter tactic makes both possible [20].

By applying voltage pulses to the machine terminals, the pulse-width modulation (PWM) method of controlling current from a DC voltage source brings the voltage fundamental as close to

the sinusoidal voltage reference as feasible. Two signals are compared in order to determine M.L.I Triangular high-frequence.

The "carrier" is a signal (Fp), and the "modulator" is a reference signal of frequency (Fm<< FP). The inverter switches' switching times are determined by where these two signals intersect[20].

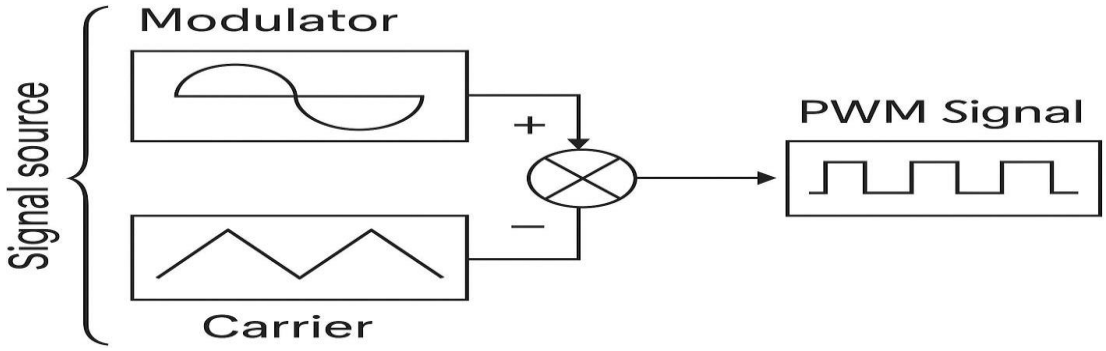


Figure (I.21): synoptic diagram of M.L.I [31]

The following is the definition of these two signals

A high-frequency signal, typically in the form of a triangle, is the carrier wave. An image signal of the intended output wave, typically a sine wave, is the modulator wave. MLI is characterized by two primary parameters: The ratio of the modulating wave's amplitude to the carrier wave's is the ML modulation index, also referred to as the harmonic ratio [20].

$$M_L = \frac{Vm}{Vp} < 1 \qquad \text{(I.14)}$$

The modulation ratio, or Mr:, is the carrier wave's frequency divided by the modulating wave's frequency [20]:

$$M_r = \frac{Fp}{Fm} \qquad \text{(I.15)}$$

**-MLI with natural sampling**

Comparing the triangular signal (carrier) with a sinusoidal signal (modulator) is the most popular and straightforward method of natural sampling, which is the process of natural selection of sampled points. The switch instants are defined by where these two signals intersect.

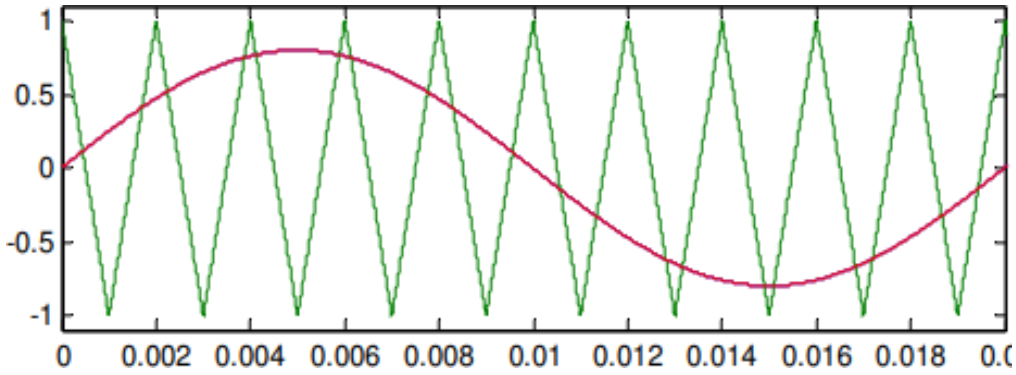


Figure (I.22): MLI with natural sampling [36]

## I.13 Motor-pump assembly

A motor-driven pump is a unit consisting of an electric motor driving a hydraulic pump [31]

### I.13.1 The motor

The motor of a pump unit converts electrical energy into mechanical energy. In the latter case, an electronic converter or inverter is required to convert direct current from a photovoltaic generator into alternating current. For this reason, the choice of a DC motor may seem, at first glance, more interesting, but we'll see that the evolution of efficient electronic converters also makes it possible to choose efficient and, above all, less expensive AC motors [31].

The motors are divided into two types:

#### I.13.1.1 DC motor

These motors are powered by DC voltages. The main advantage of DC machines lies in their simple adaptation to means of adjusting or varying their speed, torque and direction of rotation. Their main drawback is the brush/rotary commutator assembly, which wears out, is complex to manufacture and consume energy **[31].**

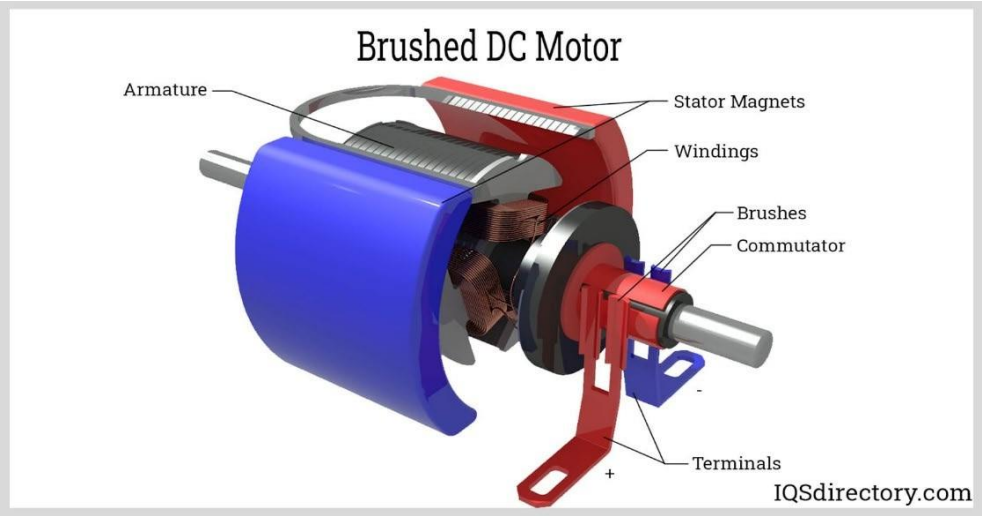


Figure (I.23): DC motor [56]

### I.13.1.2 AC motors

For low- and medium-power applications (up to a few kilowatts) the standard single-phase network is sufficient. For high-power applications, AC motors are generally supplied by a polyphase current source. The most frequently used system is the three-phase system (phases offset by 120°) used by electricity distributors [31].

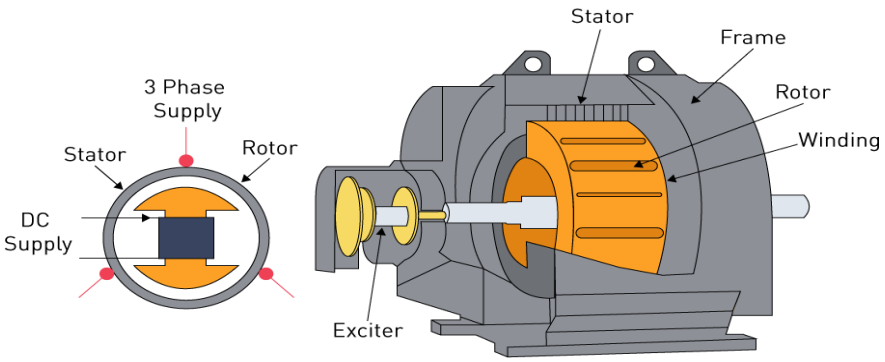


Figure (I.24): AC motor [56]

This type is division in two kinds also:

- **Synchronous motors**

The synchronous machine is often used as a generator. It is then called

“alternator”. With the exception of low-power generator sets, this machine is generally three-phase. For electricity generation, power plants use alternators with outputs of up to 1,500 MW. As the name suggests, the rotation speed of these machines is always proportional to the frequency of the currents flowing through them [31].

- **Asynchronous motors**

The asynchronous machine, also known by the Anglo-Saxon term “induction machine is an alternating-current machine with no electrical power supply to the rotor, The term comes from the currents induced in the rotor by magnetic induction. The term “asynchronous” derives from the fact that the speed of these machines is not necessarily proportional to the frequency of the currents flowing through them [20]

### I.13.2 Control of the asynchronous machine

Blaschke's work from the early 1970s introduced the concept of flow steering, which is the alignment of the flow with the “d” axis of the rotating reference frame (d-q) so that an asynchronous machine behaves like a machine with discrete content current. Therefore, the field current controls the flow, and the motor current controls the torque.

By splitting the stator current into two parts, one regulating the torque (Iqs) and the other controlling the flux (Ids), this control seeks to eliminate the coupling between the motor and field and make its operation similar to that of an AC machine [27].

- **Direct (FOC):** direct vector control involves controlling the flow, which necessitates understanding of the dynamic behavior of the rotor flux linkage and its orientation with respect to the stator reference frame [20].
- **Indirect field control (Ifoc)**: This type of vector control eliminates the need for flow knowledge by using a few approximations [20].

### I.13.3 Pump

Water pumps are usually classified according to their principle of operation, either volumetric or centrifugal. In addition to these two classifications, which we'll describe later, we also distinguish two other types of pump based on the pump's physical location in relation to the water being pumped: the suction pump and the discharge pump [31].

### I.13.4 Type of pump

#### I.13.4.1 The centrifugal pump

To achieve a higher pressure, they employ centrifugal force in conjunction with changes in the fluid's pumping speed. An impeller equipped with blades or vanes rotates to provide the fluid with kinetic energy, and speed reduction converts some of this energy into pressure. A certain motor speed is necessary for the water pressure to be high enough to exit at the end of the water supply pipe, but the centrifugal pumps drive torque is nearly zero at startup and it can operate even in extremely low sunlight The photovoltaic modules and the power input are well matched, resulting in good overall efficiency [20].

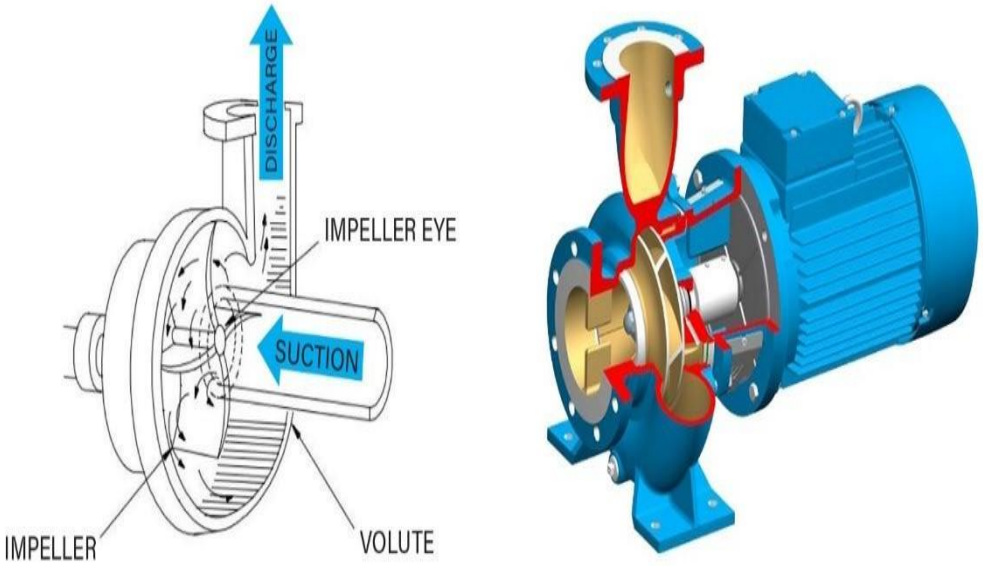


Figure (1-25): The centrifugal pump [37]

- **Torque and flow characteristic as a function of speed**

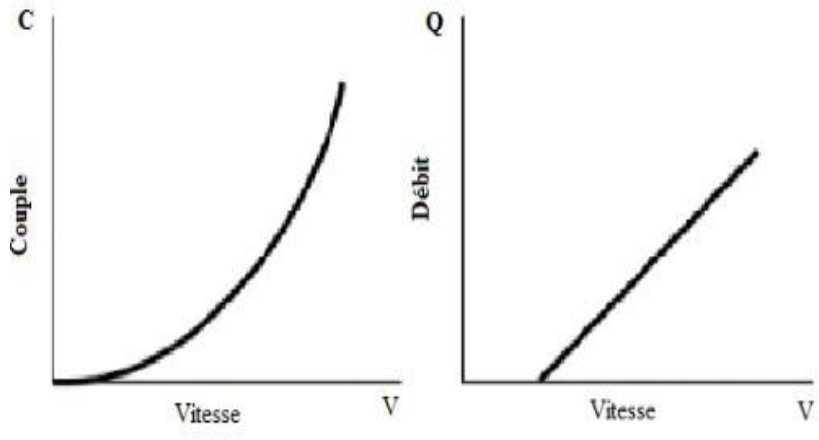


Figure(1-26) : Torque and flow characteristic as a function of speed [20]

### I.13.4.2 Volumetric pumps

In these pumps, the fluid is set in motion by a change in its volume. Positive displacement pumps are of two types: reciprocating positive displacement pumps (e.g., piston pumps, diaphragm pumps, etc.) and rotary positive displacement pumps (screw pumps, etc.). Their main advantages are:[20]

-They are designed for low flow rates (less than 5 m3/h) and high heads.

-They have good efficiency, and surface pumps are self-priming.

The starting torque of a positive displacement pump (3 to 5 times the nominal torque) and the I=f(V) characteristic of this type of pump make its operation directly on a photovoltaic panel not economically viable. To overcome the problem of generator oversizing resulting from this mismatch, an impedance matcher is used to ensure the highest possible efficiency for the entire system [20].

Figure (1-27): Volumetric pumps [20]

**Torque and flow characteristic as a function of speed**

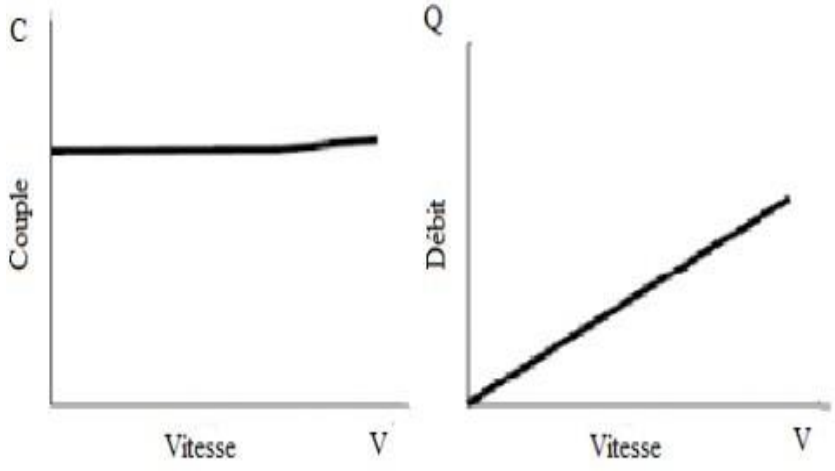


Figure:(1-28): Torque and flow characteristic as a function of speed [20]

### I.13.5 Advantages and disadvantages of pv pumping

- **Advantages**

- A sustainable and environmentally-friendly power source.
- Affordable upkeep and minimal operational costs.

- Perfect for isolated or off-grid locations.
- Self-sustained operation that does not need constant monitoring.
- Lessens reliance on non-renewable energy sources.
- Can be adjusted according to the demand for water.

➢ **Disadvantages**

- Relies on sunlight; inoperative at night or during overcast weather.
- Charging water on site is needed.
- Increased cost of installation initially.
- Less production in areas or times of the year where solar radiation is low.
- Requires skilled professionals for correct setup and configurations.

## I.14 Conclusion

In conclusion, this chapter provided a comprehensive overview of the theoretical and technical foundations of photovoltaic systems, outlining the key components involved from solar cells to electrical energy generation. A general introduction to solar-powered pumping systems was also presented, highlighting their operational characteristics and advantages, particularly in remote areas lacking access to conventional power grids. This foundational knowledge is essential for understanding the interaction between photovoltaic components and the pumping system, and it sets the stage for the following chapters, where we will analyze the system's performance and explore methods for its optimization.

# Chapter II
# PV pumping system modeling

## II.1 Introduction:

In off-grid locations, photovoltaic (PV) pumping systems provide an independent and environmentally friendly water supply option. It is possible to forecast performance, optimize the energy-water chain, and create effective control strategies by modeling these systems, from the PV generator to the pump. The electrical models that are necessary for the design and enhancement of PV pumping systems are compiled in this chapter.

## II.2 Photovoltaic panel modeling

### II.2.1 solar generator's electrical model

The solar cell is the basic component of a photovoltaic generator. Depending on its configuration that is, , the number of modules in series and parallel the electrical behavior model of the solar panel can be extended to the photovoltaic generator.

Numerous models of solar generators exist, and they are differentiated by the number of factors and the method used to calculate current and voltage. These consist of [20]:

#### II.2.1.1 Ideal model

This is the most elementary model, since the resistance is usually very large and therefore often considered infinite (and therefore neglected), while taking into account the small value of the resistance, which is assumed to be zero (=0). This model can be represented by a current generator in parallel with a diode supplying a current as shown in figure (II.1), which illustrates the equivalent circuit of an ideal solar cell [8].

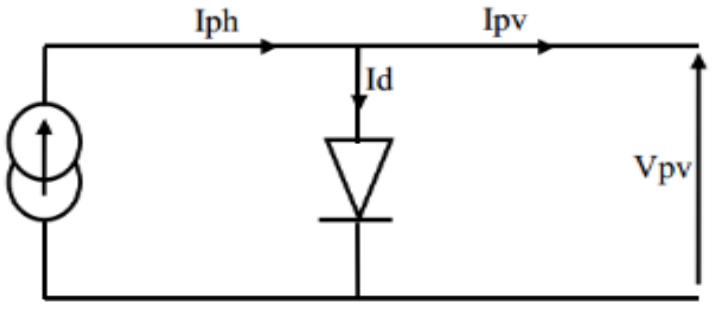


Figure (II.1): Ideal photovoltaic cell model [20]

- equation used for this model [20]:

$$I_{pv} = I_{ph} - I_d \quad \text{(II.1)}$$

- we can say that $I_{ph}$ is the same as $I_{cc}$ ,which is the short- circuit current ,with $V_{pv}$=0.

$$I_{ph} = [\, I_{cc} + k_i * (T_c - T_{ref}) \,] \quad + \frac{G}{G\,ref} \quad \text{(II.2)}$$

$k_i$ :Cell short-circuit temperature coefficient(Amperes/k)

$T_c$ : Cell temperature in kelvin (k)

G : Illuminance absorbed by the cell

$G_{ref}$: Illuminance Reference (1000/$m^2$)

Diode current : $I_d$

$$I_d = I_0 \left( \exp\left(\frac{Vd}{Vt}\right) - 1 \right) \quad \text{(II.3)}$$

$I_0$ : Saturation current of the diode

$$V_t = \left(\frac{B\,k\,T}{q}\right) \quad \text{(II.4)}$$

$V_t$ : Thermal voltage.

B: Ideality factor

K: Boltzmann constant (1.38*10-23 J/K)

q: Electron charge (1.6*10-19 C)

## II.2.1.2 Real model (5P parameters)

This model includes A $I_{Ph}$ current generator arranged in parallel with a diode, accompanied by a series resistor $R_S$ and a parallel (or shunt) resistor $R_P$. This is represented by the equivalent diagram in Figure (II.2).

The diagram shows the current generated by a single cell, a module made up of several cells, or a field made up of several modules. The relationship that defines the current generated by a photovoltaic module made up of Ns cells in series, as a function of the voltage V across its terminals [8].

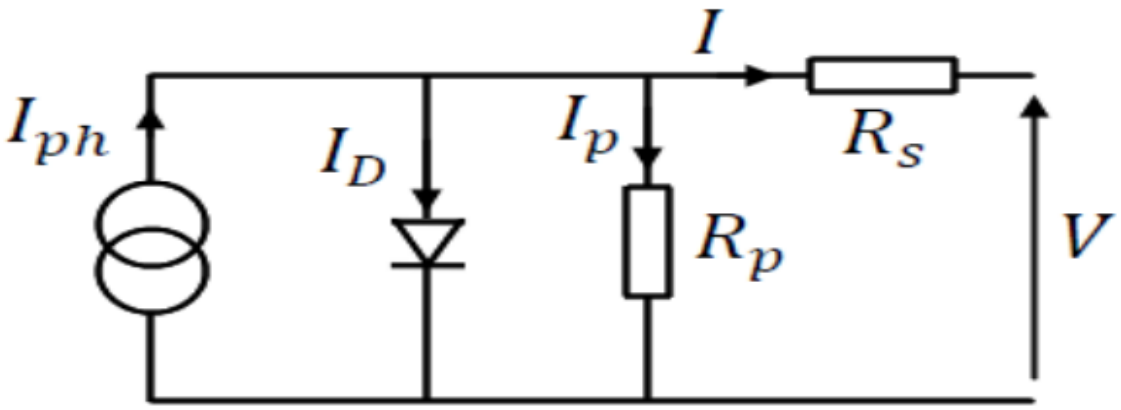


Figure (II.2): real photovoltaic cell model [20]

I: Current delivered by the cell.

V: Voltage across the cell.

$I_d$: Diode current

$I_{ph}$ : Current picture, depending on irradiation intensity

$I_p$: Current from parallel resistor

$I_0$: Diode saturation current, influenced by temperature

$R_p$: Parallel resistance, corresponding to the parallel admittance of the current generator.

$R_s$: Series resistance, representing the ohmic losses of the material and contacts

Equation used for this model:

$$I_{pv} = I_{ph} - I_d - I_p \quad \text{(II.5)}$$

Equation current of panel [39]

$I_{ph} = I_{ph} - I_0 [( \exp (\frac{V+Rs\ I}{n\ Vt}) -1 )]-(\frac{V+Rs\ I}{Rp})$. (II.6)

$I_P = (\frac{V+Rs\ I}{Rp})$. (II.7)

## II.3 DC/DC converter modeling

### II.3.1 Electric model converter

Often referred to as a parallel chopper, the boost converter is a switching power supply that raises the DC output voltage from a DC input voltage.

power source that, as the name suggests, converts a DC input voltage into a higher DC output voltage [8].

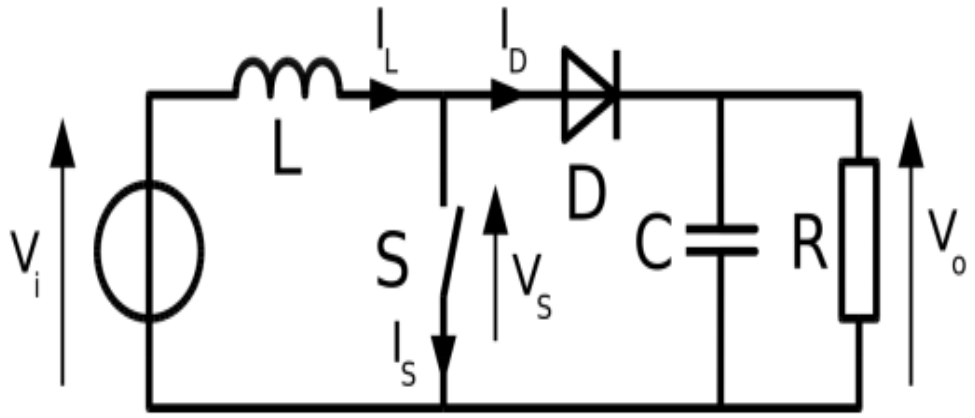


Figure(II.3) : electrical model of boost converter [8]

- When switch (S) is closed:[31]

$V_{pv} = L \frac{dIL}{dt}$ (II.8)

$0 = C \frac{dVdc}{dt} + I_{dc}$ (II.9)

- When switch (S) is opened:

$V_{pv} = L \frac{dIL}{dt} + V_{dc}$ (II.10)

$$I_L = C\frac{dVdc}{dt} + I_L \quad \text{(II.11)}$$

We can represent the converter using a single system of equations if we assume that u=1 when switch S is closed and u=0 when S is open. We presume the switches are flawless [31]

$$V_{pv} = L\frac{dIL}{dt} + V_{dc}*(1-u) \quad \text{(II.12)}$$

$$(1-u)I_L = \frac{dVdc}{dt} + I_{dc} \quad \text{(II.13)}$$

output voltage depends on the input voltage and duty cycle α in mean values. Equation (II.14) gives its expression. The duty cycle α is then adjusted to control the output voltage. [31]

$$V_{dc} = \frac{1}{1-\alpha} V_{pv} \quad \text{(II.14)}$$

$$I_{dc} = (1-\alpha) I_L \quad \text{(II.15)}$$

### II.3.2 Boost Converter Characteristic

The diagram illustrates a converter: voltage pulses between 0 and Ua.

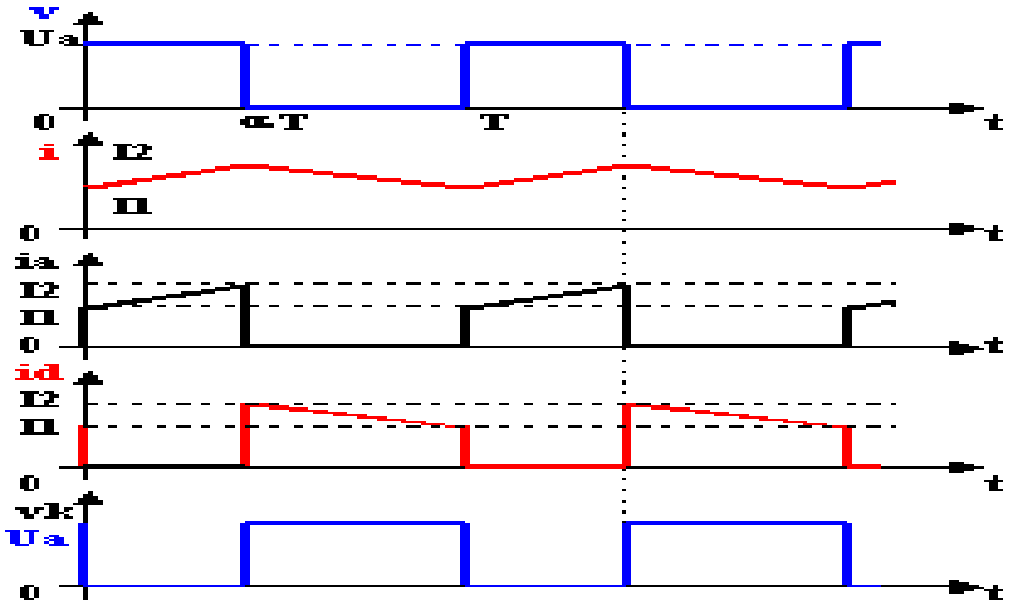


Figure(II.4): Boost Converter Characteristic

## II.4 DC/AC Modeling inverter

### II.4.1 Electrical model

To illustrate its function in the power conversion system, the inverter is modeled. To make system analysis easier, a simplified representation is used, which still captures the device's key functionalities.

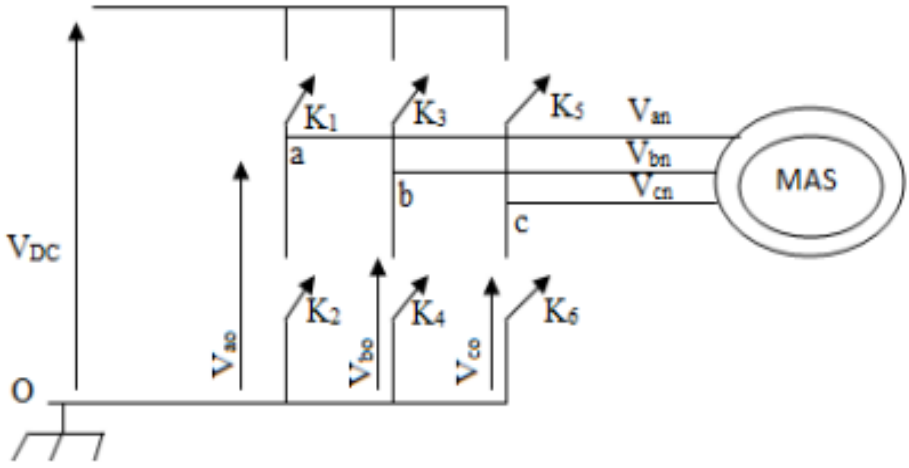


Figure (II.5): Inverter circuit connected to machine [31]

### II.4.2 Equation used

-These relationships are used to determine the compound voltages Vab, Vbc, and Vca.[31]

- $V_{ab} = V_{a0} + V_{b0} = V_{a0} + V_{b0}$
- $V_{bc} = V_{b0} + V_{c0} = V_{b0} + V_{c0}$ (II.16)
- $V_{ca} = V_{c0} + V_{0a} = V_{c0} + V_{a0}$

With: Vao, Vbo, and Vco are the continuous voltages at the inverter's input. For these final voltages, we used point "O" as a reference. The CHARLE relation produces the following three continuous input voltages:[31]

$-V_{a0} = V_{an} - V_{n0}$

$-V_{b0} = V_{bn} - V_{n0}$ (II.17)

$-V_{c0} = V_{cn} - V_{n0}$

The load's or the inverter's output's phase voltages are Van, Vbn, and Vcn, while the load's neutral voltage with respect to point "O" is Vno.[31]

The load is assumed to be balanced:[31]

$$V_{an} + V_{bn} + V_{cn} = 0 \quad \text{(II.18)}$$

We will remplaced equation (II.17) in equation (II.16) we get :[31]

$$\begin{cases} \text{Van} = \frac{1}{3}(2\text{Va0} + \text{V b0} + \text{VC0}) \\ \text{Vbn} = \frac{1}{3}(2\text{Vb0} - \text{V a0} - \text{VC0}) \\ Vcn = \frac{1}{3}(2Vc0 - Vb0 - Vc0) \end{cases} \quad \text{(II.19)}$$

-Assuming :[31]

$$\begin{cases} Va0 = VDC * S1 \\ Vb0 = VDC * S2 \\ Vc0 = VDC * S3 \end{cases} \quad \text{(II.20)}$$

-intercepter (ki) status :[31]

S(i)=1, ki is ferme

S(i)=0,ki is open

So :

$$\begin{bmatrix} Va \\ Vb \\ VC \end{bmatrix} = \frac{U0}{3}\begin{bmatrix} 2 & -1 & -1 \\ -1 & 2 & -1 \\ -1 & -1 & 2 \end{bmatrix}\begin{bmatrix} S1 \\ S2 \\ S3 \end{bmatrix} \quad \text{(II.21)}$$

- Va Vb Vc : simple voltages
- U0 : compound voltag

## II.5 Asynchronous motor modeling

Given the non-linearity of the electrical and magnetic circuits found in the different parts of the motor as a result of resistances, inductances, and metallic
and magnetic components, we added some simplifying for this asynchronous motor mathematical model [40]. In the slots, the coils of the three phases are symmetrically and geometrically well-spaced.

-Additionally, winding resistances are independent of operating temperature.

It is believed that the current density is constant across the conductor cross-section.

The skin effect is ignored, and the air gap thickness is constant. [40]

-On both the stator and rotor, the magnetic circuit is laminated, and saturation is minimal.

-To generate the rotating field, the stator and rotor currents generate magnetomotive forces that are distributed in the air gap in a sinusoidal manner [40].

### II.5.1 Electrical model

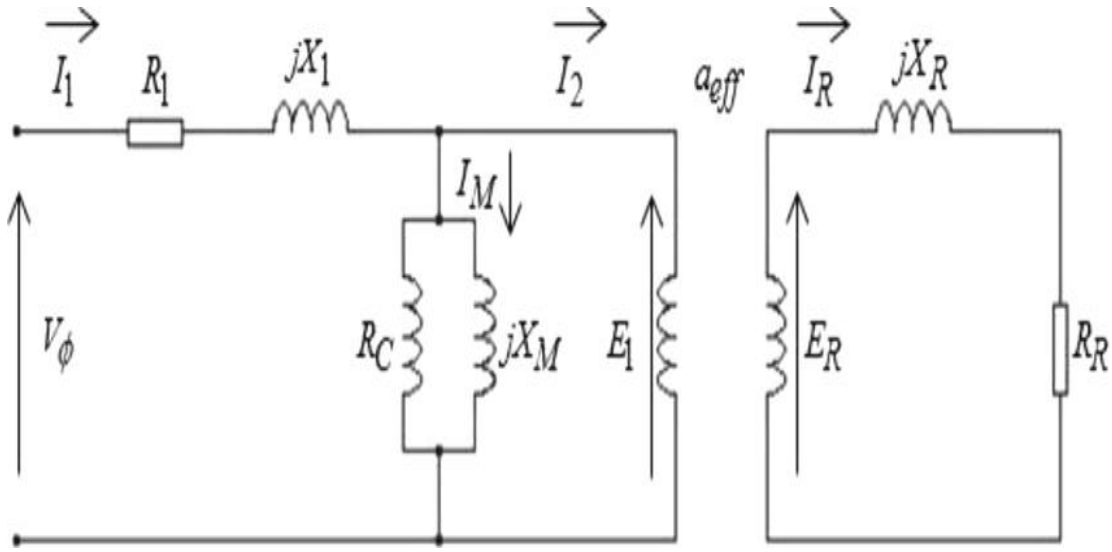


Figure(II.6) : Electrical model [39]

### II.5.2 Equation used

$$Zr = R1 + J(x1 + Xr) \quad \text{(II.22)}$$

- Slip:

$$S=\frac{Ns-Nr}{Ns} \quad \text{(II.23)}$$

- Ns: synchronism speed
- Nr: rotor speed

### II.5.2.1 Electrical equation

-At stator index 's' and rotor index 'r', the mesh law equations are used to relate the motor parameters such as resistances, currents, and flux linkages to the applied electrical voltages. These equations, based on Kirchhoff's voltage law, describe how the voltage is distributed between ohmic losses in the windings and the time-varying magnetic flux. This relationship is fundamental for understanding the dynamic behavior of the asynchronous machine and serves as the basis for building accurate mathematical models. Moreover, it plays a key role in the implementation of advanced control strategies, particularly vector control, where precise tracking of flux and torque components is essential for efficient and decoupled operation.[40]

- In stator [40]

$$V_{sa} = R_s I_{sa} + \frac{d\Phi\, sa}{dt}$$

$$V_{sb} = R_s I_{sb} + \frac{v\, d\Phi\, sb}{dt} \quad \text{(II.24)}$$

$$V_{sc} = R_s I_{sc} + \frac{d\Phi\, sc}{dt}$$

- In rotor :[40]

$$V_{ra} = R_r I_{s\,ra} + \frac{d\Phi ra}{dt}$$

$$V_{rb} = R_r I_{rb} + \frac{d\Phi rb}{dt} \quad \text{(II.25)}$$

$$V_{rc} = R_r I_{rc} + \frac{d\,\Phi rc}{dt}$$

Matrix form of equations (II.24) and (II.25) [40]:

- In stator:

$$\begin{bmatrix} Vsa \\ Vsb \\ VsC \end{bmatrix} = \begin{bmatrix} Rs & 0 & 0 \\ 0 & Rs & 0 \\ 0 & 0 & Rs \end{bmatrix} \begin{bmatrix} Isa \\ Isb \\ IsC \end{bmatrix} + \frac{d}{dt} \begin{bmatrix} \Phi sa \\ \Phi sb \\ \Phi sc \end{bmatrix} \quad \text{(II.26)}$$

- In rotor:

$$\begin{bmatrix} Vra \\ Vrb \\ VrC \end{bmatrix} = \begin{bmatrix} Rr & 0 & 0 \\ 0 & Rr & 0 \\ 0 & 0 & Rr \end{bmatrix} \begin{bmatrix} Ira \\ Irb \\ IrC \end{bmatrix} + \frac{d}{dt} \begin{bmatrix} \Phi ra \\ \Phi rb \\ \Phi rc \end{bmatrix} \quad \text{(II.27)}$$

**II.5.2.2 Magnetic equations**:[40]

- In stator:

$$[\varphi sabc] = [Ls][Isabc] + [Msr][Irabc] \quad \text{(II.28)}$$

- In rotor:

$$[\varphi rabc] = [Lr][Irabc] + [Mrs][Isabc] \quad \text{(II.29)}$$

- [Ls]: stator inductance matrix
- [Lr]: rotor inductance matrix
- [Msr]: inductance matrix of the magnetic coupling between stator and rotor

**II.5.2.3 Mechanical equation:[40]**

$$T_{em} = Tr + J + \frac{d\omega}{dt} + f\,\omega \quad \text{(II.30)}$$

- $T_{em}$ :The motor's electromagnetic torque
- $T_r$ : the load resisting torque
- J:the moment of inertia of the rotor and all rotating parts.
- F: the coefficient of friction.
- ω: rotational speed of the rotor, typically expressed in rad/s

**II.5.3 Park transformation:**

-Time-varying three-phase (abc) quantities are transformed into two-axis (d-q) components in a rotating reference frame using the Park transformation. By making their differential equations simpler, this conversion makes mathematical modeling of electrical machines easier. Variables like currents, voltages, and flux linkages consequently become almost constant in steady-state conditions, making analysis and control simpler, especially in sophisticated techniques like Field-Oriented Control (FOC).

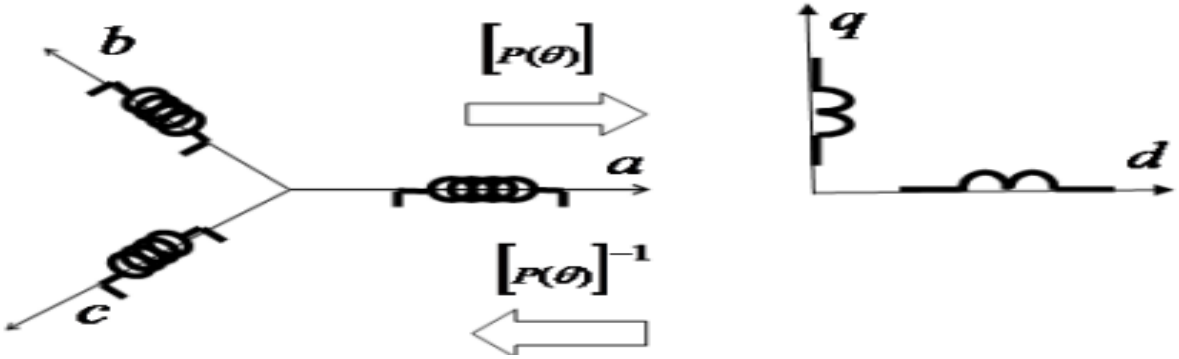


Figure (II.8): Park transformation [40]

- The matrix used for park transformation:

$$(TP)0 = \sqrt{\frac{2}{3}}\begin{bmatrix} \cos(\theta) & \cos(\theta - \frac{2\pi}{3}) & \cos(\theta - \frac{4\pi}{3}) \\ -\sin(\theta) & -\sin(\theta - \frac{2\pi}{3}) & -\sin(\theta - \frac{4\pi}{3}) \\ \frac{1}{\sqrt{2}} & \frac{1}{\sqrt{2}} & \frac{1}{\sqrt{2}} \end{bmatrix} \quad \text{(II.31)}$$

- Equation of asynchronism motor in biphasic (d ,q) :[31]
- Stator [31]

$$-V_{sd} = R_S I_{sd} + \frac{d\Phi sd}{dt} - w_s \Phi sq \quad \text{(II.32)}$$

$$-V_{sq} = R_S I_{sq} + \frac{d\Phi sq}{dt} - w_s \Phi sd$$

- Rotor:[31]

$$0 = R_r I_{rd} + \frac{d\Phi rd}{dt} + (w_s - w)\,\Phi rq \quad \text{(II.33)}$$

$$0 = R_r I_{rq} + \frac{d\Phi rq}{dt} + (w_s - w)\,\Phi rd$$

Definition of element:[31]

- $V_{sd}$ , $V_{sq}$ : direct stator voltage and quadratic
- $I_{sd}$, $I_{sq}$ : direct stator current and quadratic
- Φrd , Φrq: direct rotor flux and quadratic
- Φsd , Φsq: direct stator flux and quadratic
- ws, wr: Pulsation of stator and rotor quantities [rd/s].
- $w = p.\Omega = w_s - w_r$ : mecanique pulsation

➢ Stator and rotor fluxes are expressed in PARK's reference frame in function of current by the following relation [31]:

$$\begin{bmatrix} Qsd \\ Qsq \\ Qrd \\ Qrq \end{bmatrix} = \begin{bmatrix} Ls & 0 & M & 0 \\ 0 & Ls & 0 & M \\ M & 0 & Lr & 0 \\ 0 & M & 0 & Lr \end{bmatrix} \cdot \begin{bmatrix} Isd \\ Isq \\ Ird \\ Irq \end{bmatrix} \quad \text{(II.34)}$$

- $L_S = ls + M$ : Cyclic stator inductance.
- $L_r = l_r + M$: Cyclic stator inductance.
- ls : Stator leakage inductance.
- $l_r$ : rotor leakage inductance.
- M : Mutuel inductance

- Electromagnet torque [31] :

$$Te = P\frac{M}{Lr}\,(\Phi rd\ Isq - \Phi rq\ Isd) \quad \text{(II.35)}$$

- Mechanical equation [31]:

$$J\frac{d.\Omega}{dt} = Te - Tr - J\,\Omega \qquad (II.36)$$

### II.5.4 Indirect Field-Oriented Control of Induction Motor (IFOC):

-The vectorial control of the asynchronous machine primarily consists of controlling the flux and couple as is naturally the case for a continuous current machine, as well as dynamically and separately (in a manner decoupled) [31].

- Therefore, vectorial control entails selecting an axis system (d, q) in order to control the flow by one current component (Isd) and couple it by another component (Isq). Thus, it is possible to create a law that guarantees the breakup of the couple and the flow [31].

- In control we use the following equation:
- flux:

$$\begin{cases} \Phi rd = \Phi r \\ \Phi rq = 0 \end{cases} \qquad (II.37)$$

- **Equation of tension :** [31]
- Stator:

$$\begin{cases} Vsd = RS\,Isd + \frac{d\Phi sd}{dt} - ws\,\Phi sq \\ Vsq = RS\,Isq + \frac{d\Phi sq}{dt} - ws\,\Phi sd \end{cases} \qquad (II.38)$$

$$\psi ds = Ls\,Ids + Lm\,Idr \qquad (II.39)$$

$$\psi qs = LIqs + LmIqr \qquad (II.40)$$

- **Flux Equation**:[31]

$$\Phi s = Ls\,Isq + M\,Irq \qquad (II.41)$$

$$\Phi sd = Ls\,Isd + M\,Ird \qquad (II.42)$$

$$\Phi r = M\,Isd + Lr\,Isd \qquad (II.43)$$

$$0 = M\,Isq + Lr\,Irq \qquad (II.44)$$

- Rr: rotor resistance
- Lr: rotor inductance

## Torque equation :

$$Te = \frac{3}{2}\frac{p}{2}\frac{Lm}{Lr}\ \Phi r\ isq \quad \text{(II.45)}$$

- Te : electromagnet torque
- p: number of poles
- Lm: Mutual Inductance Represents the magnetic coupling between the stator and rotor windings.
- Lr: Rotor Inductance
- isq : Quadrature Axis Current Component

**Slip speed :**

$$Wsl = \frac{Rr}{Lr}\frac{Isq}{Isd} \quad \text{(II.46)}$$

$$Ws = Wr + Wsl \quad \text{(II.47)}$$

## II.6 centrifugal pump modeling

- Thus, the electrical model of the pump system is essentially the asynchronous motor model because the pump is mechanically coupled to the motor shaft. Their difference lies primarily in the mechanical conversion aspect, not in their electrical representation.

### II.6.1 Pump parameters and equations

#### II.6.1.1 Head(h)

**General Formula for Pump Head Calculation:**

$$Hm = Hg + Hp + Hf \quad \text{(II.48)}$$

Hg: Geometric head – the vertical height between the suction surface and the discharge point.

- Hp: Pressure head – the difference in pressure between the pump's outlet and inlet, converted into meters of water column.
- Hf: Friction head losses –losses due to friction in pipes, fittings, valves, etc.

$$H = H_m \times \left(\frac{N}{Nm}\right)^2 \quad \text{(II.49)}$$

H: Developed head (m)

$H_m$: Reference head (m)

N: Actual speed (rpm)

$N_m$: Reference speed (rpm)

### II.6.1.2 Flow Rate (Q)

$$\Phi = \Phi_m \times \left(\frac{N}{Nm}\right)^2 \quad \text{(II.50)}$$

$\Phi$: Actual flow rate ($m^3/s$)

$\Phi r_m$: Reference flow rate ($m^3/s$)

$Ns$ : Actual speed (rpm)

$N_m$: Reference speed (rpm)

### II.6.1.3 Hydraulic Power (P)

$$P = \rho \times g \times Q \times H \quad \text{(II.51)}$$

P: Hydraulic power (W)

ρ: Density of water ($kg/m^3$), typically 1000 $kg/m^3$

g: Gravitational acceleration (9.81 $m/s^2$)

$\Phi$: Flow rate ($m^3/s$)

H: Head (m)

### II.6.1.4 Resistive torque

$$\omega = \frac{2\Pi n}{60} \quad \text{(II. 52 )}$$

$$T_r = \left(\frac{P}{\omega}\right) \quad \text{(II.53)}$$

Tr : Load torque (Nm)

P: Hydraulic power (W)

ω: Angular speed (rad/s)

N: Actual rotational speed (rpm)

## II.7Techniques Mppt

### II.7.1 Perturb and Observe (P&O)

the Perturb and Observe (P&O) algorithm is a simple and commonly used method for maximizing the power delivered by a photovoltaic system. It works by slightly modifying the system voltage or current, then observing the power variation.

-If the power increases after the modification, the algorithm continues in the same direction.

-If the power decreases, it reverses the direction of the chang

This process repeats itself in a loop, causing the operating point to oscillate around the maximum power point (MPP).

- Perturb and Observe (P&O) algorithm, which is frequently used for Maximum Power Point Tracking (MPPT) in photovoltaic systems, is shown in the following figure show as working.

#### II.7.1.1 How it work

- $\Delta p > 0$ and $\Delta V > 0$ : Increase voltage
- $\Delta p > 0$ and $\Delta V < 0$: decrease voltage
- $\Delta p < 0$ and $\Delta V > 0$ : Increase voltage
- $\Delta p < 0$ and $\Delta V < 0$ : : decrease voltage

#### II.7.1.2 Diagramme used for this methode

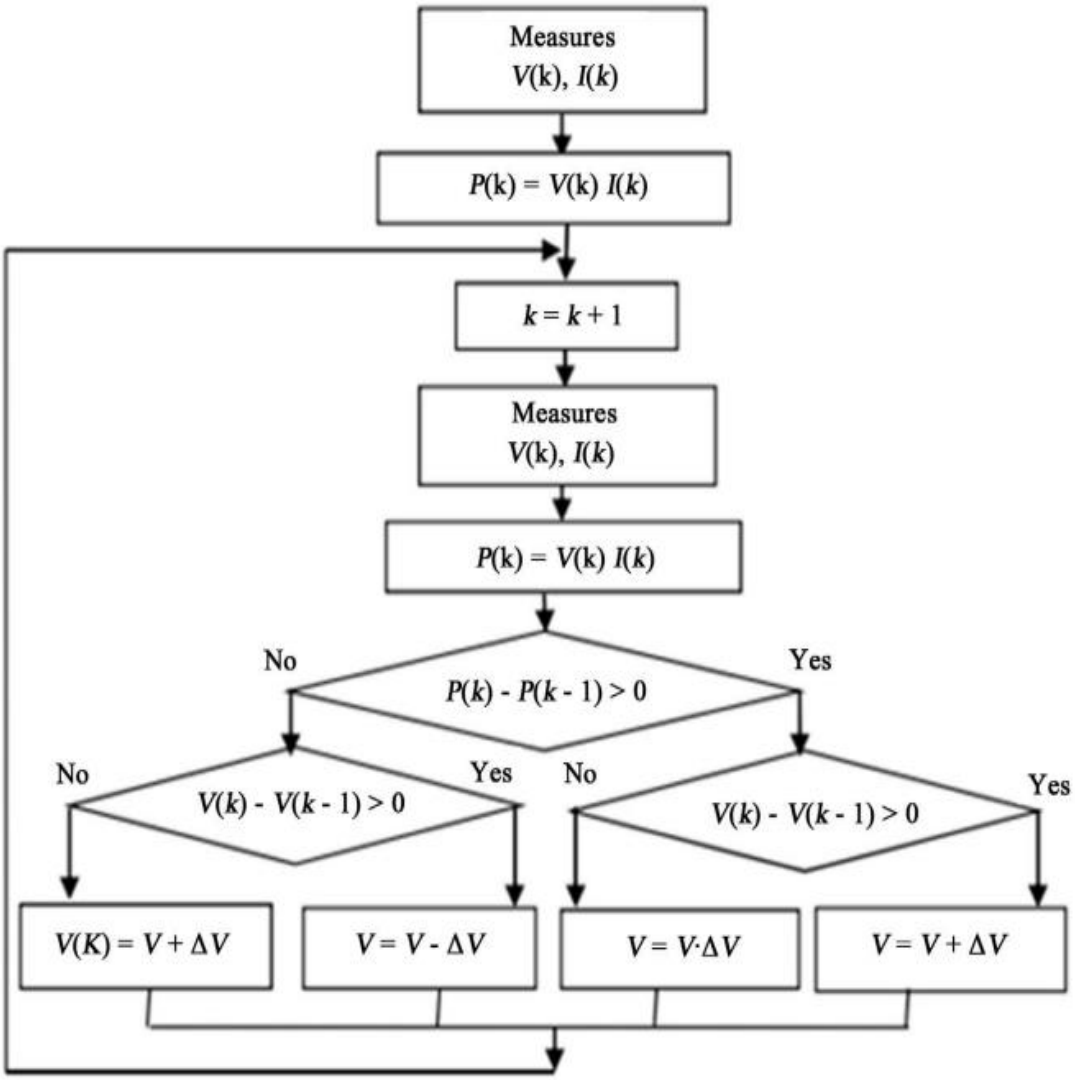


Figure(II.9): Perturb and Observe organigrame[53]

- diagram below illustrates the operating principle of the Perturb and Observe (P&O) algorithm used
- in MPPT, with the I–P curve serving as a key reference for analyzing its tracking performance ″.

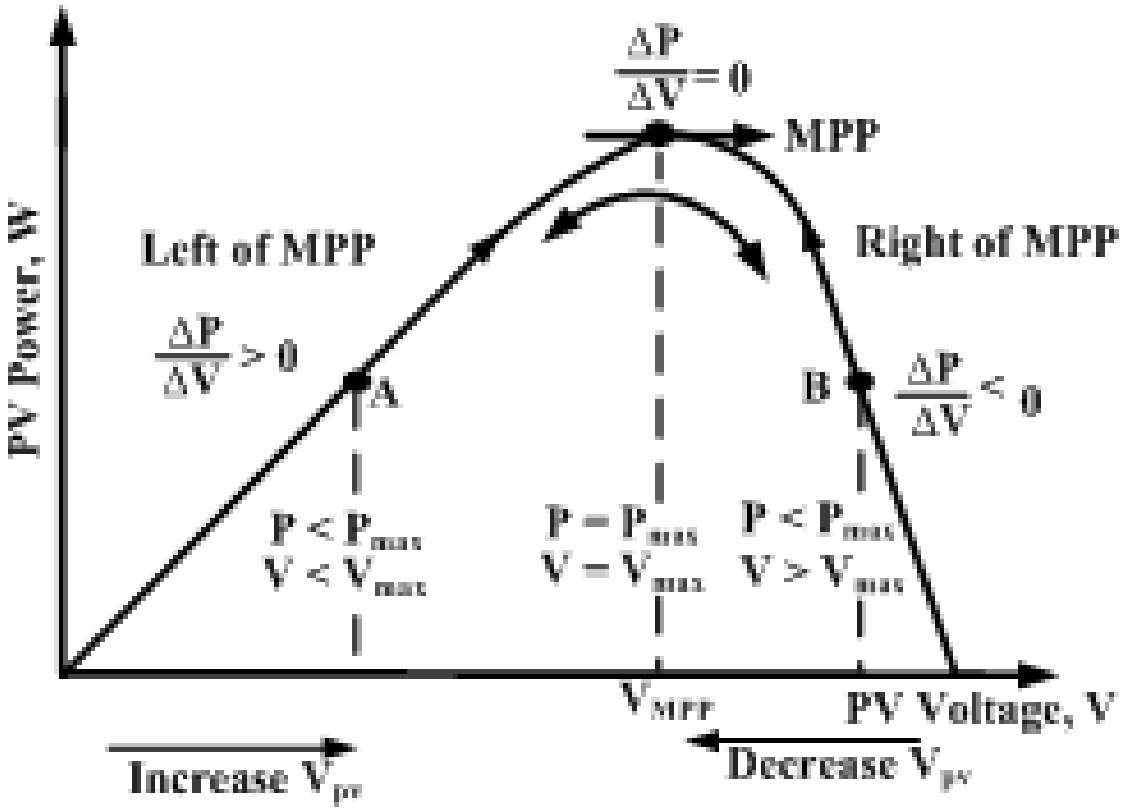


Figure (II.10): Perturb and Observe behavior [54]

### II.7.1.3 Advantage and disadvantage of this method

- **Advantages**

- The P&O algorithm doesn't require a thorough understanding of the PV module's characteristics and is very easy to implement. For standalone systems or embedded systems in PV-based pumping, this makes it ideal**.[44]**
- Low Price and Easy Computation The system cost is kept to a minimum because doesn't require sophisticated calculations or sensors. It functions well with basic
- microcontrollers.[45]
- Sufficient Performance in Consistent Situations The algorithm tracks the MPP with a respectable level of accuracy when the temperature and irradiance remain constant.[46]

- **Disadvantages**

- Movement Around MPP Even in stable conditions, there is a constant oscillation around the maximum power point, which results in minor but noticeable energy losses. This is a major disadvantage.[47]
- Poor Performance in Conditions That Change Quickly When the irradiance fluctuates rapidly, the P&O algorithm may interpret the resulting power change as the result of its own perturbation, which could lead to incorrect decisions.[48]

### II.7.2 Incremental Conductance INC method

The algorithm continuously measures the incremental conductance ($\frac{dI}{dV}$)

and the instantaneous conductance $\frac{I}{V}$ to determine the position of the operating point relative to the MPP.

#### II.7.2.1 How it works

- Measure current I and voltage V from the PV array.
- Calculate $\Delta I$ and $\Delta V$ (the changes since the last sample).
- Compute $\frac{dI}{dV} = \frac{\Delta I}{\Delta V}$
- compare it with $\frac{I}{V}$
- If $\frac{dI}{dV} = -\frac{I}{V}$ : the système is in the mpp
- If $\frac{dI}{dV} > -\frac{I}{V}$ : increase the voltage
- If $\frac{dI}{dV} < -\frac{I}{V}$ : decrease the voltage

### II.7.2.2 Diagram used for this method

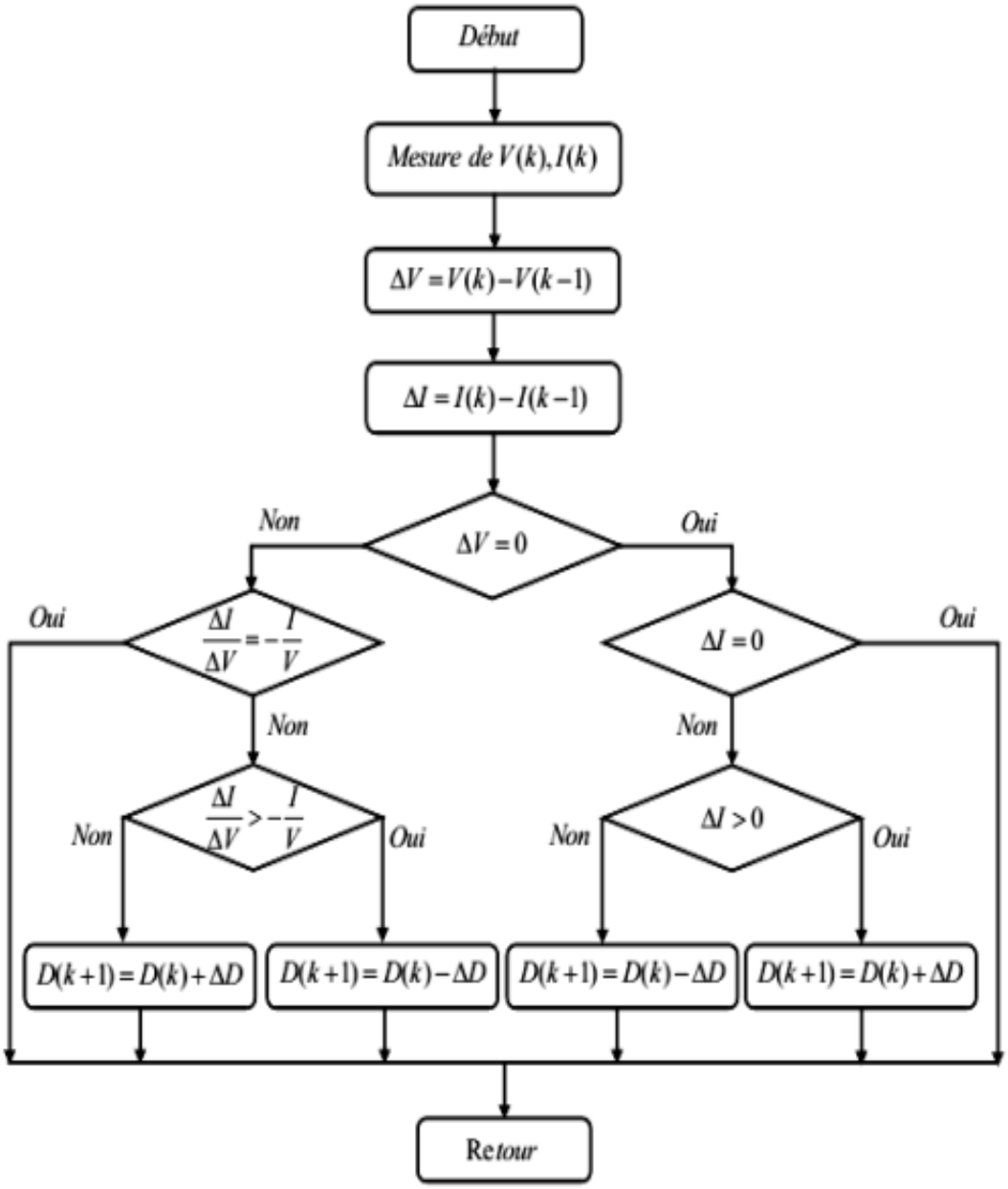


Figure (II.11): Incremental Conductance (INC) diagram

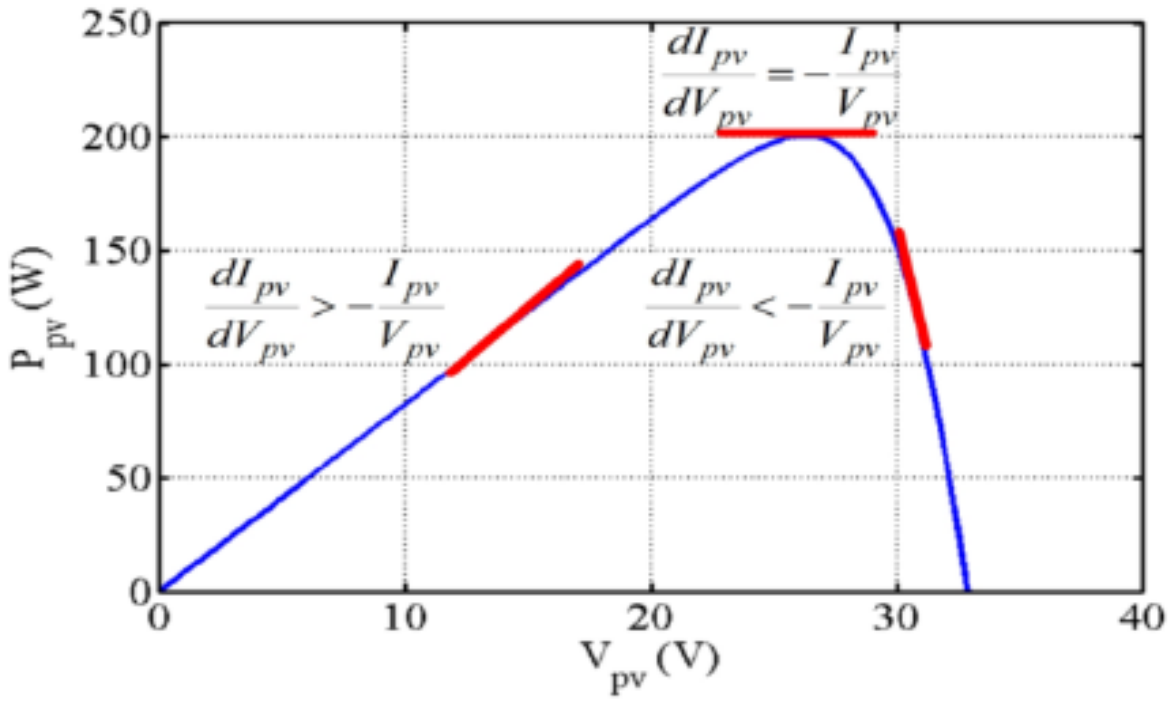


Figure(II.12): Incremental Conductance (INC) behaviors[43]

### II.7.2.3 Advantage and disadvantage of this method

- **Advantages**

- Higher Accuracy Near MPP The INC algorithm can precisely determine the MPP by comparing the instantaneous conductance (I/V) with the incremental conductance (ΔI/ΔV), which reduces oscillations around the MPP.[49]
- Improved Adaptability to Changing Circumstances The INC algorithm avoids the confusion between natural variations and perturbations and reacts more efficiently to rapid changes in temperature or irradiance than P&O.[50]
- Flexibility in Response to Nonlinear PV Features The INC approach can more precisely adjust to the nonlinear behavior of PV modules because it is based on differential relationships.[51]

- **Disadvantage**

- Enhanced Intricacy Compared to P&O, the algorithm's implementation is more complicated because it necessitates the computation of derivatives (ΔI ΔV)[50].

- An increased computational burden The INC method requires more processing power from the controller since The INC method requires more processing power from the controller since [51]
- Noise Sensitivity in Measurements If the voltage and current sensors are inaccurate or the measurements are noisy, calculating $\Delta I$ and $\Delta V$ may introduce errors. Erroneous tracking or instability may result from this.[52]

## II.8 Conclusion

Photovoltaic pumping systems represent a sustainable and autonomous solution for water supply in remote areas, where conventional grid access is unavailable or unreliable. Through accurate modeling of each component ranging from the PV generator to the electric motor and hydraulic pump it becomes possible to predict system behavior, evaluate performance under varying environmental conditions, and design effective control strategies. The electrical models presented in this chapter lay the groundwork for optimizing the entire PV pumping system, ensuring efficient energy conversion and reliable water delivery. Such models are essential for enhancing the design, improving operational reliability, and promoting the broader adoption of PV-powered water pumping solutions.

# Chapter III
# PV
# Pumping
# Simulink

## III.1 Introduction

To validate its performance for various environmental and operational conditions. The system componentslike the PV generator, DC-DC boost converter, MPPT controller, inverter, induction motor, and the pumpwere modelled and simulated using MATLAB/Simulink.

Two of the MPPT control methods, Perturb and Observe (P&O) and Incremental Conductance (INC), were implemented in order to obtain maximum possible power from the PV array under varied solar irradiance. The motor control was also performed with the use of the Indirect Field-Oriented Control (IFOC) method in order to yield efficient and stable induction motor performance.

The simulation output provides some observations of the electrical and mechanical system behavior and places particular emphasis on efficiency in power tracking, voltage and current waveforms, response to torque, motor speed regulation, and total pumping performance. Comparative analysis between the two MPPT schemes is also conducted to determine the optimal practice for practical applications.

## III.2 System part Simulation

### III.2.1 Panel modeling in MATLAB \ SIMULINK

The image illustrates the modeling of a photovoltaic (PV) panel in MATLAB/Simulink. The simulation includes input ports for solar irradiance and ambient temperature, allowing dynamic analysis of the panel's performance under varying environmental conditions

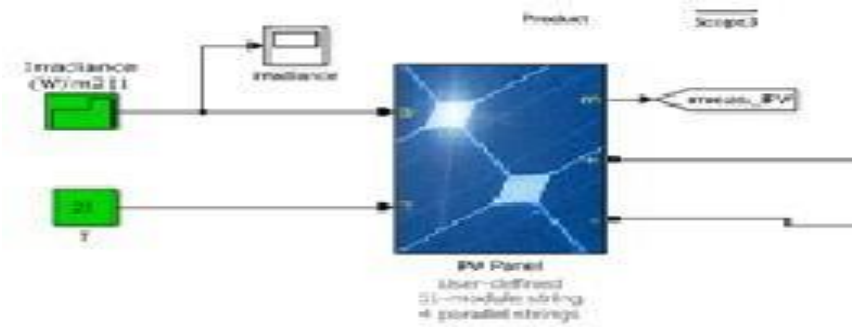

Figure (III.1): Panel modeling in MATLAB \ SIMULINK

Table III.1: panel Technical

| Parameter | Value |
|---|---|
| Parallel strings | 4 |
| Series-connected modules per string | 11 |
| Maximum Power (W) | 270.116 |
| Open circuit voltage $V_{oc}$ (V) | 37.9 |
| Voltage at maximum power point $V_{mp}$ (V) | 30.8 |
| current at maximum power point $I_{mp}$ (A) | 8.77 |
| Short-circuit current $I_{sc}$ (A) | 9.07 |
| Temperature coefficient of $V_{oc}$(%/°C) | -0.4 |
| Temperature coefficient of $I_{sc}$ (%/°C) | 0.05 |
| Cells per module (Cell number) | 60 |

### III.2.1.1 characteristic of a panel

The figure (III.2) (III.3) show characteristic (I-V) (P-V) inSTC condition(1000w/m2; 25°C)

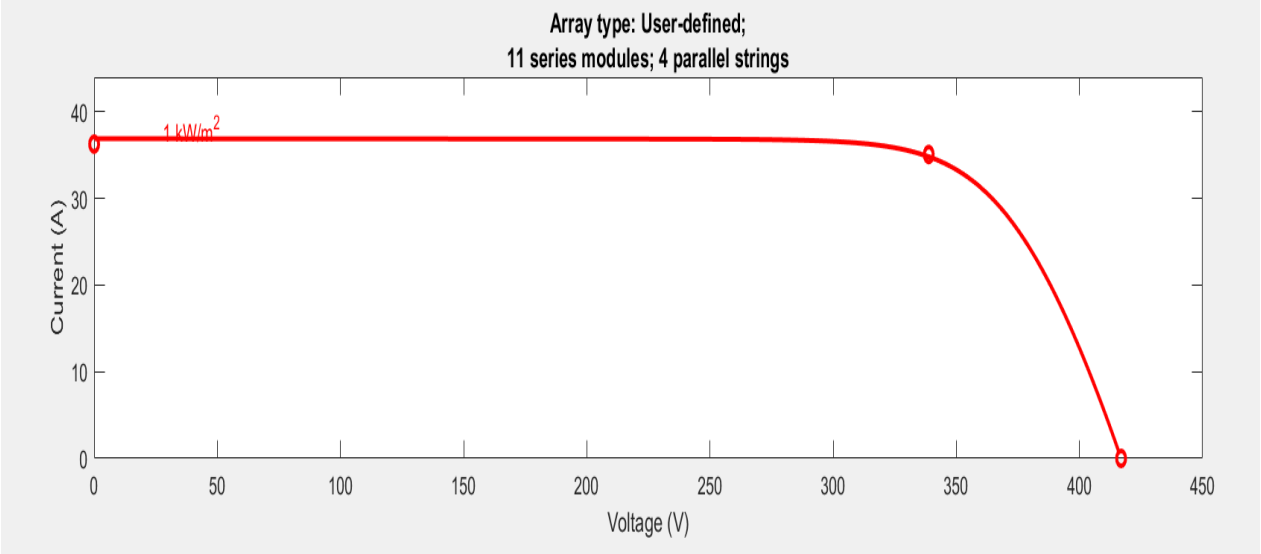


Figure (III.2): (I-V) characteristic ofPV generator

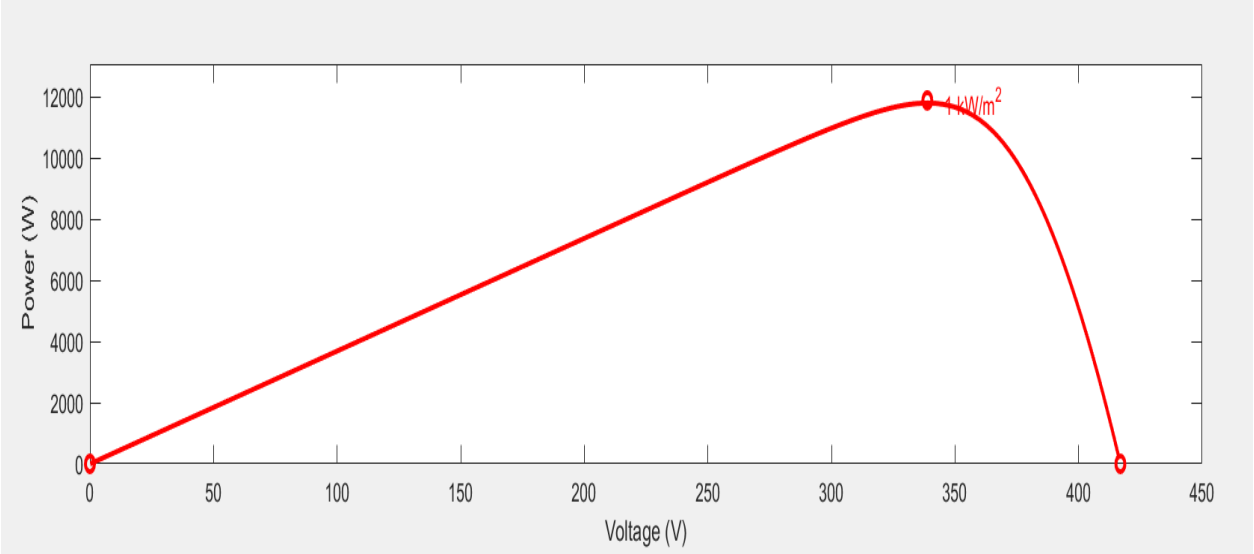


Figure (III.3): (P-V) characteristic of a panel

### III.2.1.2 Variation effectof temperaturein panel

The figure (III.4) (III.5) show characteristics (current–voltage and power–voltage curves) were recorded under constant solar irradiance and varying ambient temperature conditions.

Where :E=1000W/m2; Ta= [25 50 40]C°

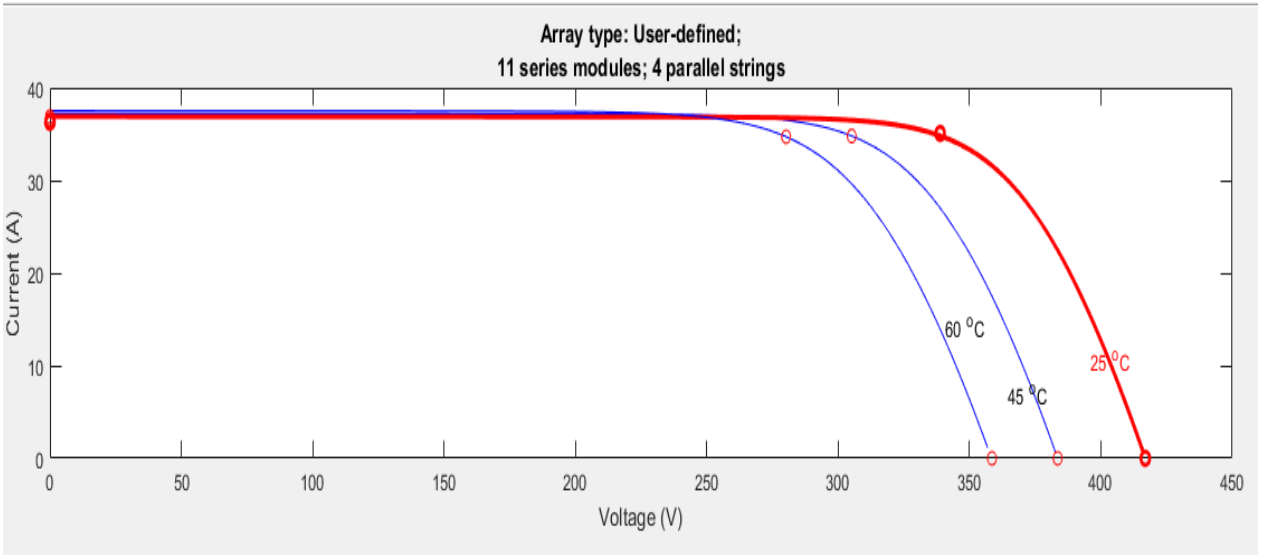


Figure (III.4): Temperature effect in (I-V) characteristic

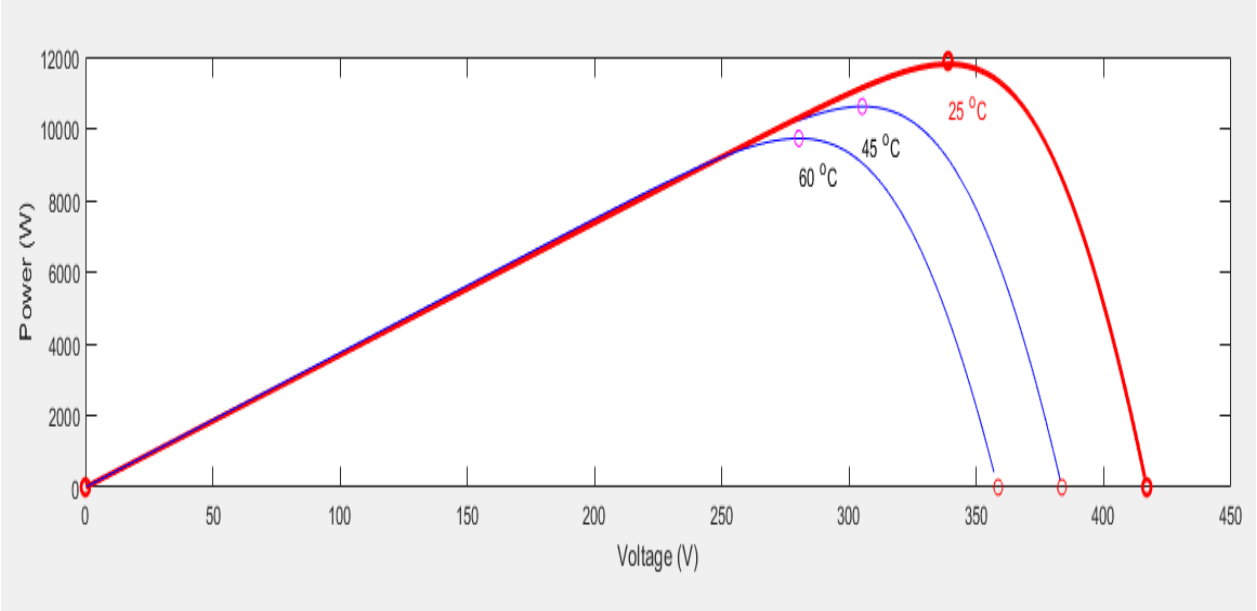


Figure (III.5):Temperatureeffect in (P-V) characteristic

- PV performance decreases with heat, so thermal effects must be considered in PV system design
- Higher temperatures cause more electrons to recombine, which lowers voltage output; current is less affected. This behavior is common for solar panels.

### III.2.1.3 PV Performance Under Fluctuating Irradiance

In the figure bellow (I-V)(P-V)werepresent the Impactof Varying Solar Irradiance on Photovoltaic Panel Performance under Constant Temperature Conditions

T=25c° I=[0.6kw/m$^2$, 0.8kw/m$^2$, 1kw/m$^2$]

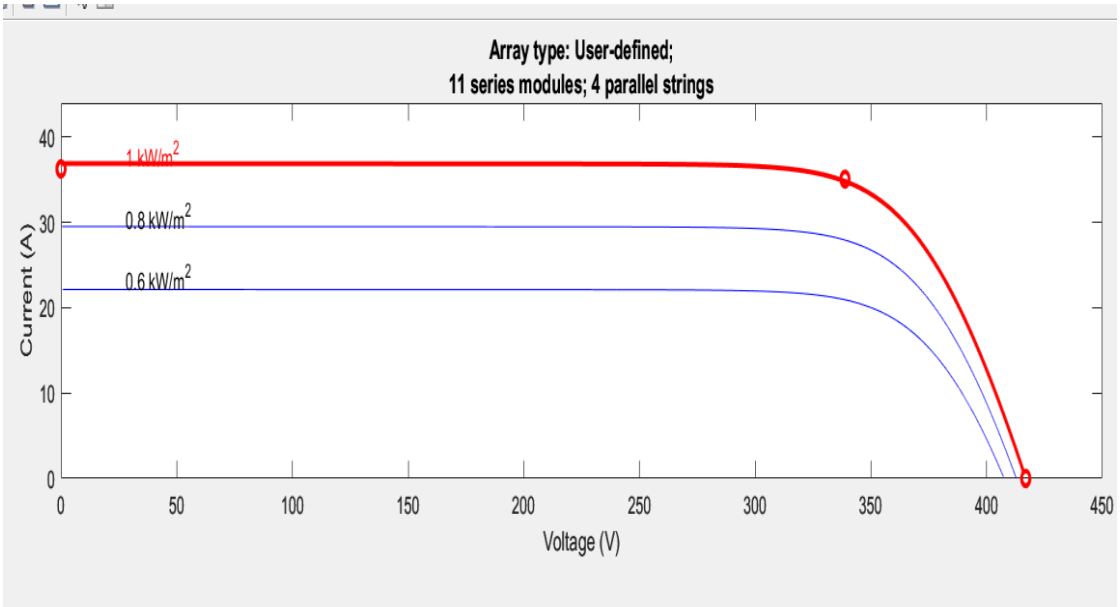


Figure (III.6): irradiation effect in (I-V) characteristic.

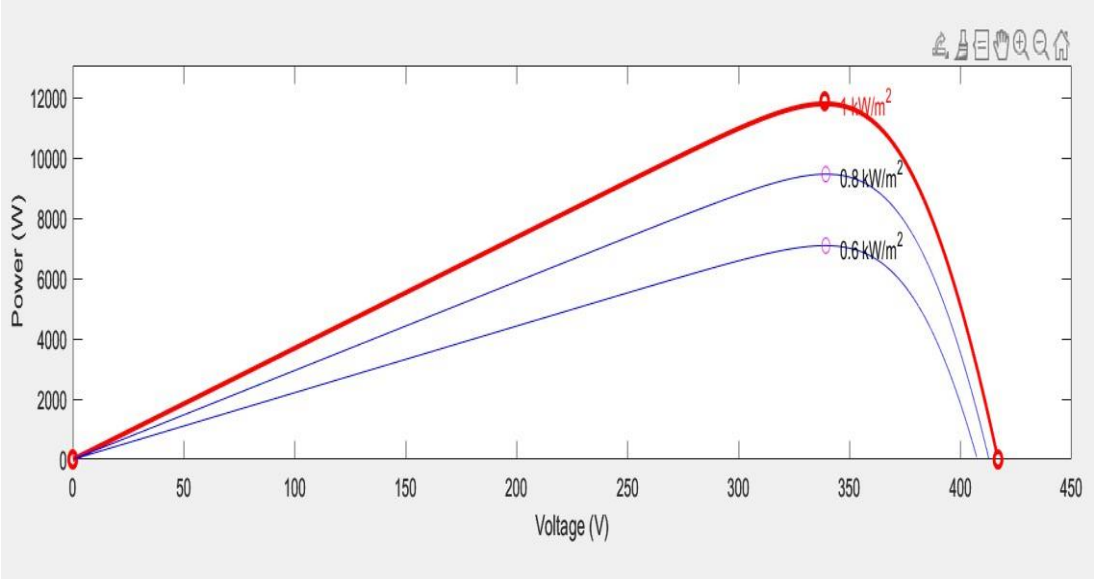


Figure (III.7): irradiation effect in (P-V) characteristic of a PVgenerator.

- With current rising with increasing irradiance, voltage staying constant up to the open-circuit point (35–40 V), and a power peak before decreasing, the graph displays the I–V characteristics of a user-defined solar module under various irradiance levels (1, 0.8, and 0.6 kW/m²)

### III.2.2 Boost DC/DC converter parameters

Table(III.2):Boost DC-DC converter parameters

| C1=C2(F) | R(ohm) | L(H) |
|---|---|---|
| 6*10^-4 | 30 | 3*10^-3 |

### III.2.2.1 Boost DC\DC converter modeling in MATLAB \SIMULINK

Following figure show simulation of DC /DC converter controlled by Mppt:

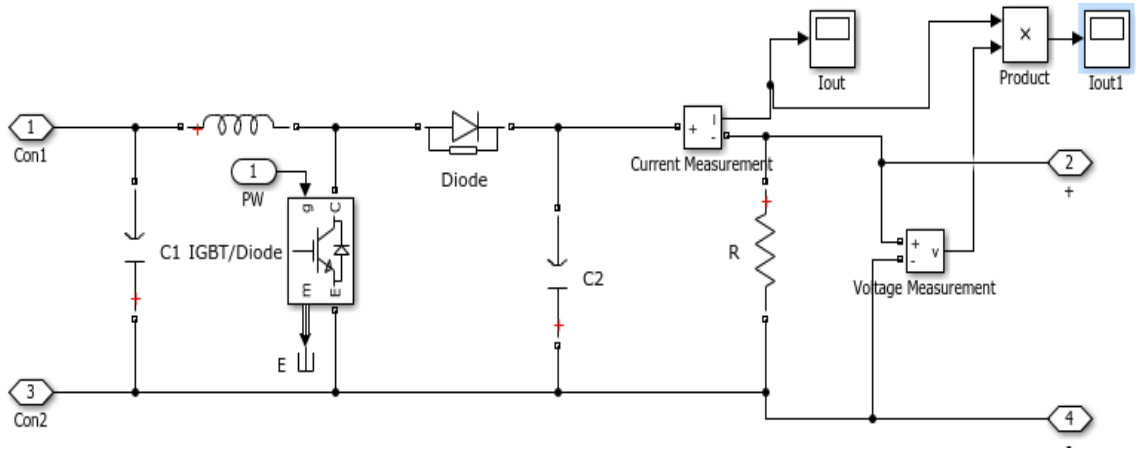


:

Figure (III.8):modeling DC\DC in MATLAB/Simulink

This figure show converter voltage and current and power output in standard

condition :

(1000w\m2 ; 25°C)

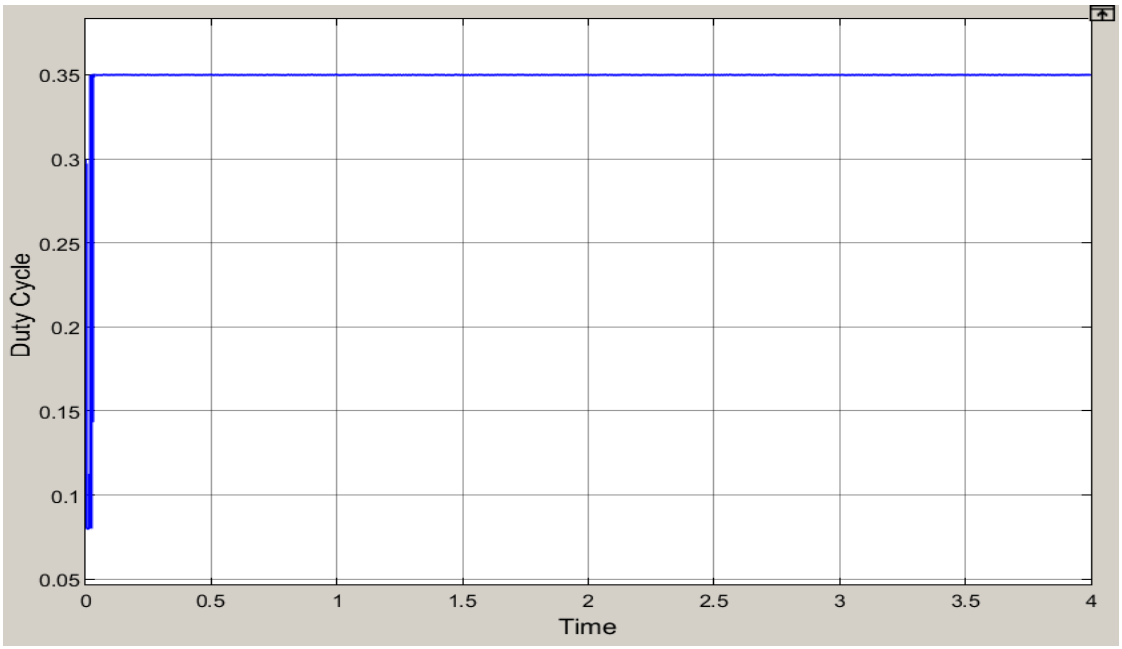


Figure(III.9):Converter Duty Cycle

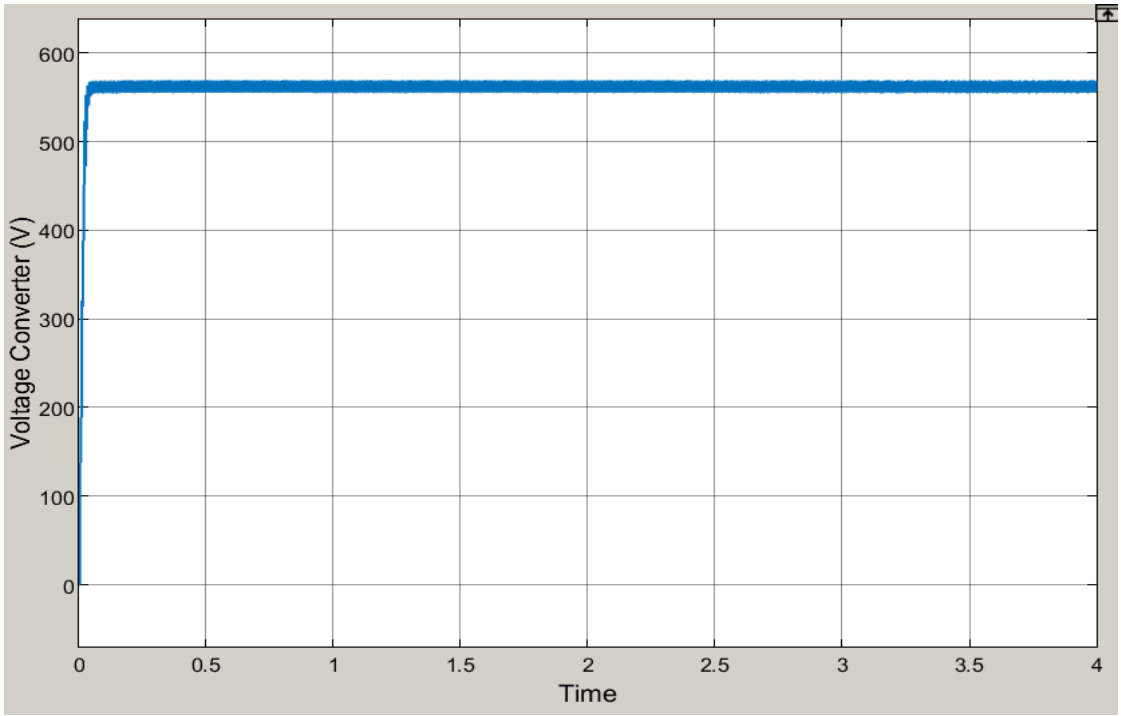


Figure(III.10):Voltage Converter (V)

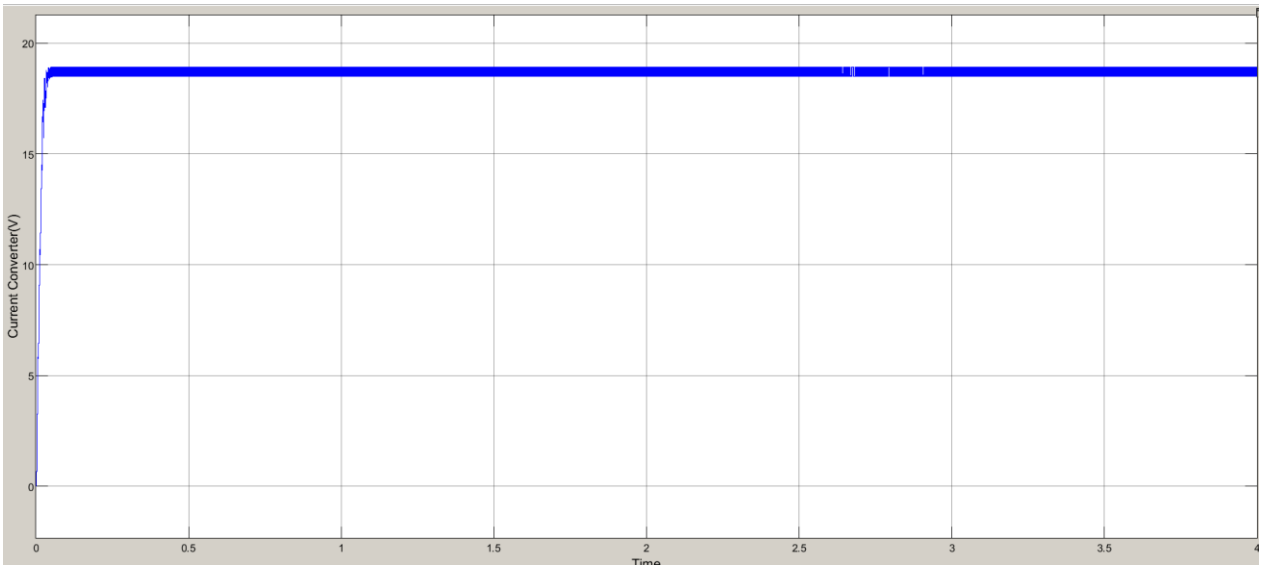


Figure(III.11):Current Converter ( A)

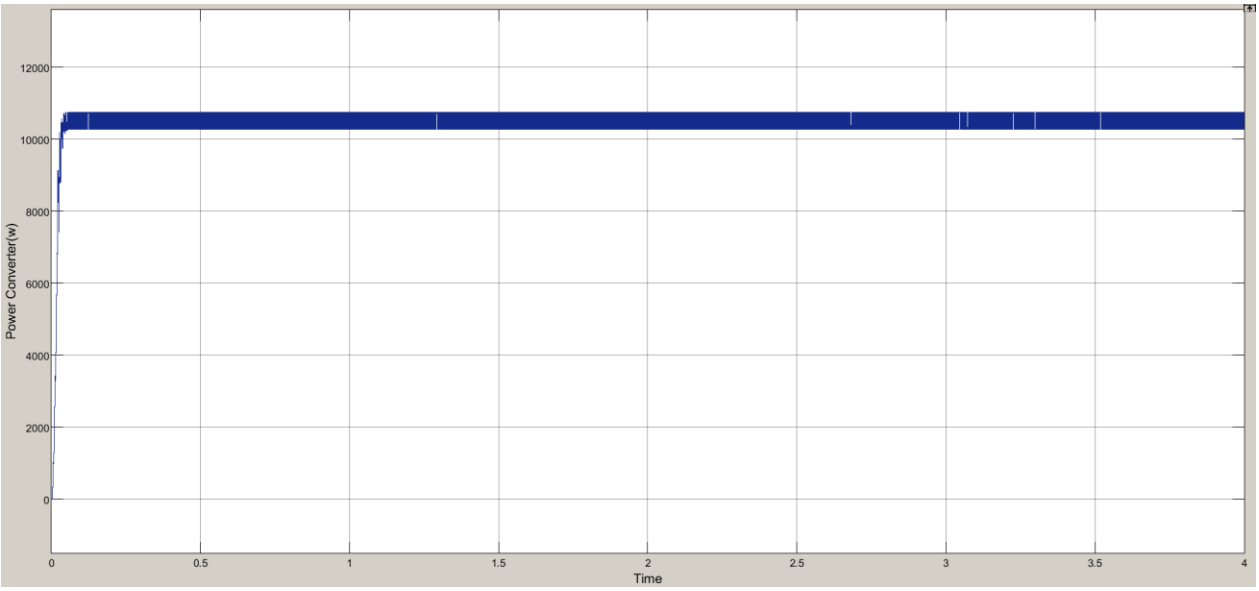


Figure(III.12):Power Converter (w)

### III.2.3 Inverter control modeling in MATLAB \Simulink

In order to carry out this simulation, the previously established equations were applied. The simulation was conducted under varying solar irradiance conditions, and the following results were obtained and analyzed accordingly.

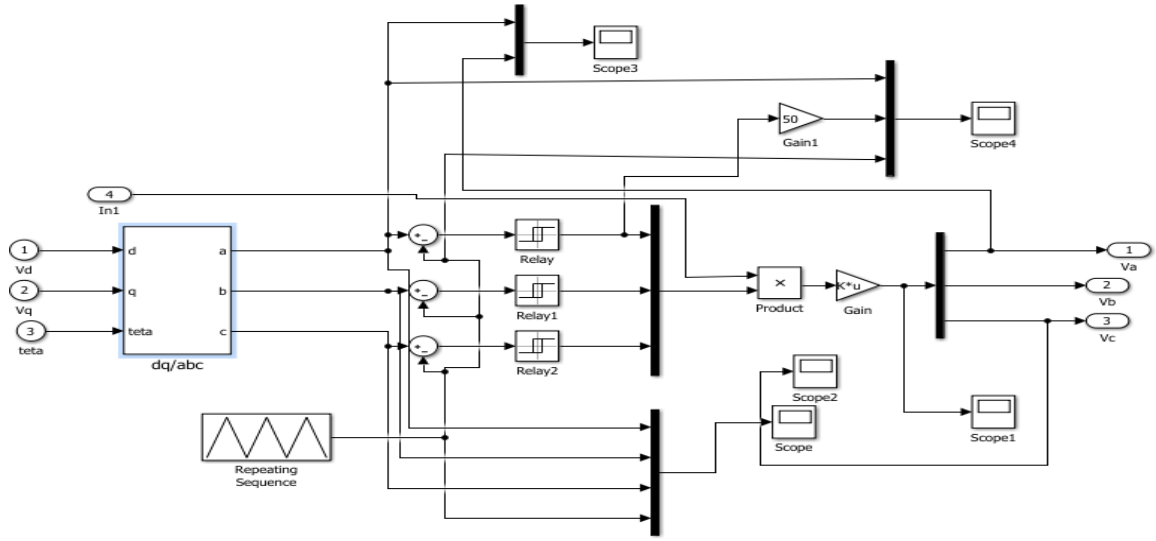


Figure(III.13):Invert control modeling in MATLAB \Simulink

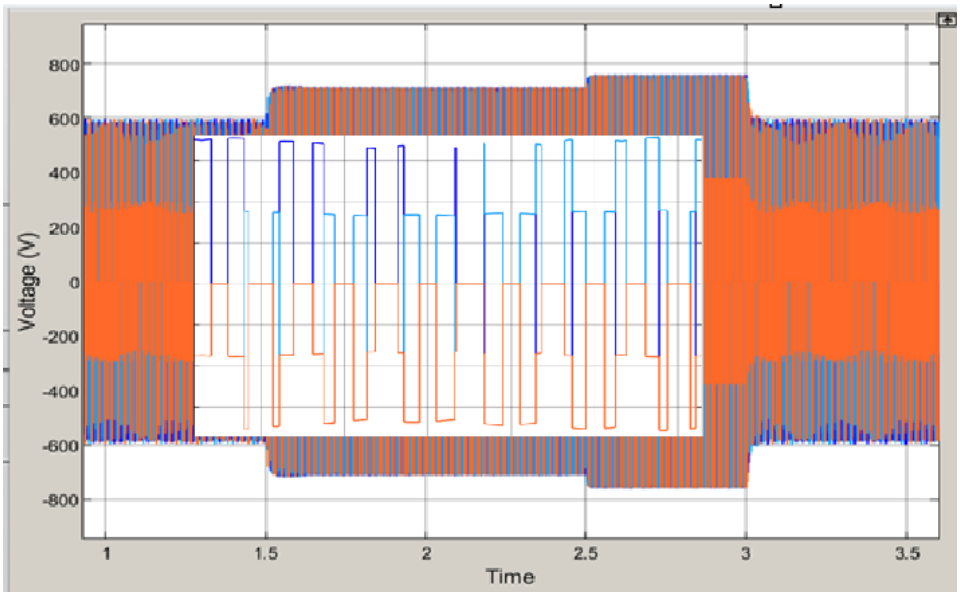


Figure(III.14): Voltage Phase

- Image shows the results of MLI l Inverter control, highlaiting its effectiveness in generating a sinusoidal output waveform, which reflects the inverter's efficient performance."

### III.2.4 Induction motor modeling in MATLAB\Simulink

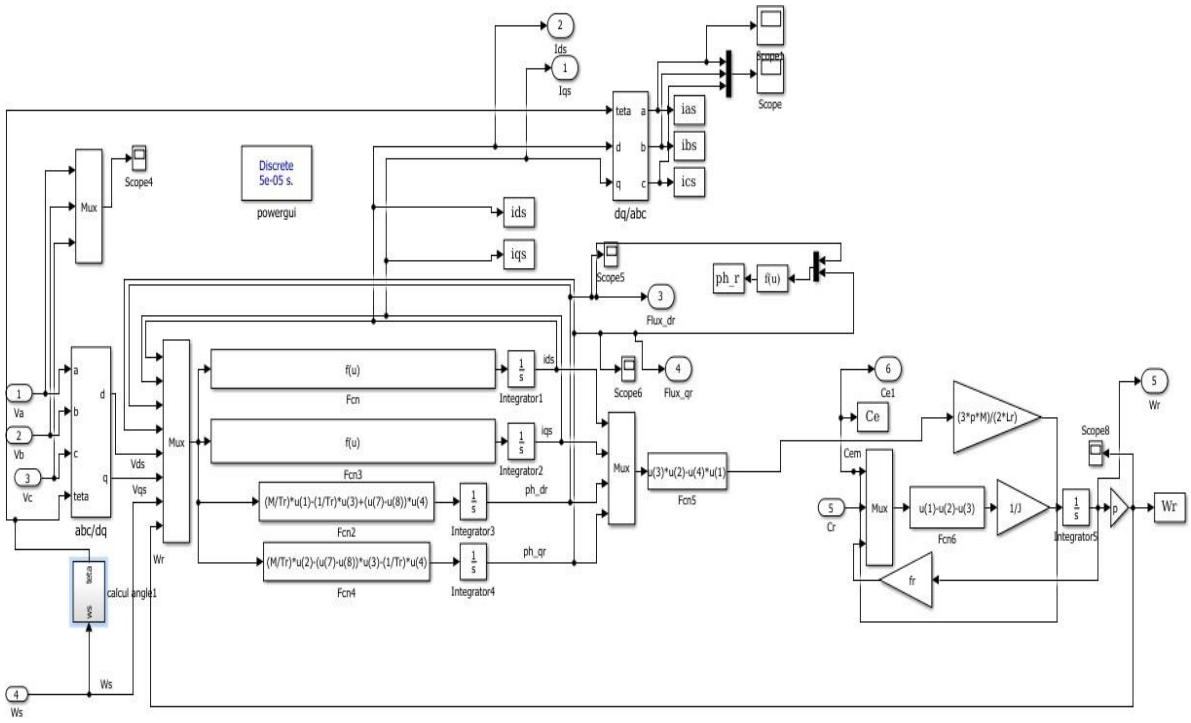


Figure(III.15): induction motor modeling in MATLAB\Simulink.

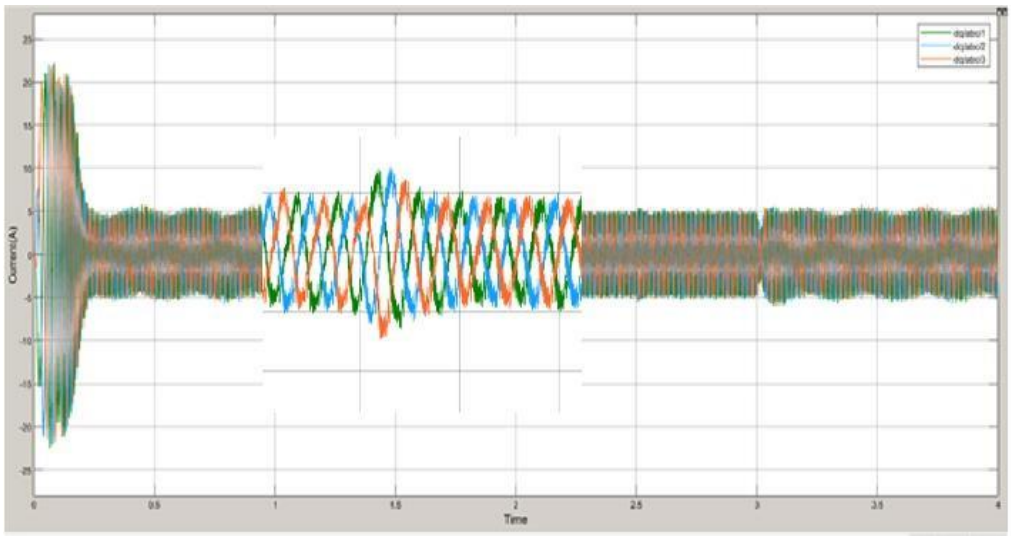


Figure(III.16): Phase Current (A)

- The figure(III.16) illustrate the three-phase current response of the system under MPPT and FOC control. At start-up, high transient currents are observed, which quickly settle into balanced and

stable sinusoidal waveforms. This indicates an effective control strategy and good dynamic performance. Minor disturbances around 1.5 s and 3 s correspond to changes in solar irradiance, showing the system's ability to adapt without losing overall stability.

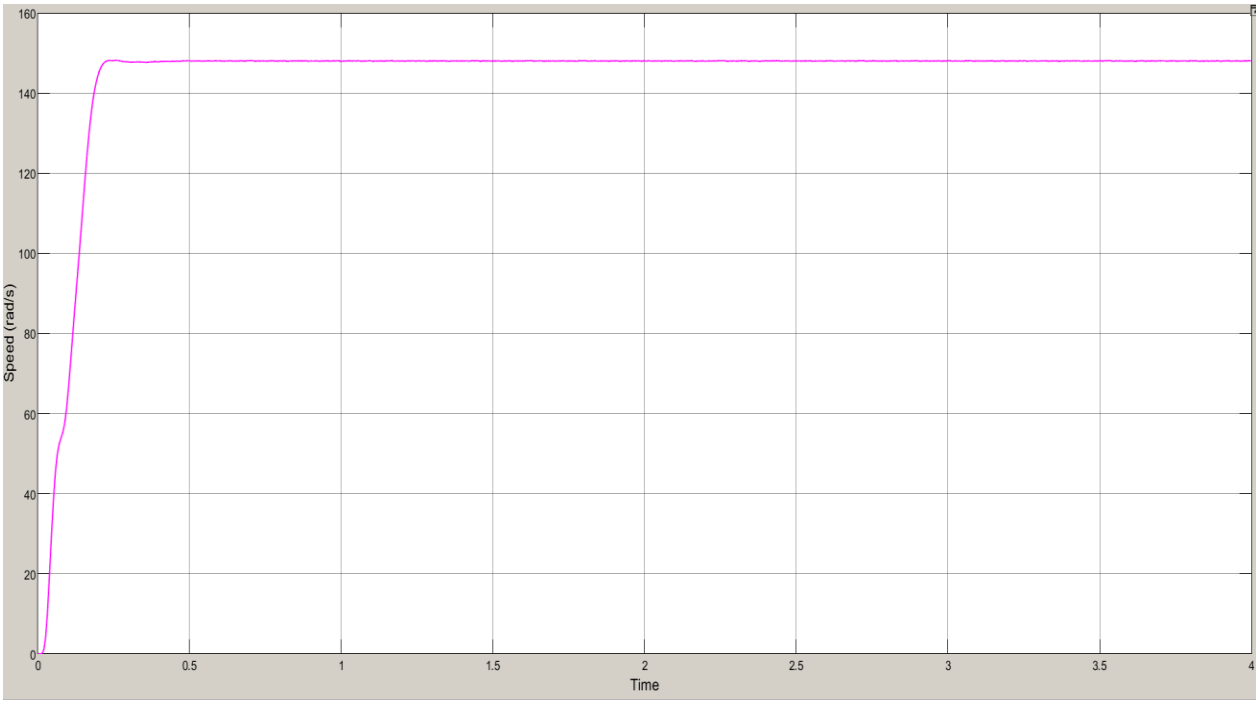


Figure(III.17):Induction motor speed (rad \s)

- Motor speed curve shows a smooth and continuous increase until it reaches the steady- state value, without overshoot or oscillations. This indicates fast dynamic response and high stability of the IFOC and MLI-based control system, ensuring accurate speed tracking and reliable operation in PV water pumping applications.

### III.2.5 pump simulation

To simulate the pump, we utilized the corresponding equations governing its behavior, as previously discussed.

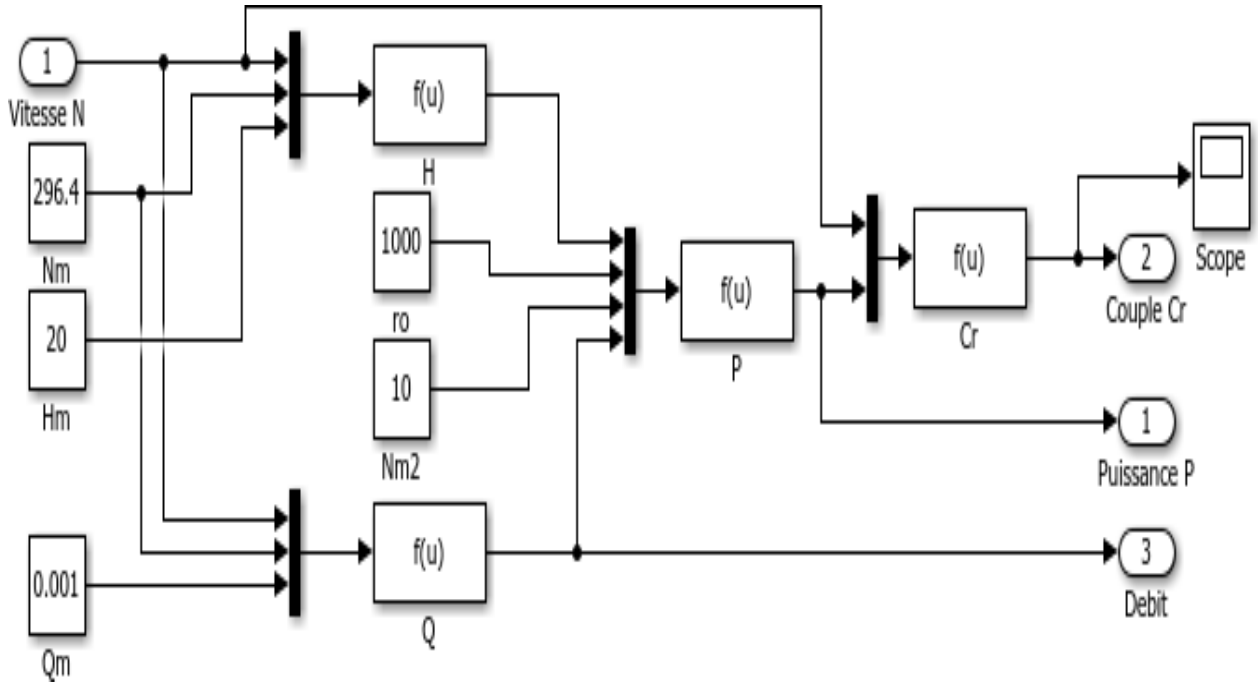


Figure(III.18) :pump  modeling in MATLAB \smiling

### III.3 Simulation Results and MPPT Algorithm Comparison in the PV Water Pumping System

To simulate a sudden change in climate, we varied the solar radiation value between two states: one with a maximum value and the other with a minimum value.  This modification aims to investigate the system's response to these abrupt fluctuations, determine whether the MPPT algorithm can effectively track the maximum power point in these situations, and assess the PV system's overall stability.

#### III.3.1 Perturbed and observe method

By applying this method in the simulation, we obtained the results shown below Under :

- **STC [1000 w/m$^2$, 25C]**

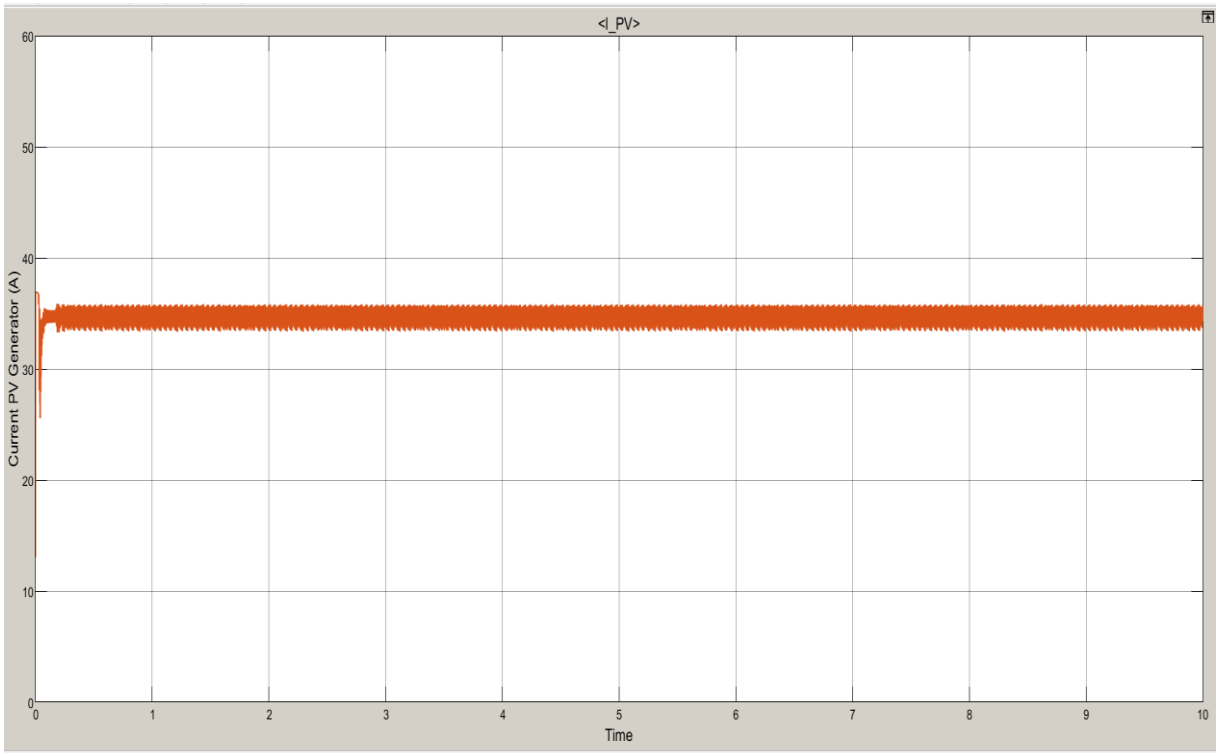


Figure(III.19): Current PV Generator(A)Under (STC)

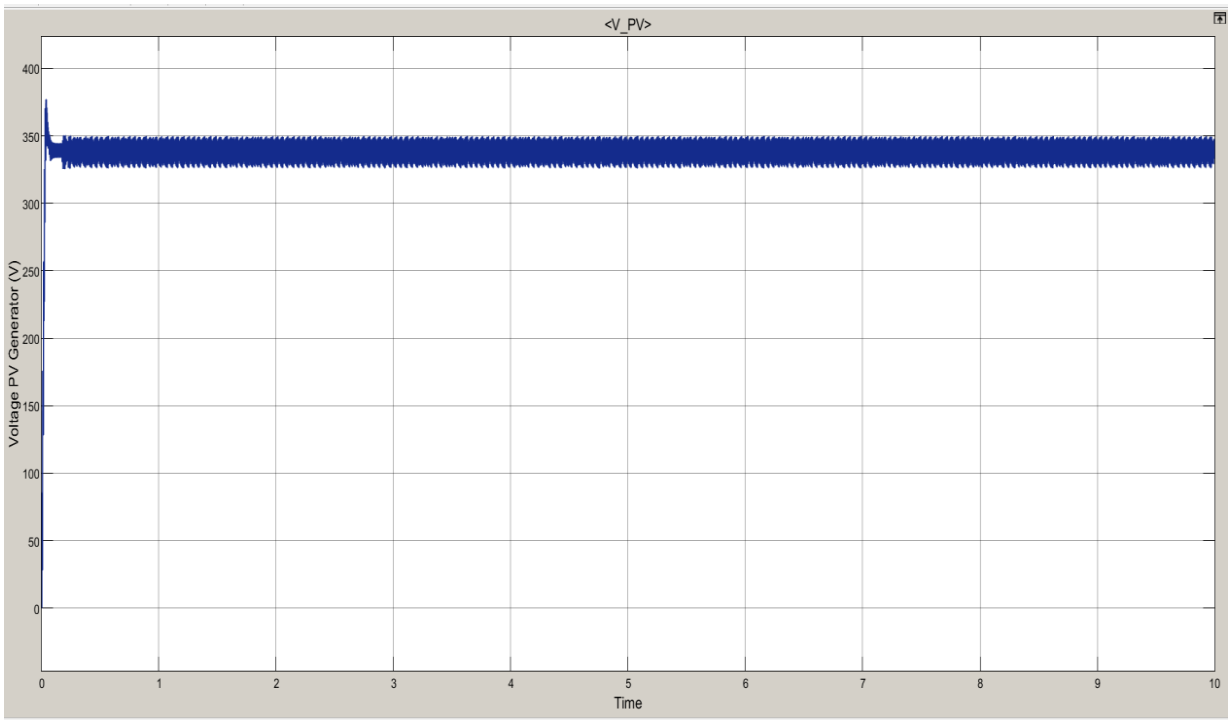


Figure(III.20): Voltage PV Generator(V) Under (STC)

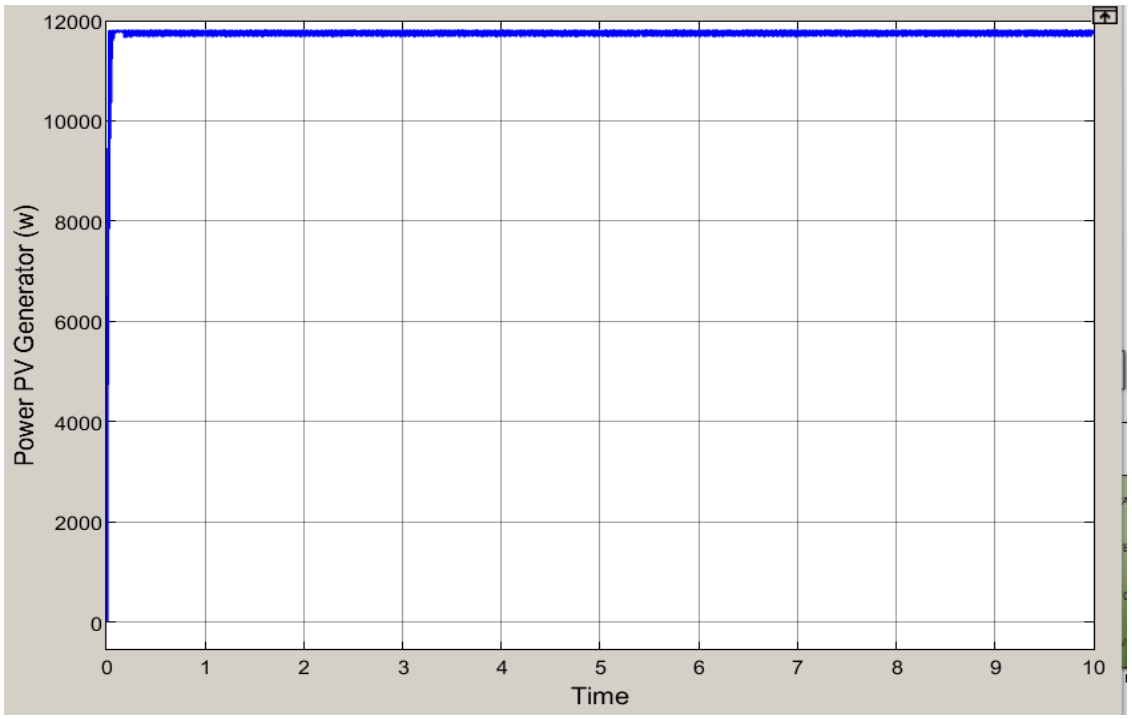


Figure(III.21): Power PV generator (W) Under (STC)

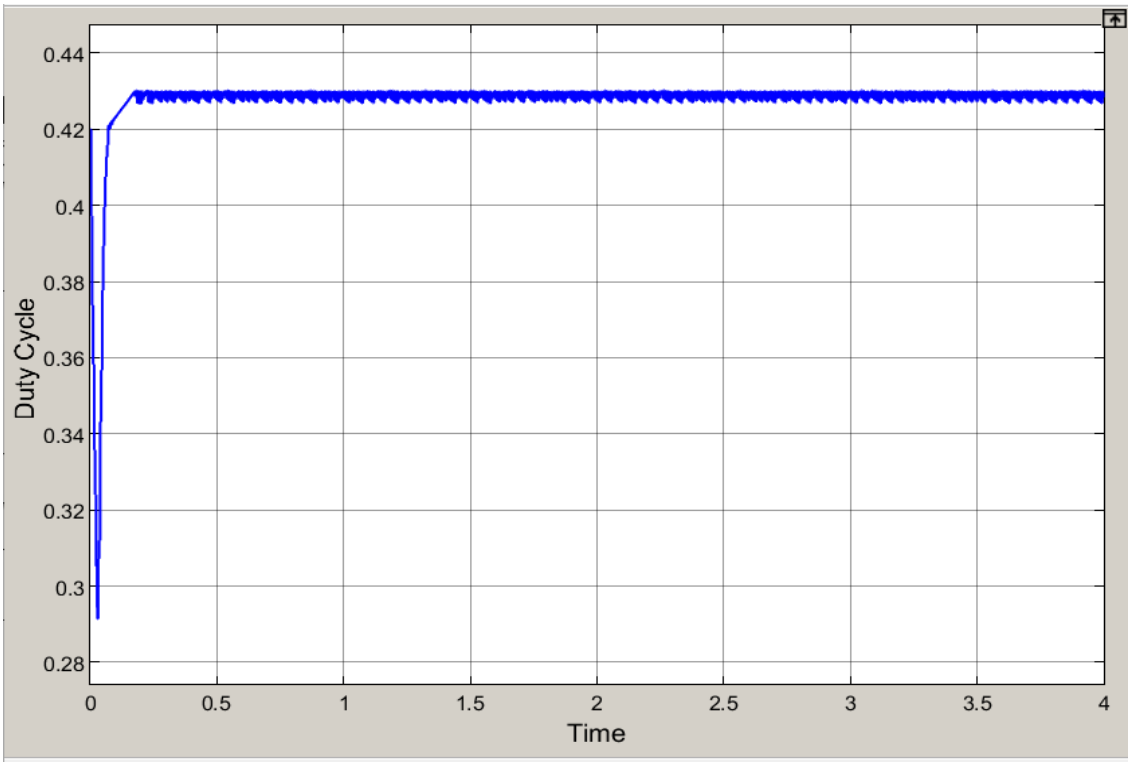


Figure(III .22) :Duty Cycle Converter

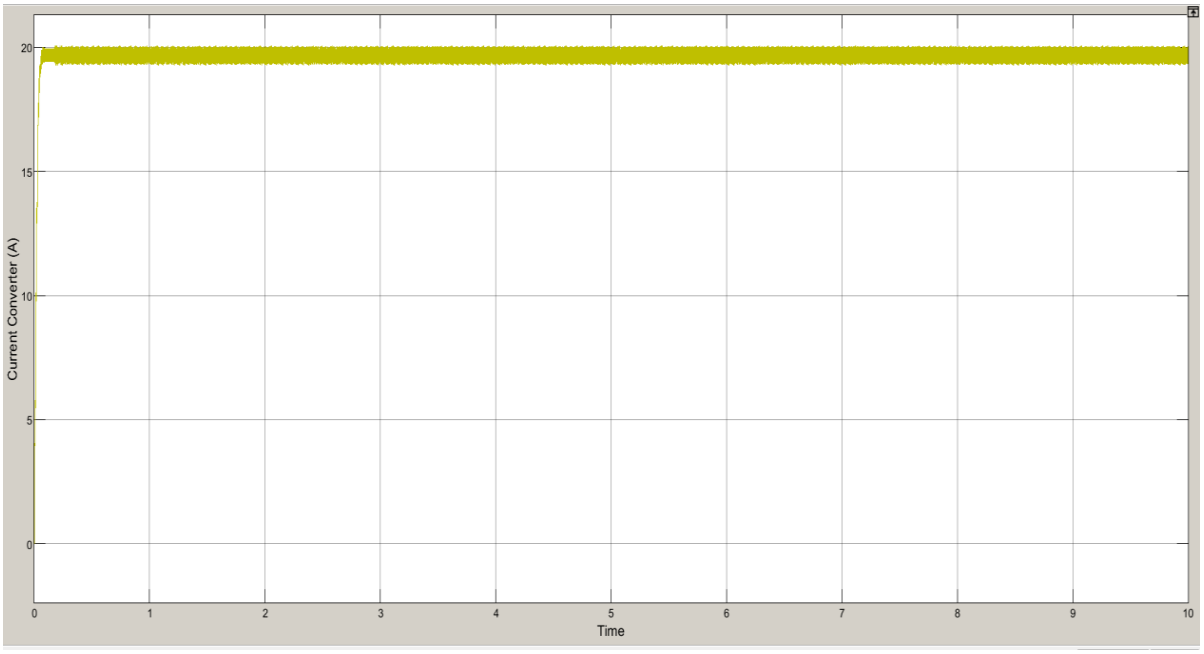


Figure(III.23): Current Converter (A) Under (STC)

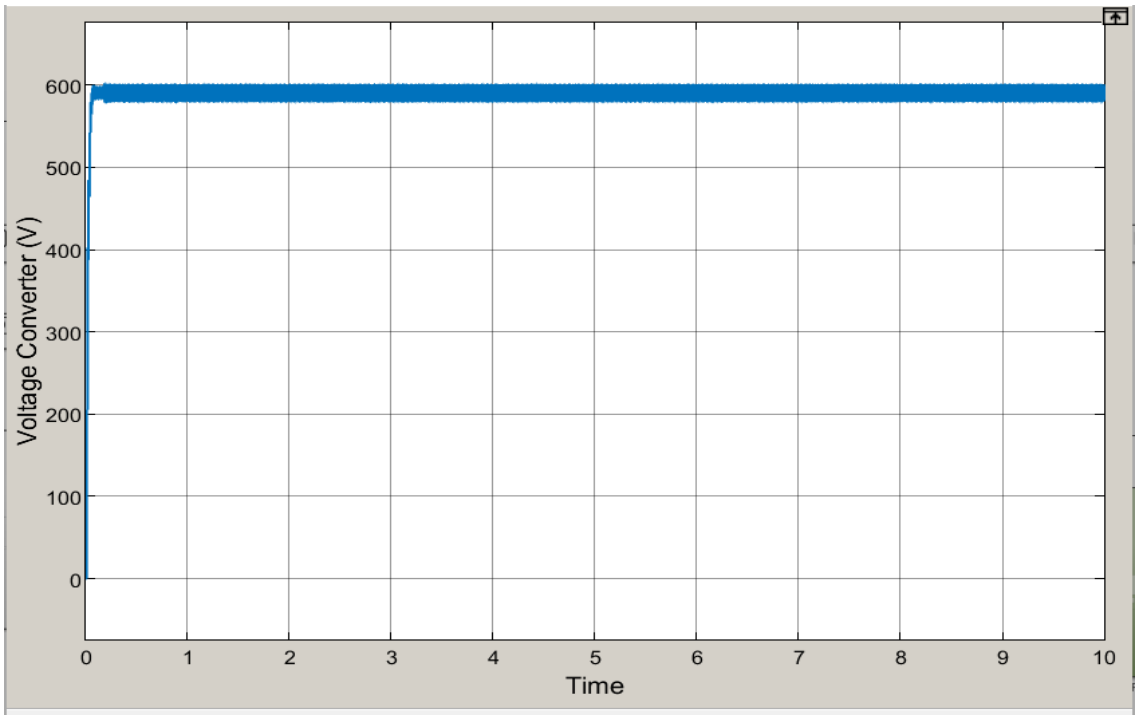


Figure(III.24):Voltage Converter(V) Under (STC)

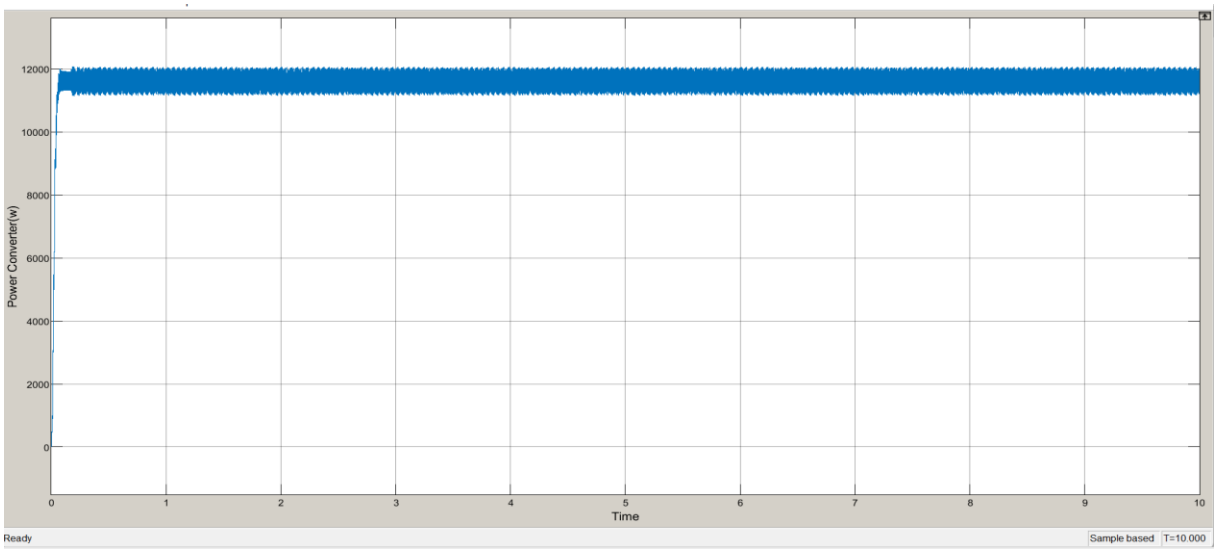


Figure(III.25): Power Converter (w) Under (STC)

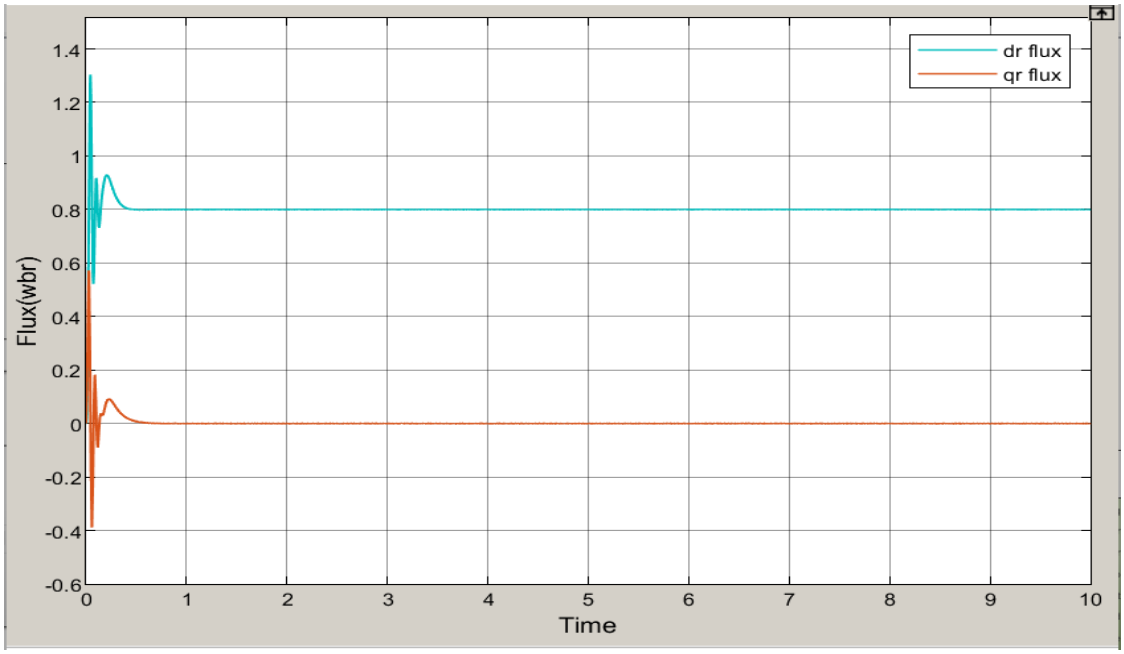


Figure(III.26):Flux (wb) Under (STC)

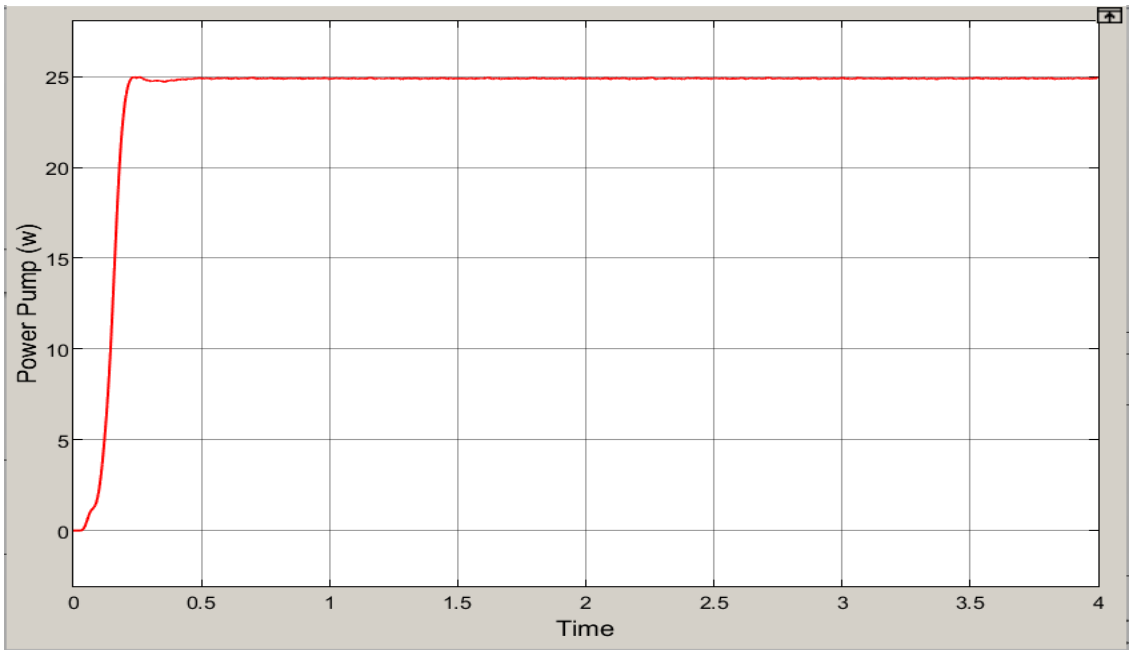


Figure(III.27):Power Pump (w)Under (STC)

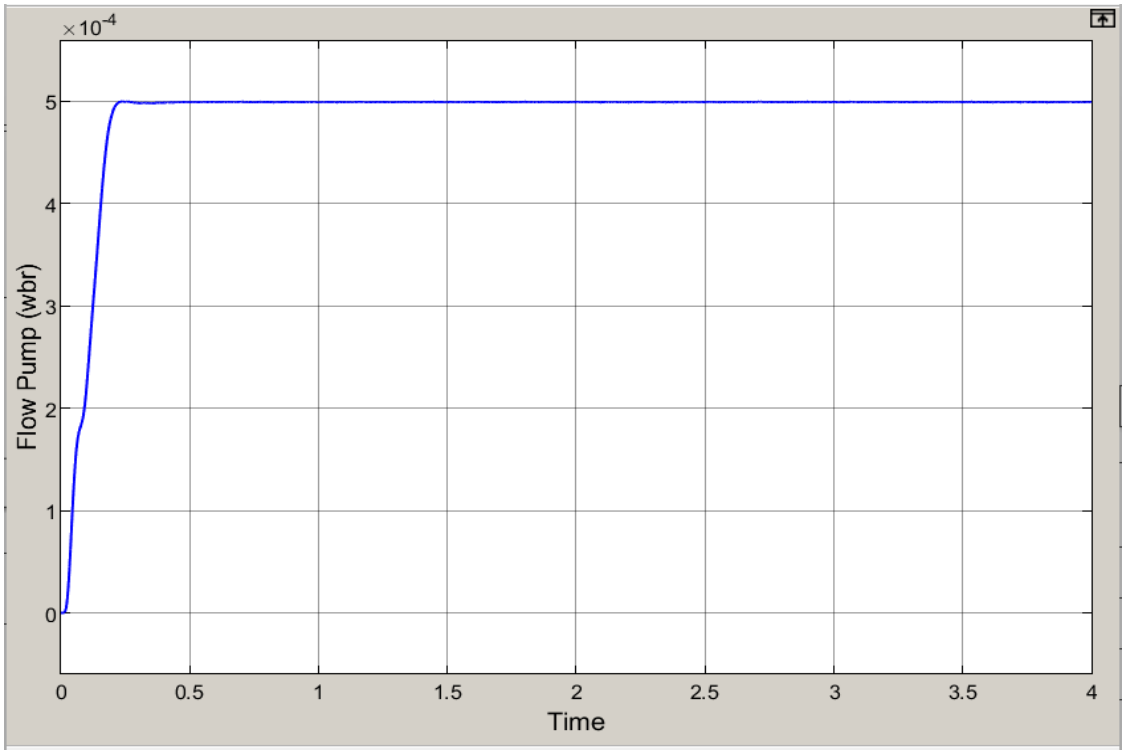


Figure(III.28): flow pump (wb)Under (STC)

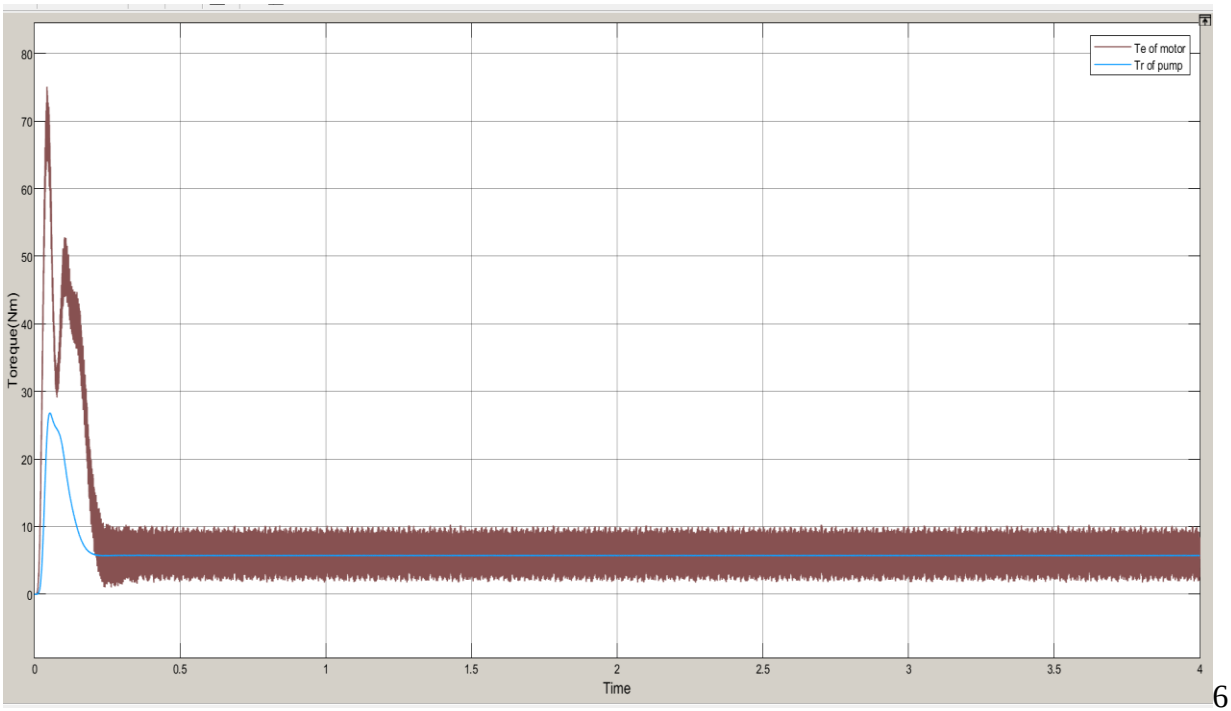


6

Figure(III.29): Torque (Nm)

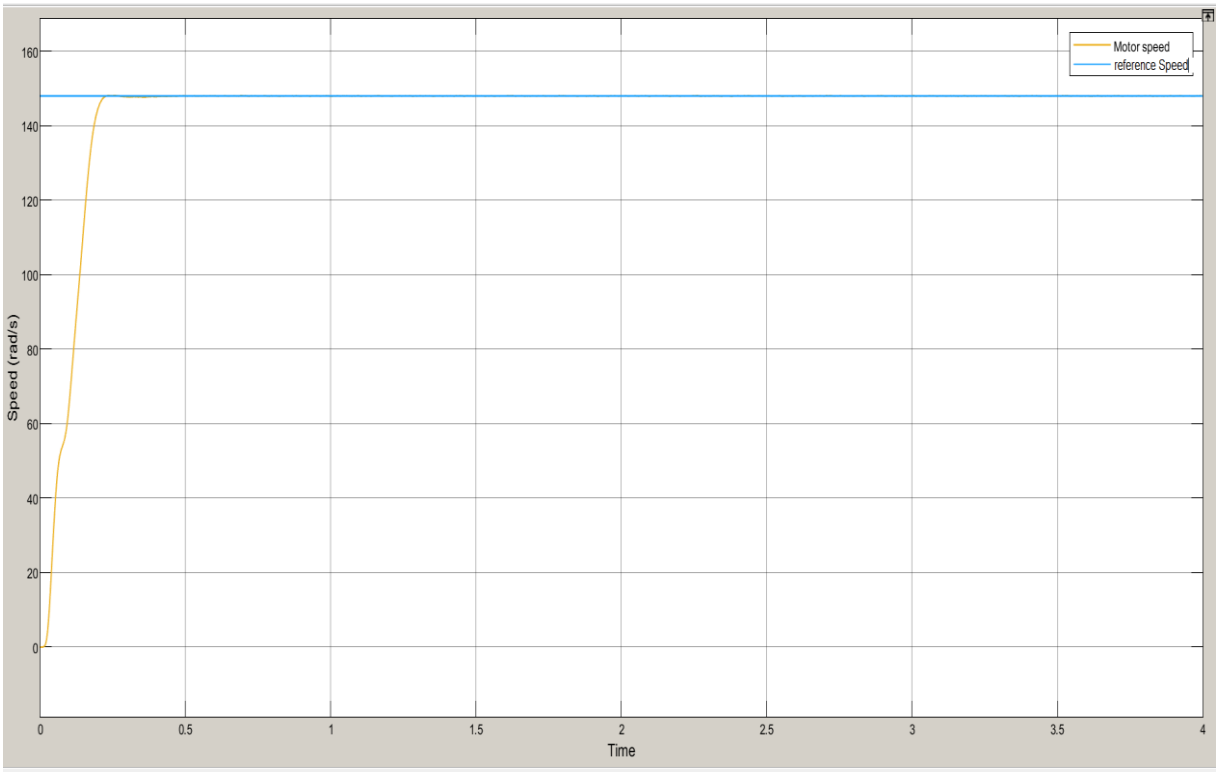


Figure(III.30):Speed (rad\s)Under (STC)

- **Varying irradiation and fixed temperature I(w\m$^2$)=[500 800 1000 500]**

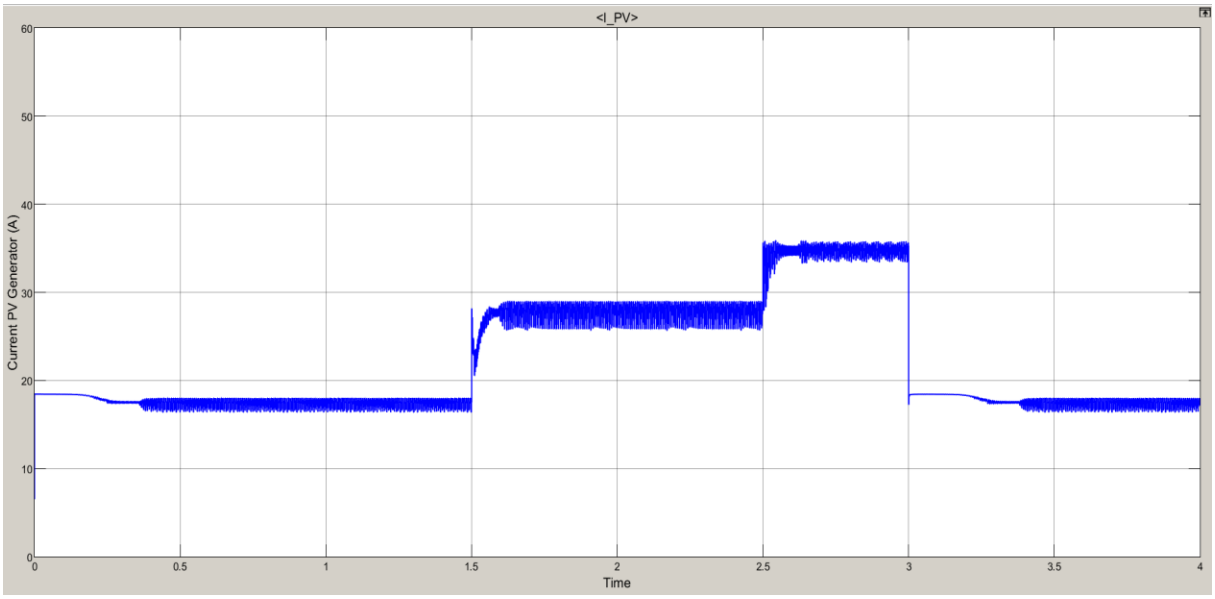


Figure(III.31) :Current PV Generator (A)

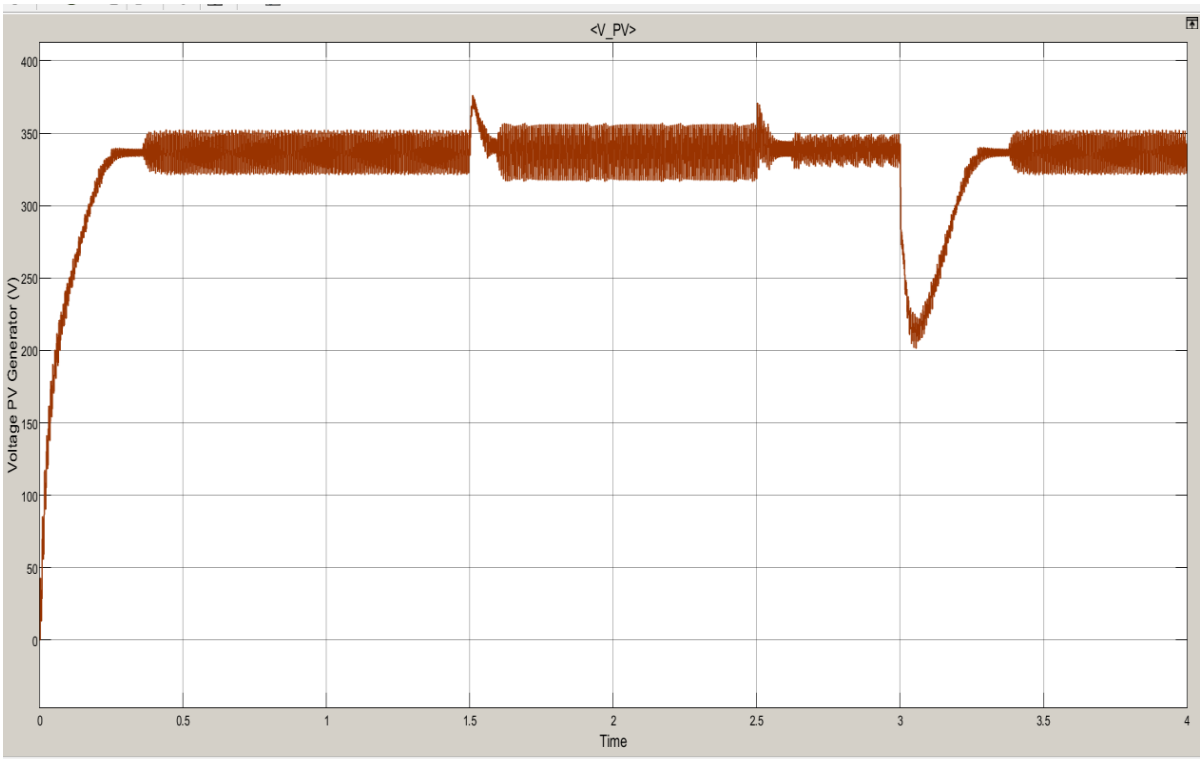


Figure(III.32) : Voltage PV Generator (v)

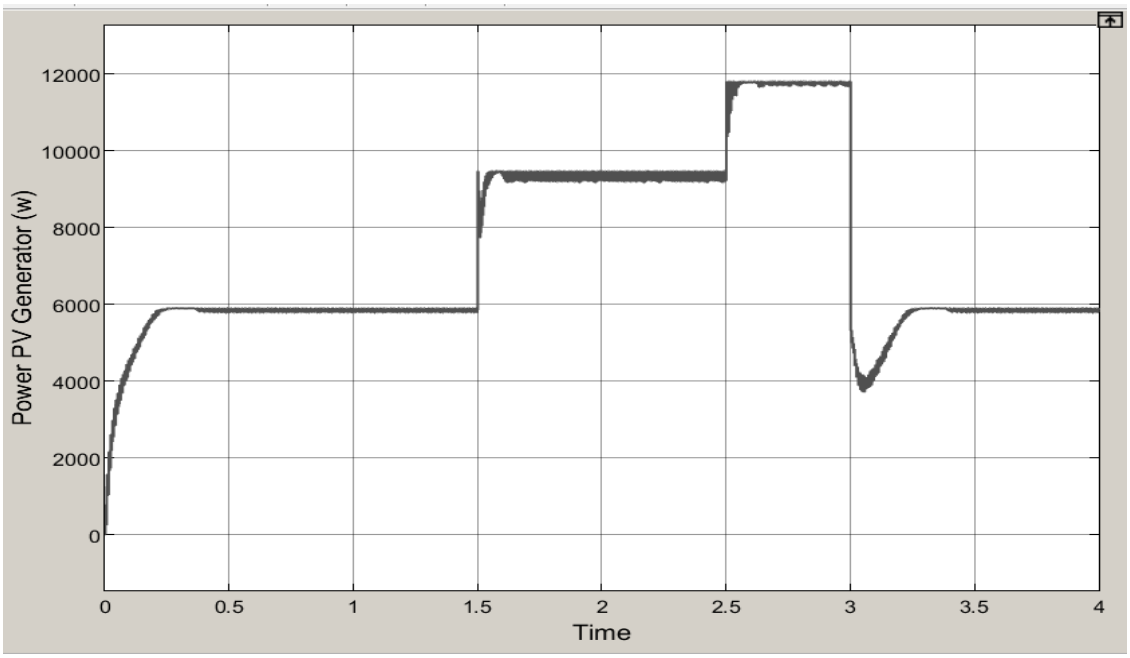


Figure(III.33) : Power PV  Generator (W)

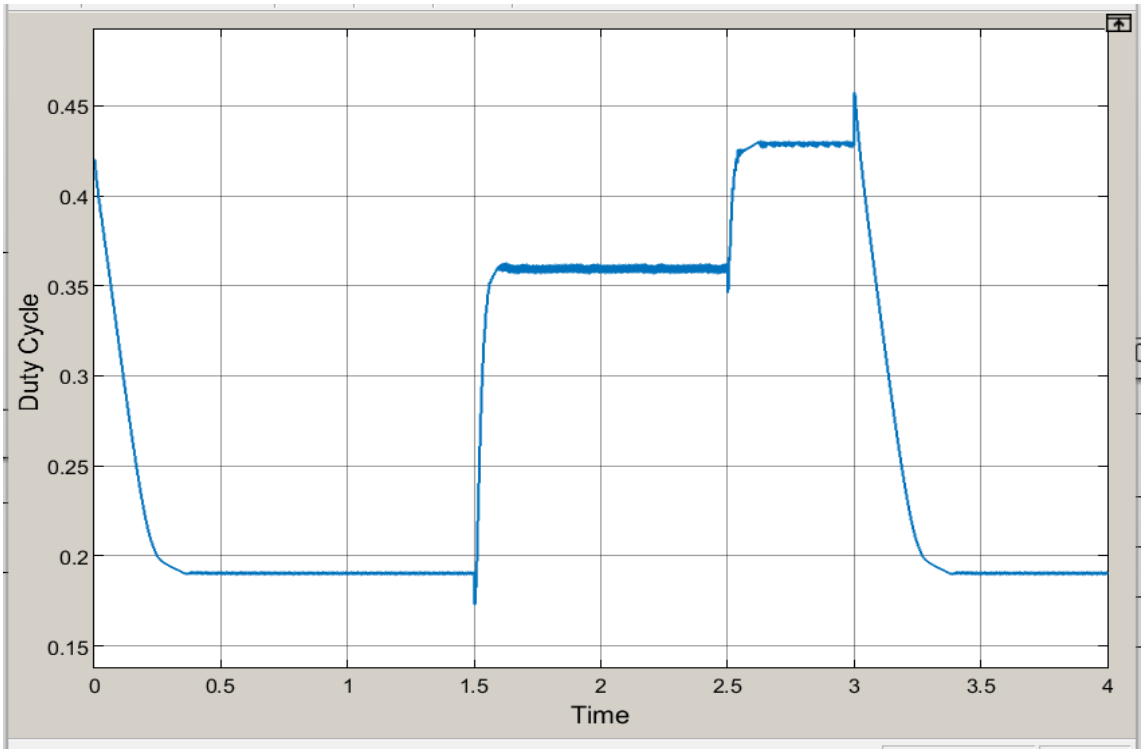


Figure(III.34): Duty Cycle Converter

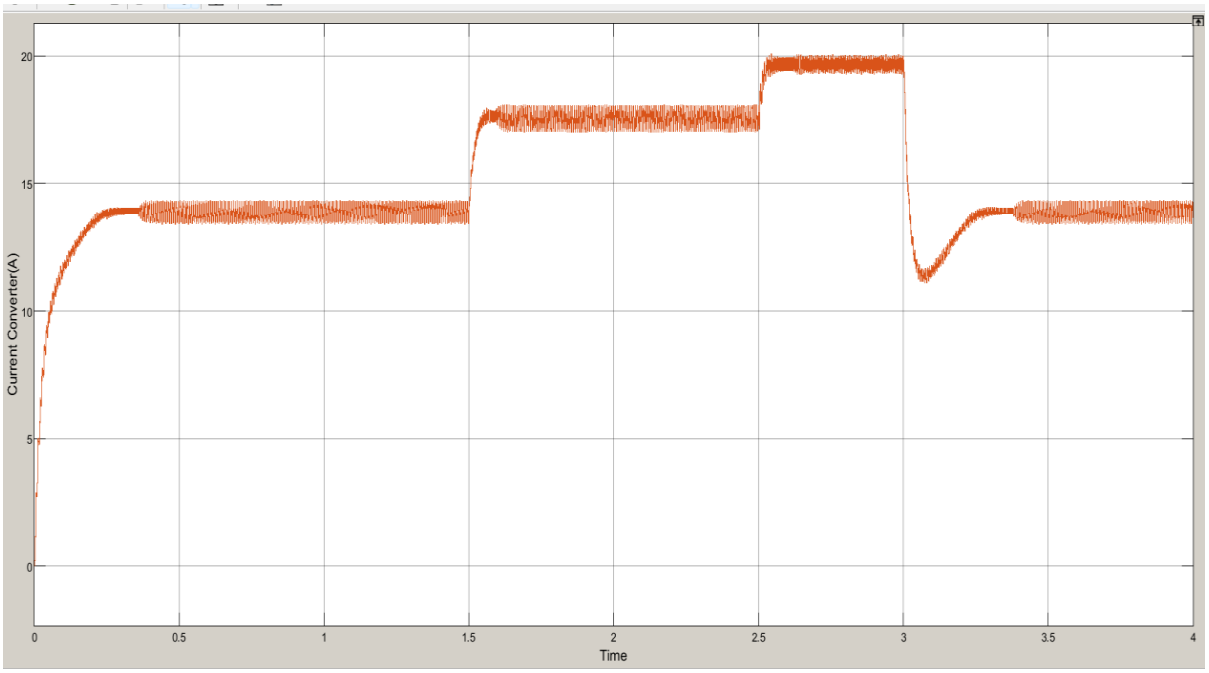


Figure(III.35): Current Converter (A)

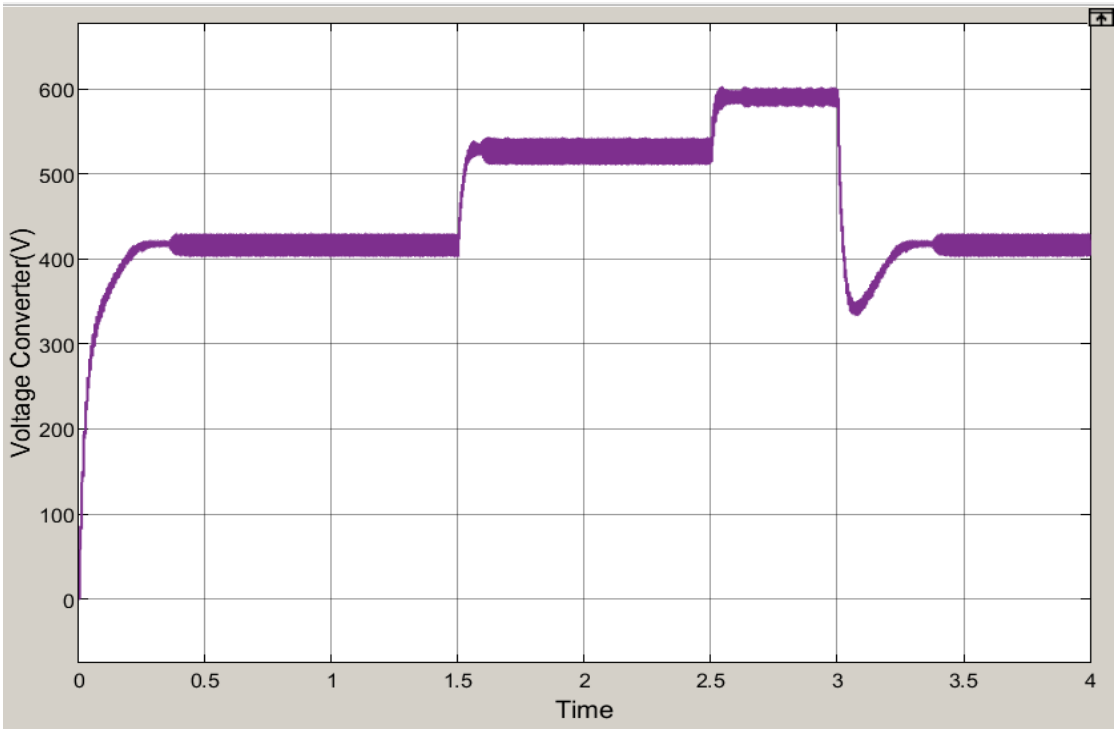


Figure(III.36): Voltage Converter (V)

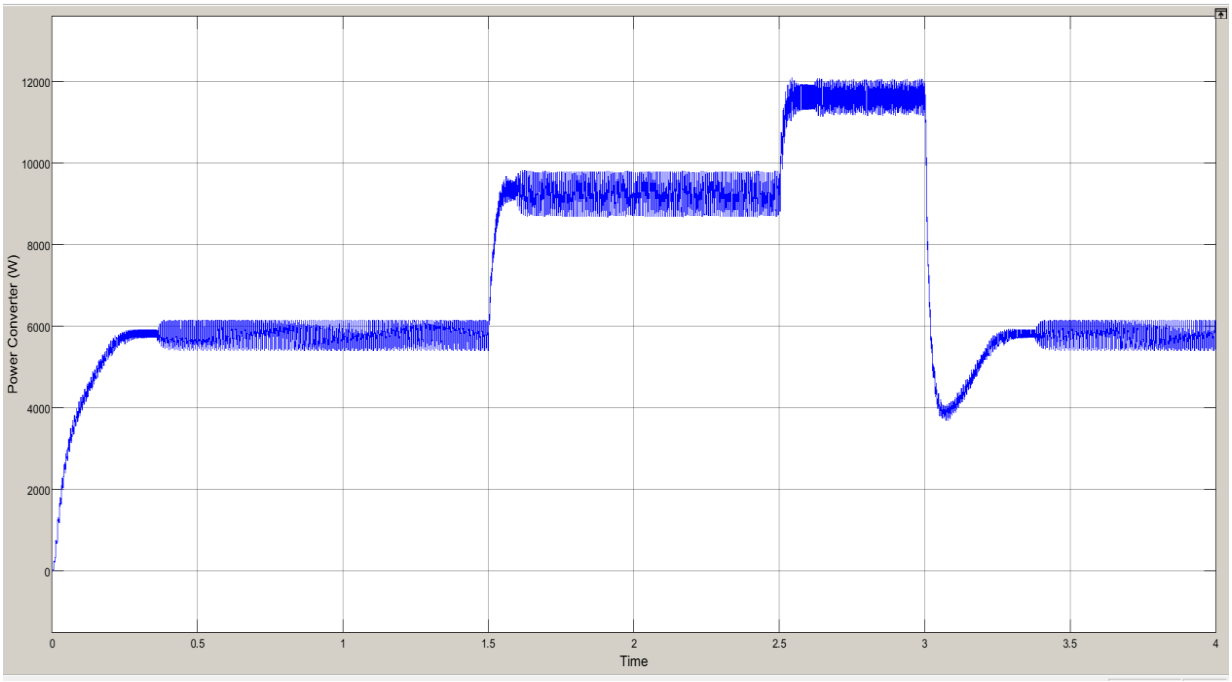


Figure (III.37):Power Converter (w)

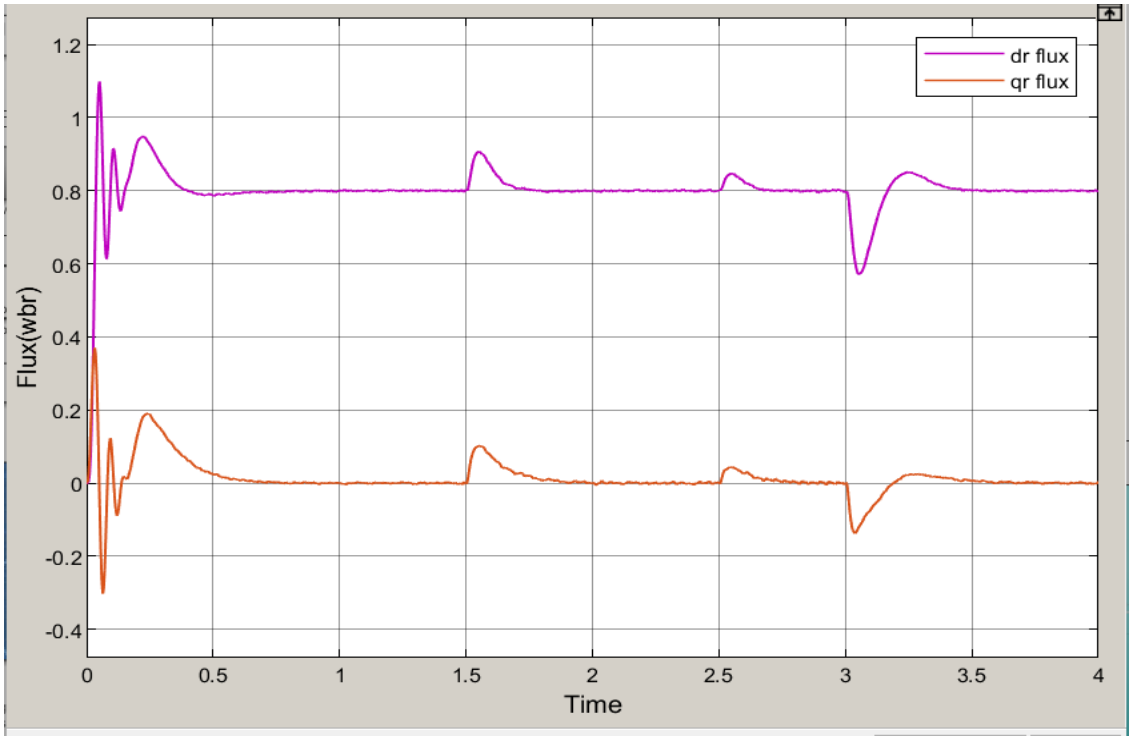


Figure(III.38): Flux (wb)

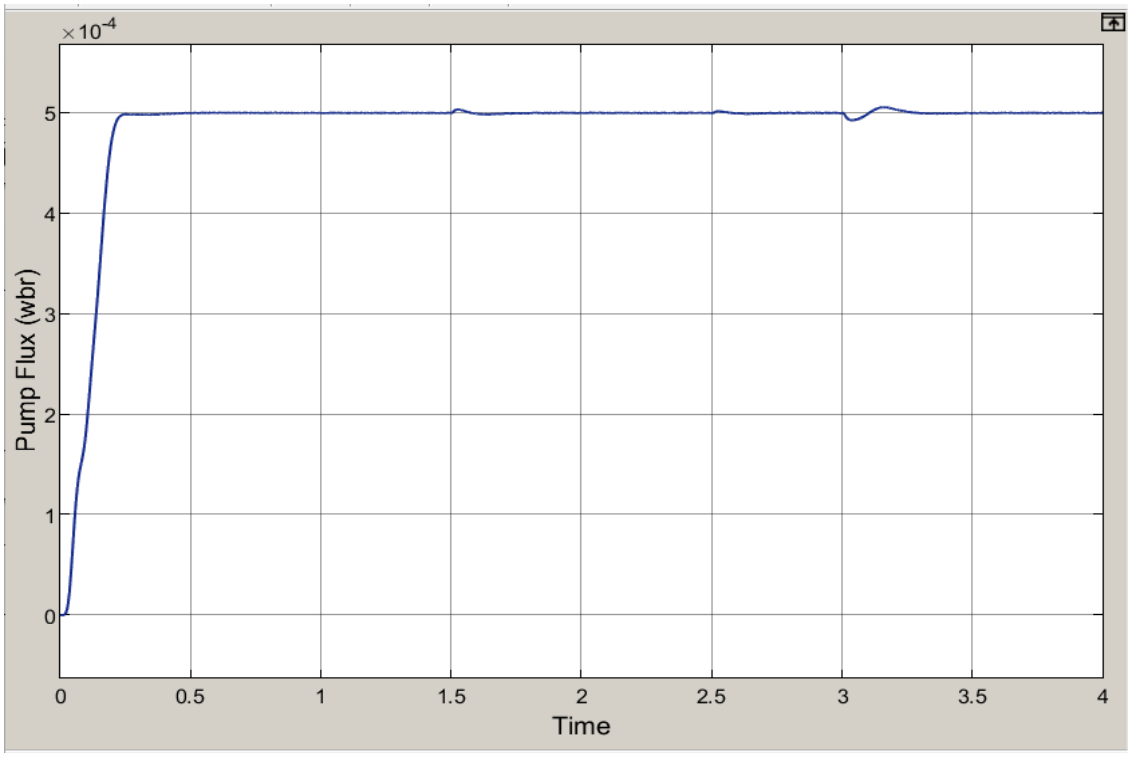


Figure(III.39): Flux  Pump(wb)

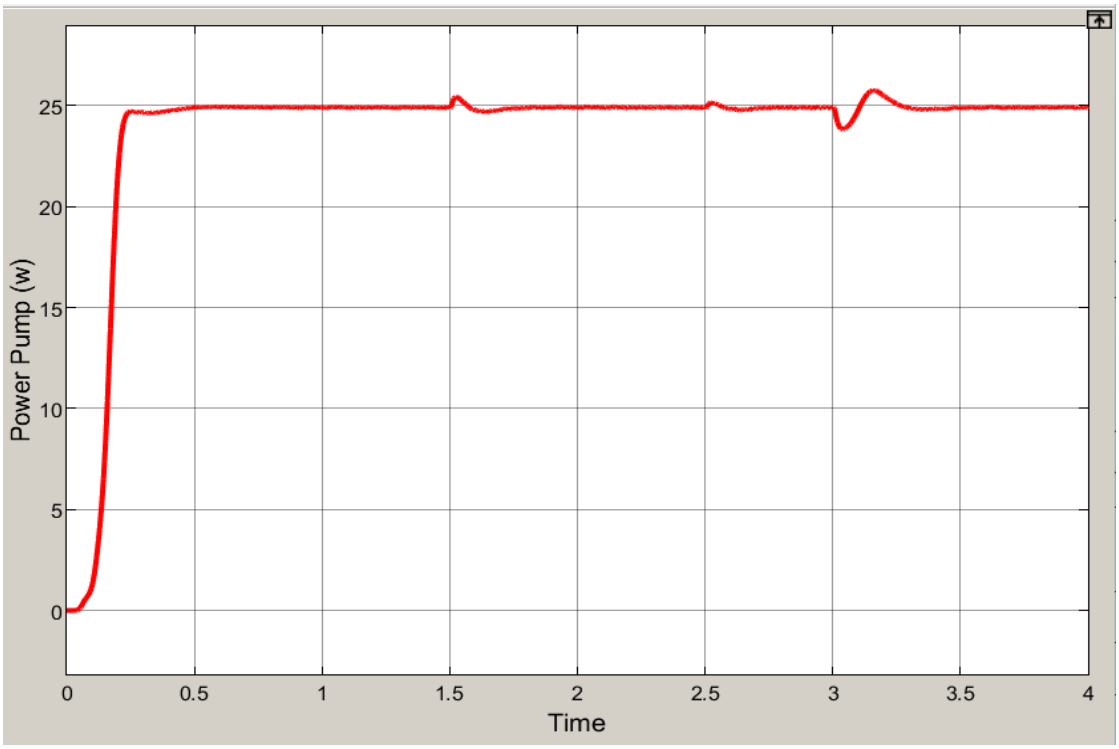


Figure(III.40):Power Pump(w)

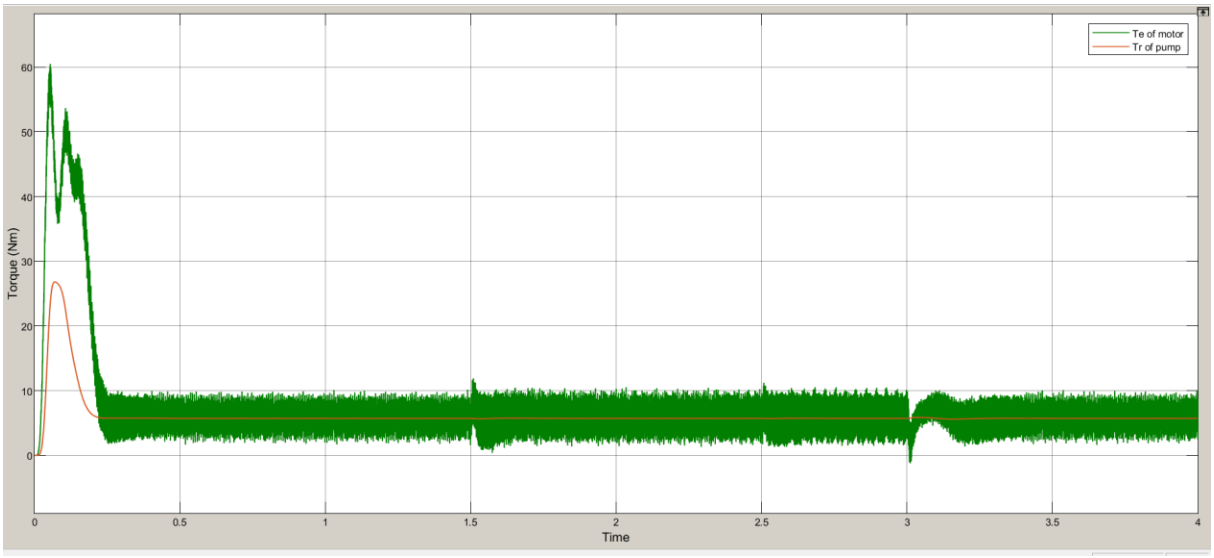


Figure(III.41):Torque (Nm)

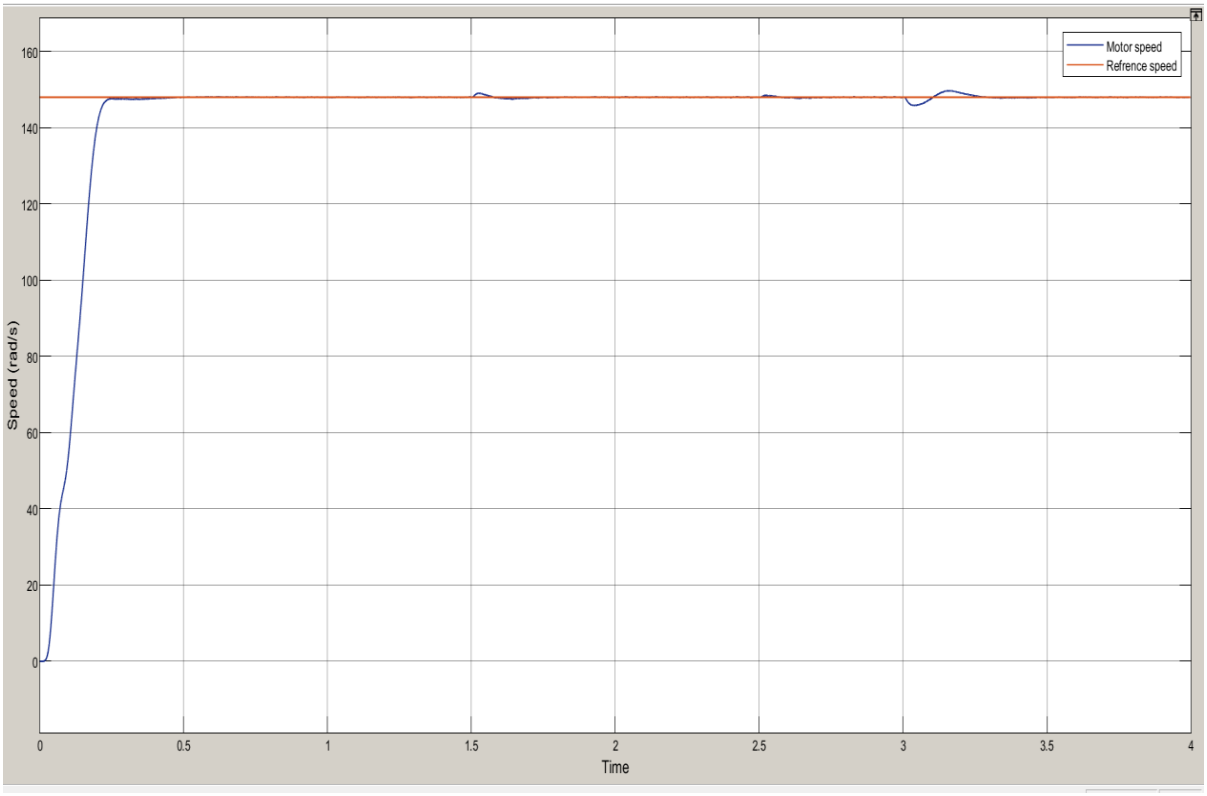


Figure(III.42):Speed(rad/s)

- Following the implementation of the simulation and the application of the Maximum Power Point Tracking (MPPT) algorithm based on Perturb and observe the strategy, the system's behavior was analyzed under varying solar irradiance levels. The obtained results revealed noticeable dynamic fluctuations at lower irradiance values500(w/$m^2$), whereas the response became more stable and consistent at higher irradiance levels, particularly at 1000(W/m2). These findings highlight the effectiveness of the algorithm in tracking the maximum power point across a wide range of operating conditions. However, the observed oscillations represent a technical limitation that may compromise the overall stability of the system, especially under rapidly changing irradiance conditions.

### III.3.2 Incremental Conductance method

- **In standard condition (1000 w\m25C)**

This figure showed power generated by Pv generator

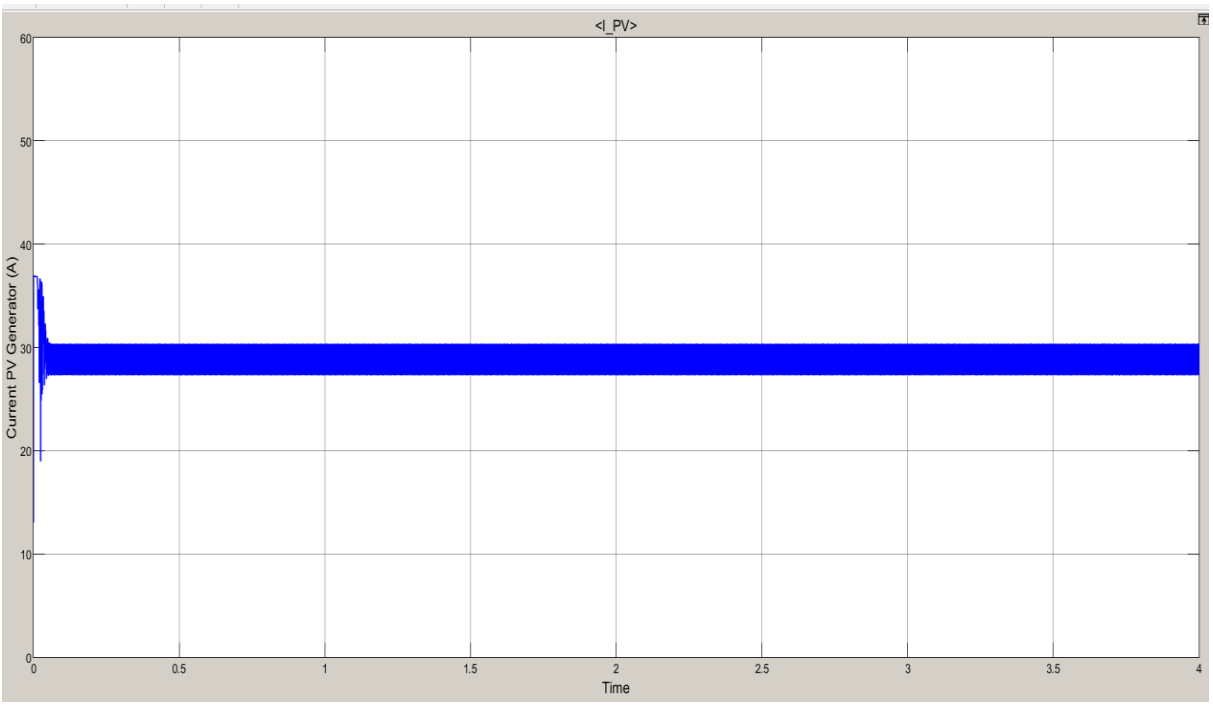


Figure(III.43):Current PV Generator (A)

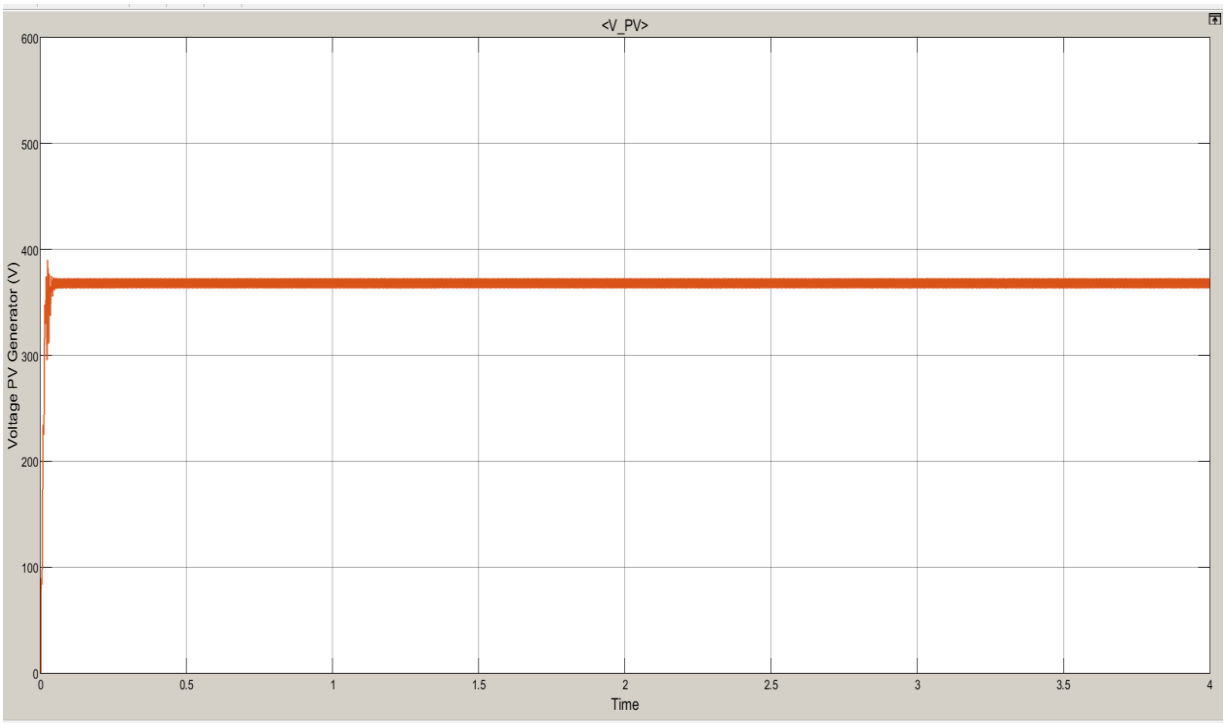


Figure(III.44):Voltage PV Generator(V)

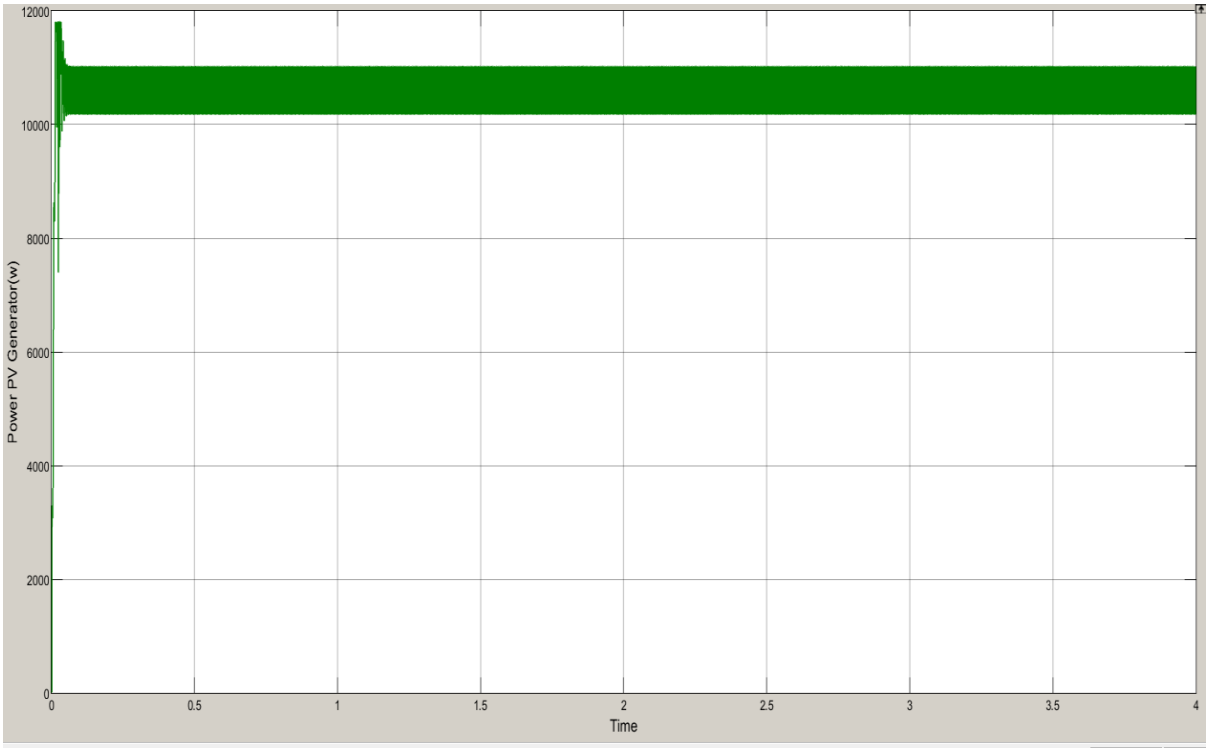


Figure(III.45):Power PV Generator (w)

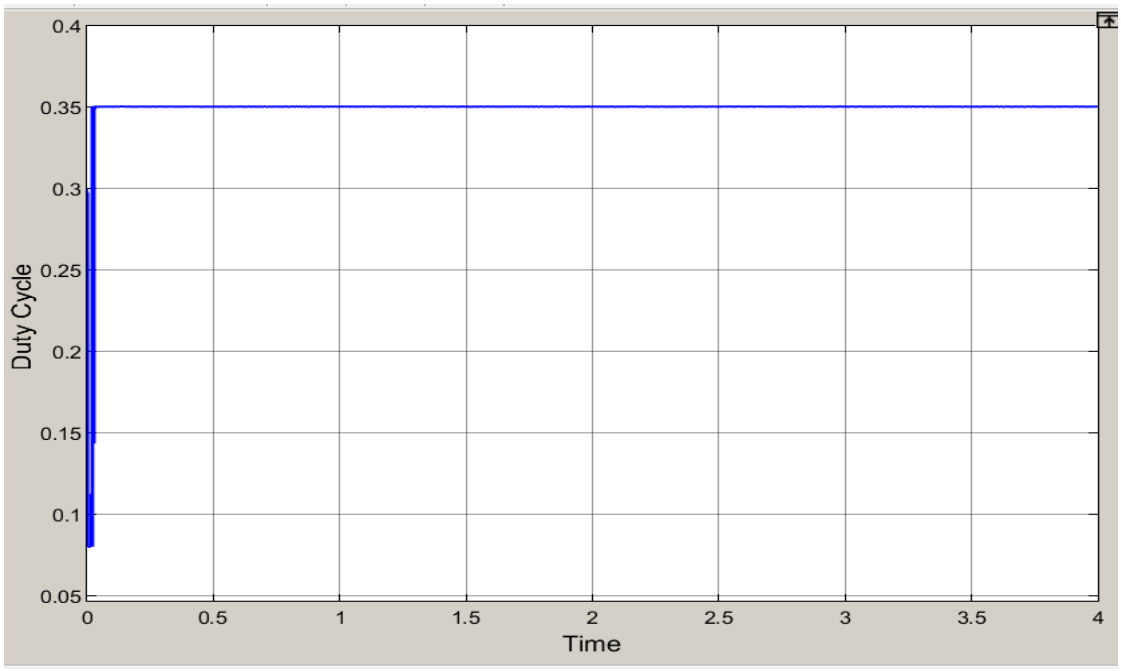


Figure(III.46):Converter Duty Cycle

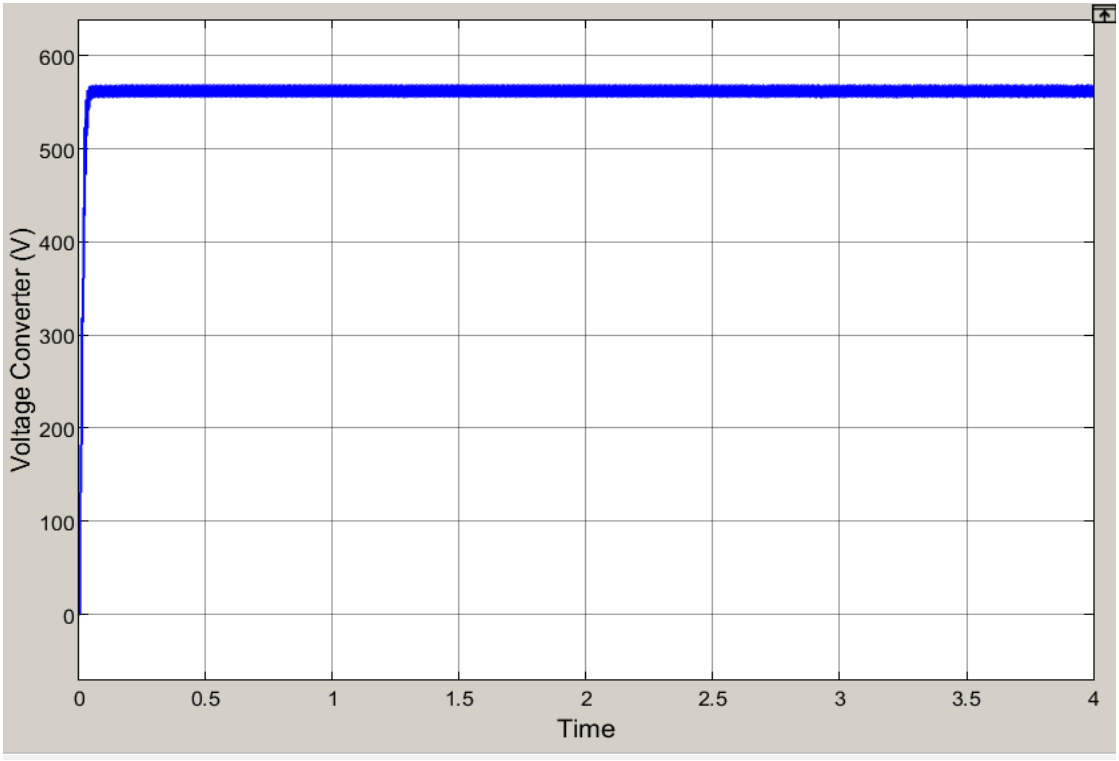


Figure(III.47):Voltage Converter(V)

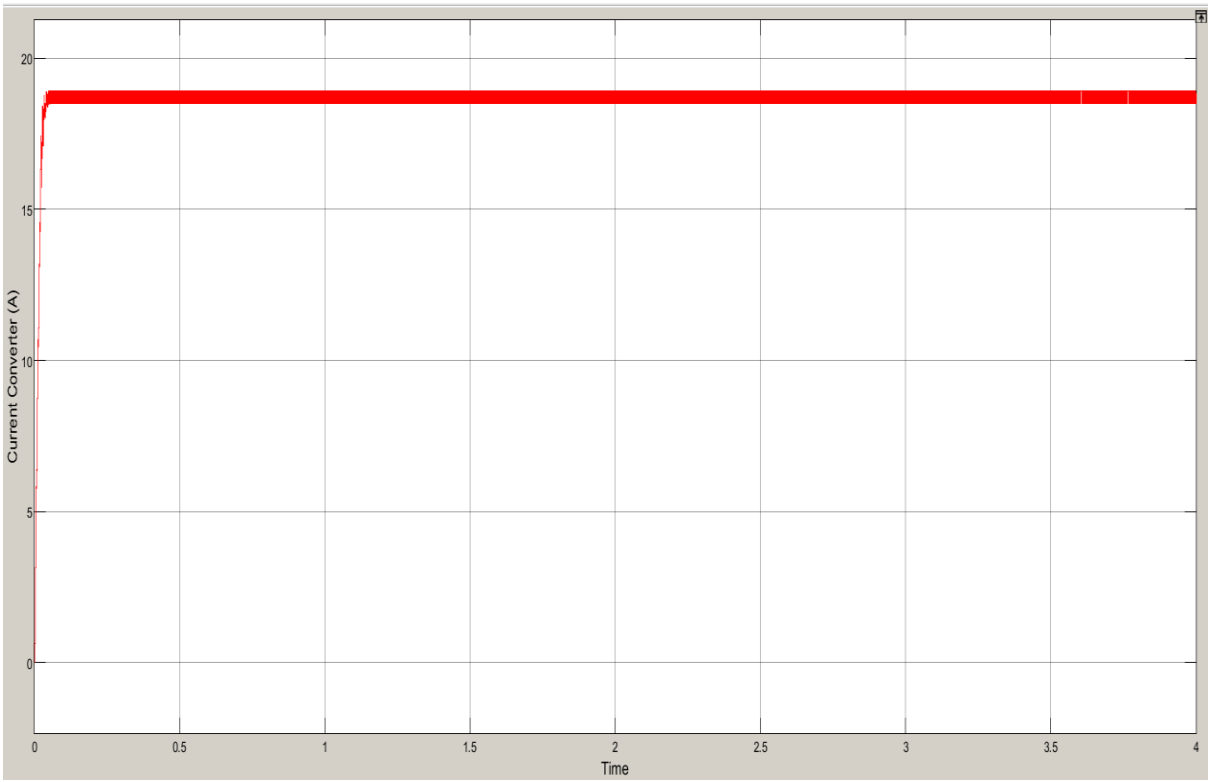


Figure(III.48):Current Converter (A)

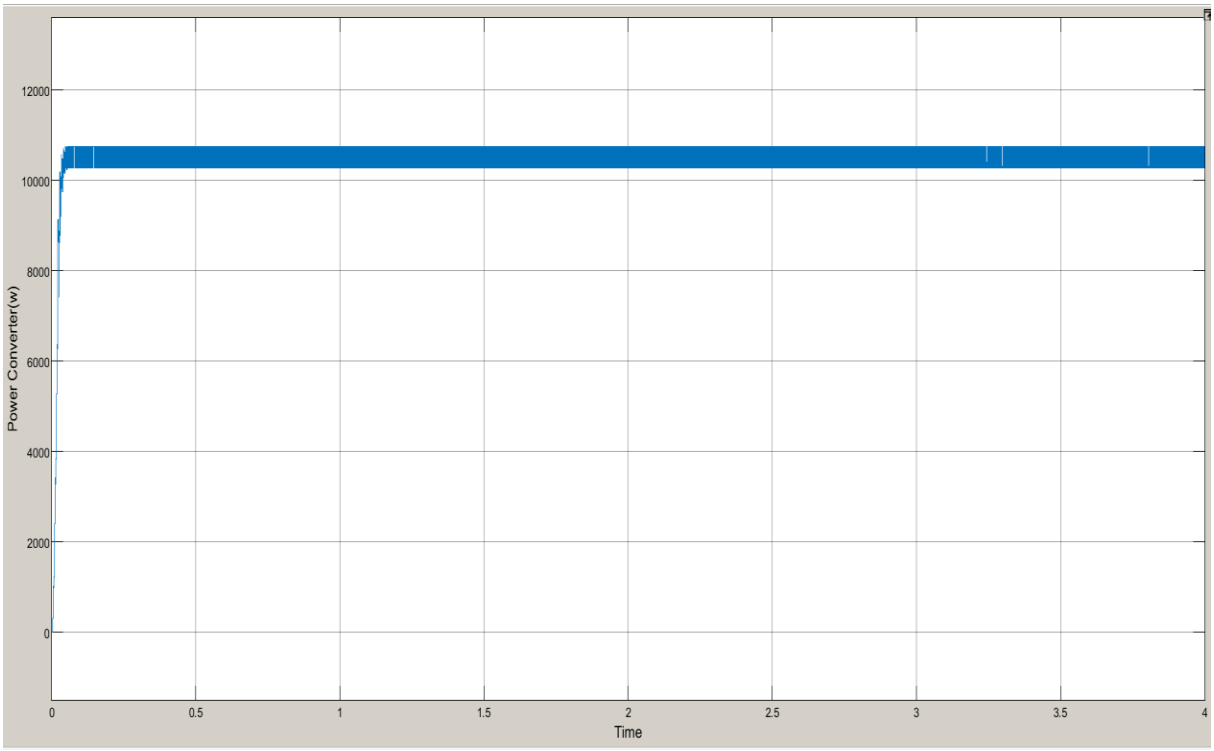


Figure (III.49):Power Converter(w)

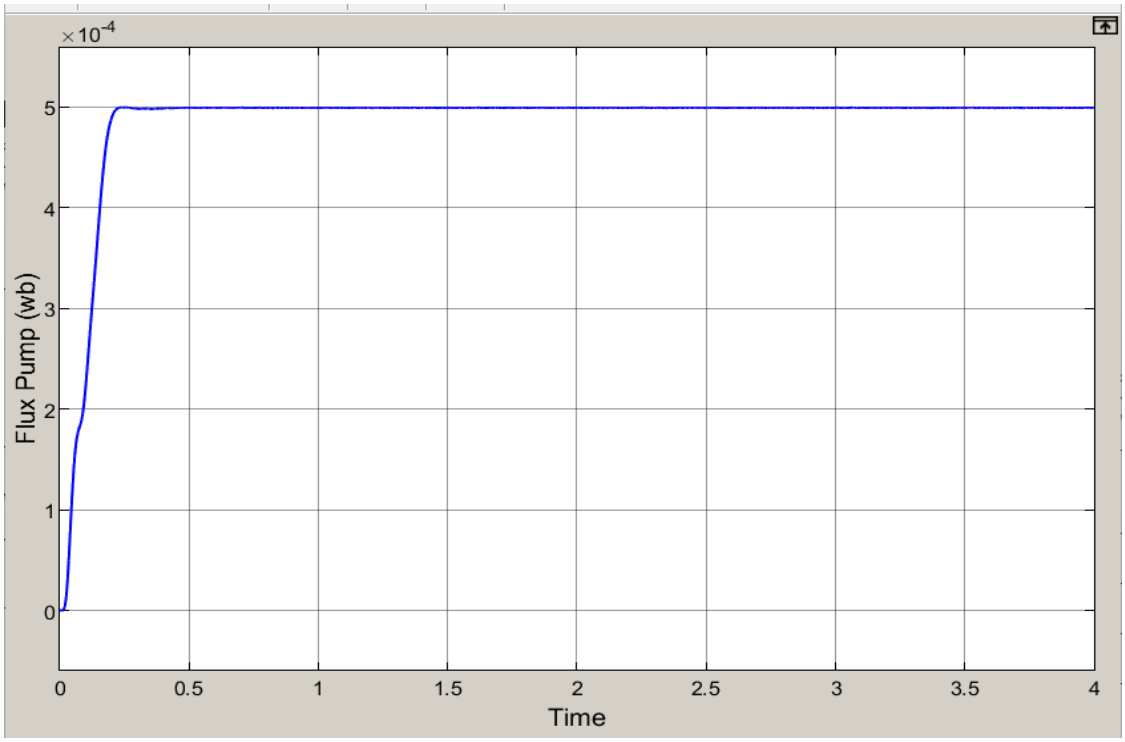


Figure(III.50):Flux Pump (wb)

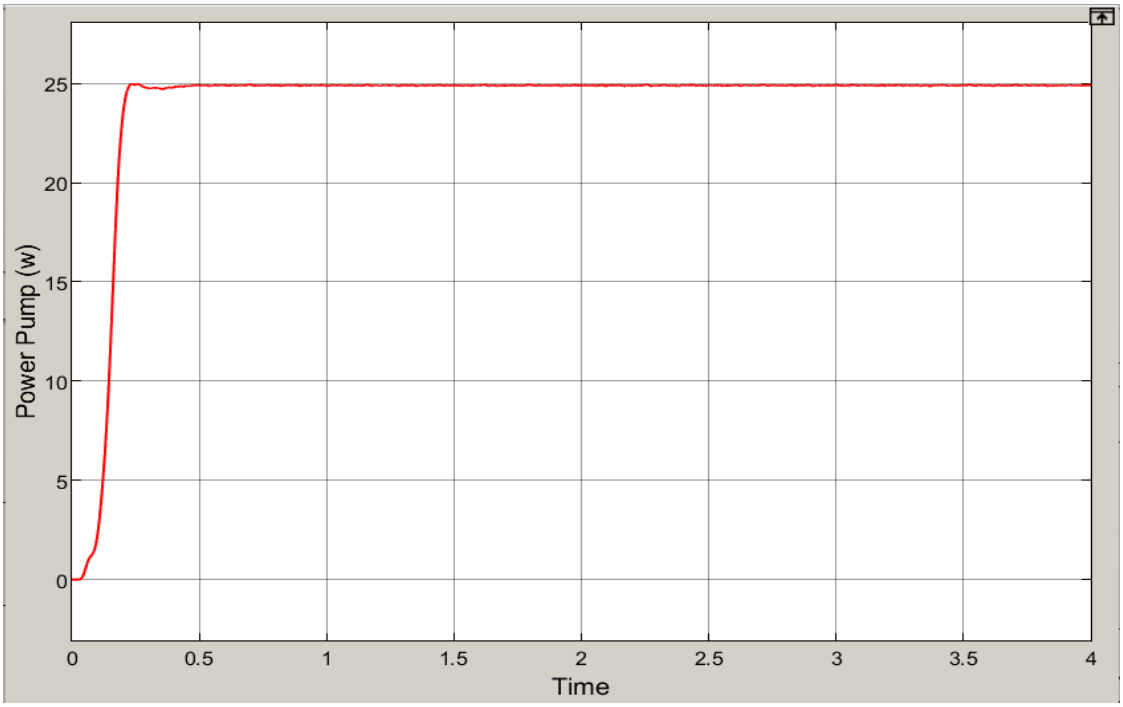


Figure(III.51):Power Pump(w)

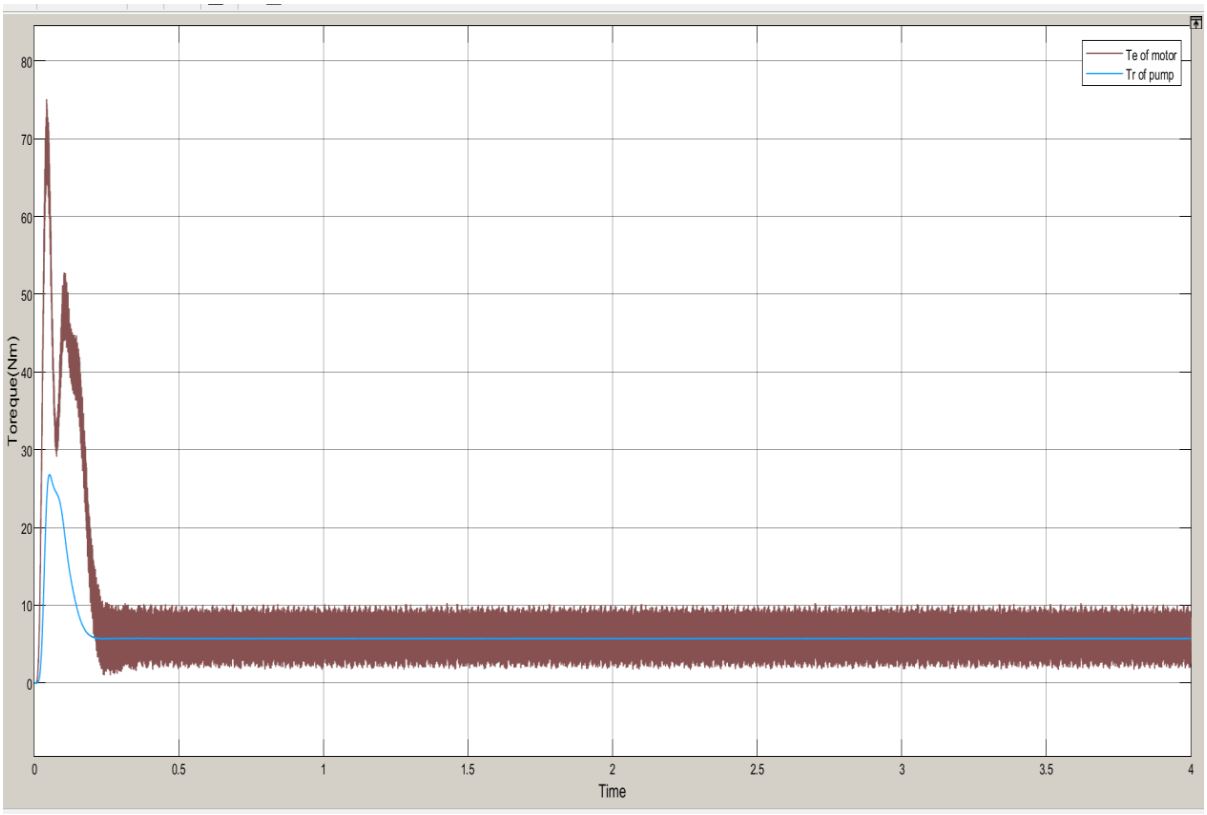


Figure(III.52): Torque(Nm)

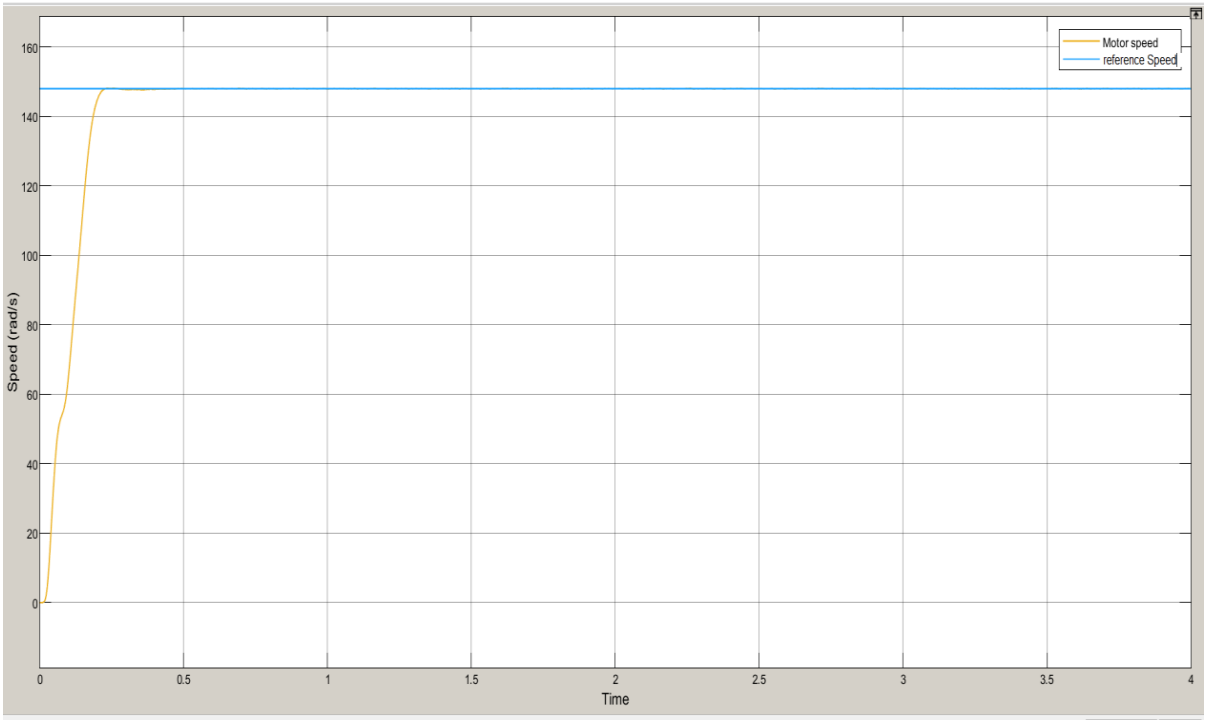


Figure(III.53):Speed(rad/s)

- **By varying irradiation and fixed temperature, I(w\m$^2$) =[500 800 1000 500] T=25C**

A simulation was conducted to evaluate the performance of the photovoltaic system under varying solar irradiance levels while keeping the temperature constant. This was done to assess the impact of the Maximum Power Point Tracking (MPPT) algorithm on system efficiency and stability.

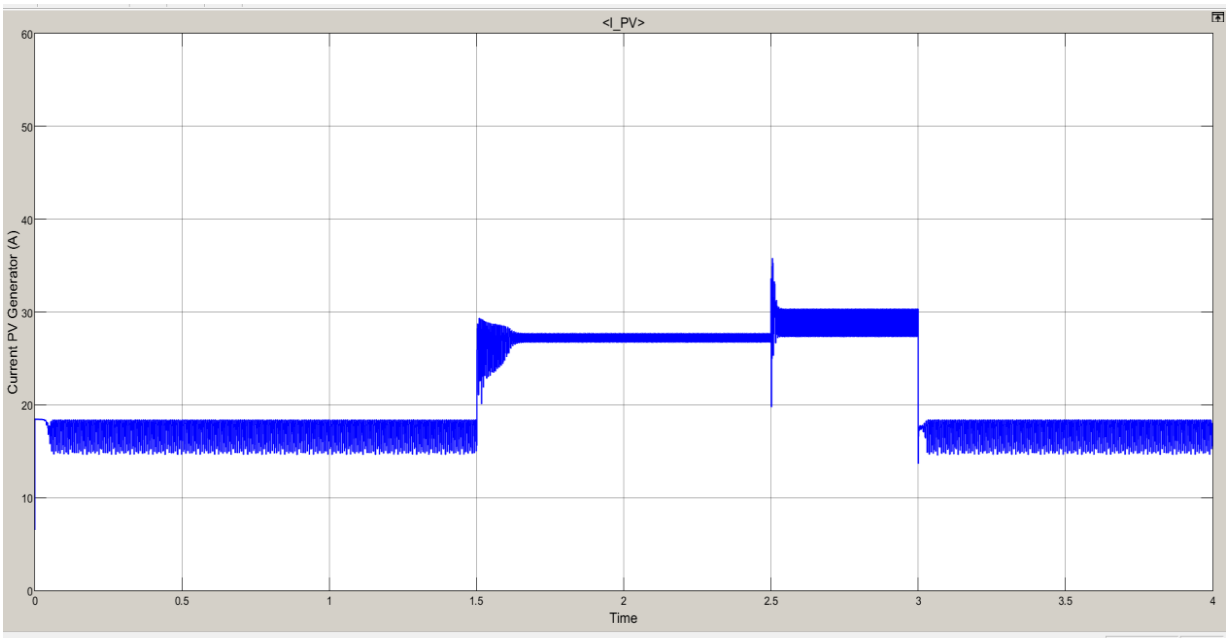


Figure(III.54): Current PV Generator (A)

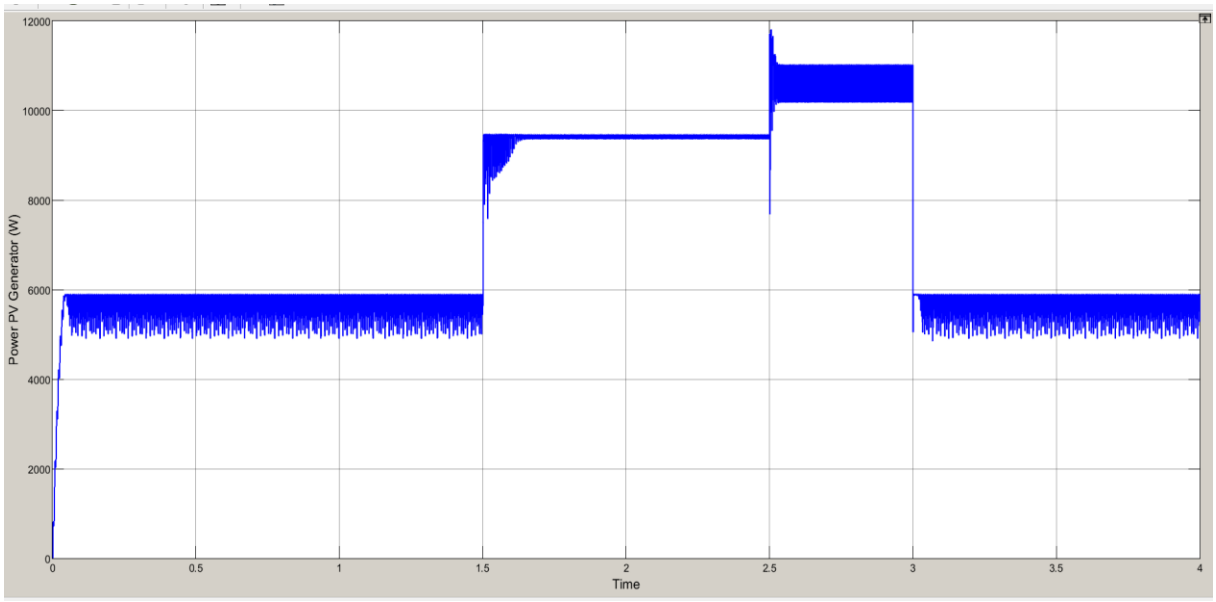


Figure(III.55):Power PV Generator (w)

- Image illustrates the power output of the photovoltaic generator, showing that the generated power varies proportionally with the solar irradiance levels. This highlights the dependency of PV power production on the intensity of solar radiation.
- This figure represent power PV generator system parameters under the control of the Incremental Conductance (INC) MPPT algorithm. Slight oscillations in voltage, current, and power can be observed as the system adapts to changing environmental conditions. These minor fluctuations are typical of the INC method, which tracks the Maximum Power Point (MPP) by comparing incremental and instantaneous conductance. Compared to the P&O algorithm, INC provides more accurate and stable tracking, especially under rapidly varying irradiance or temperature conditions

**Voltage generated by PVgenerated**

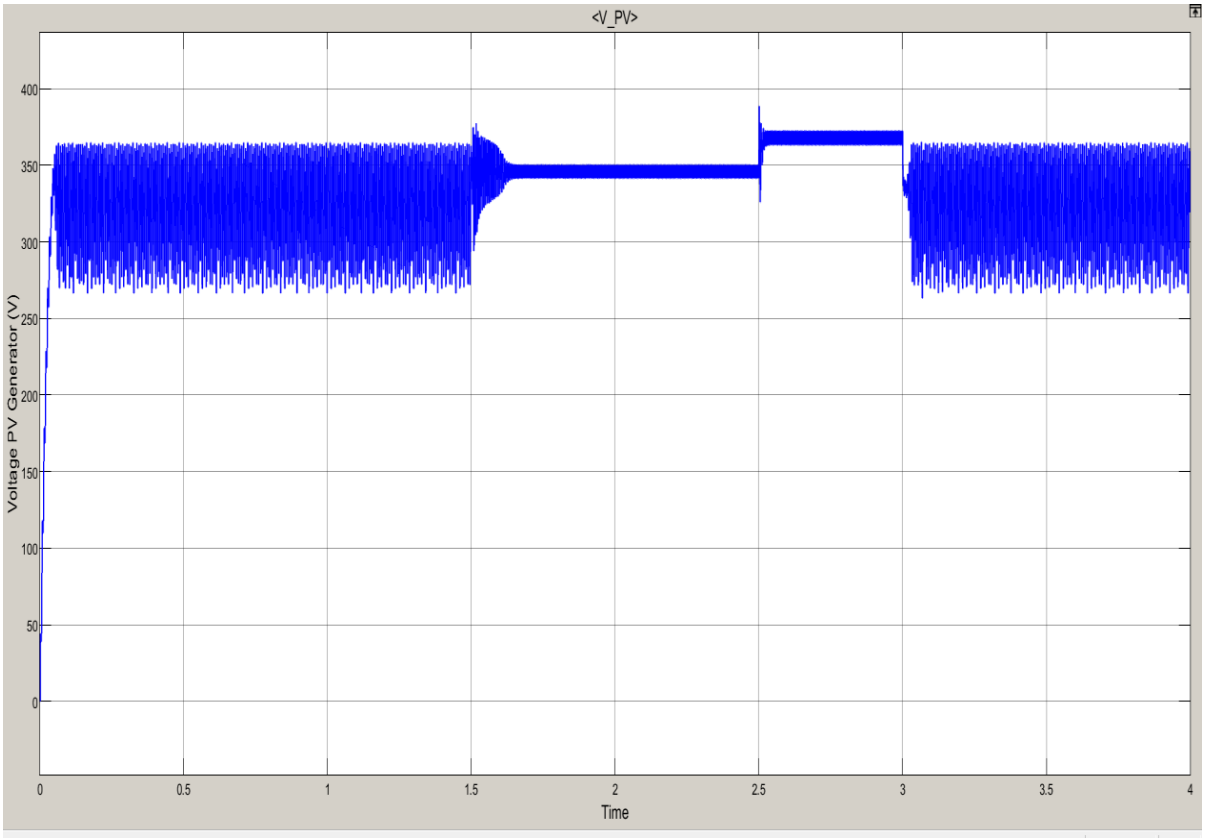


Figure(III.56):Voltage PV Generator (V)

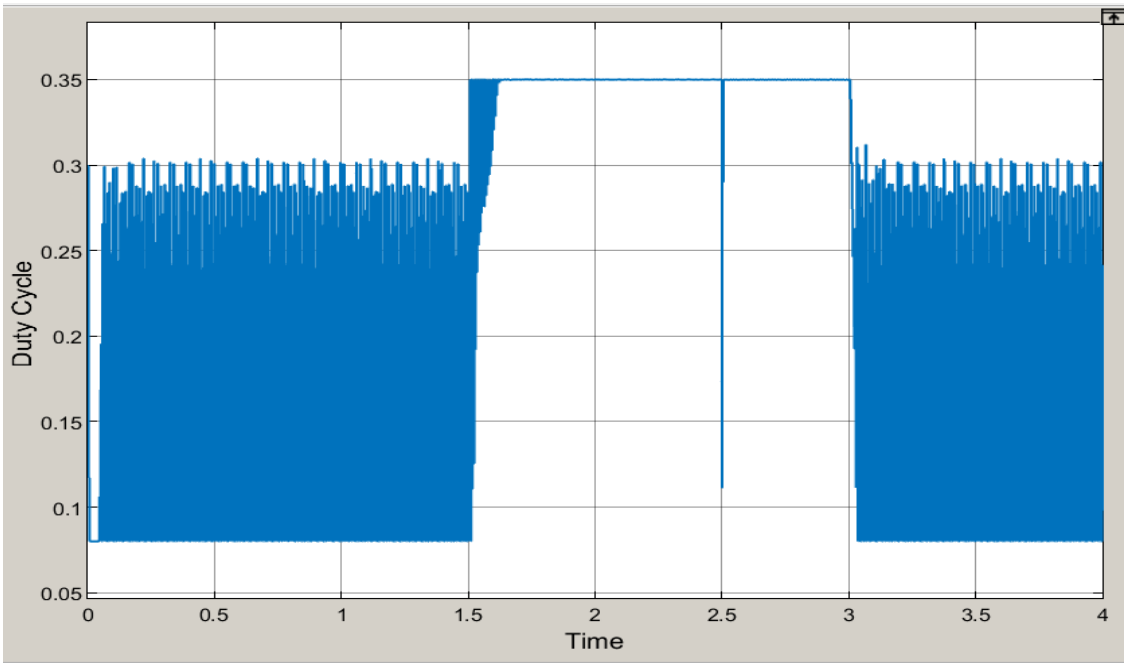


Figure(III.57):Duty Cycle Converter

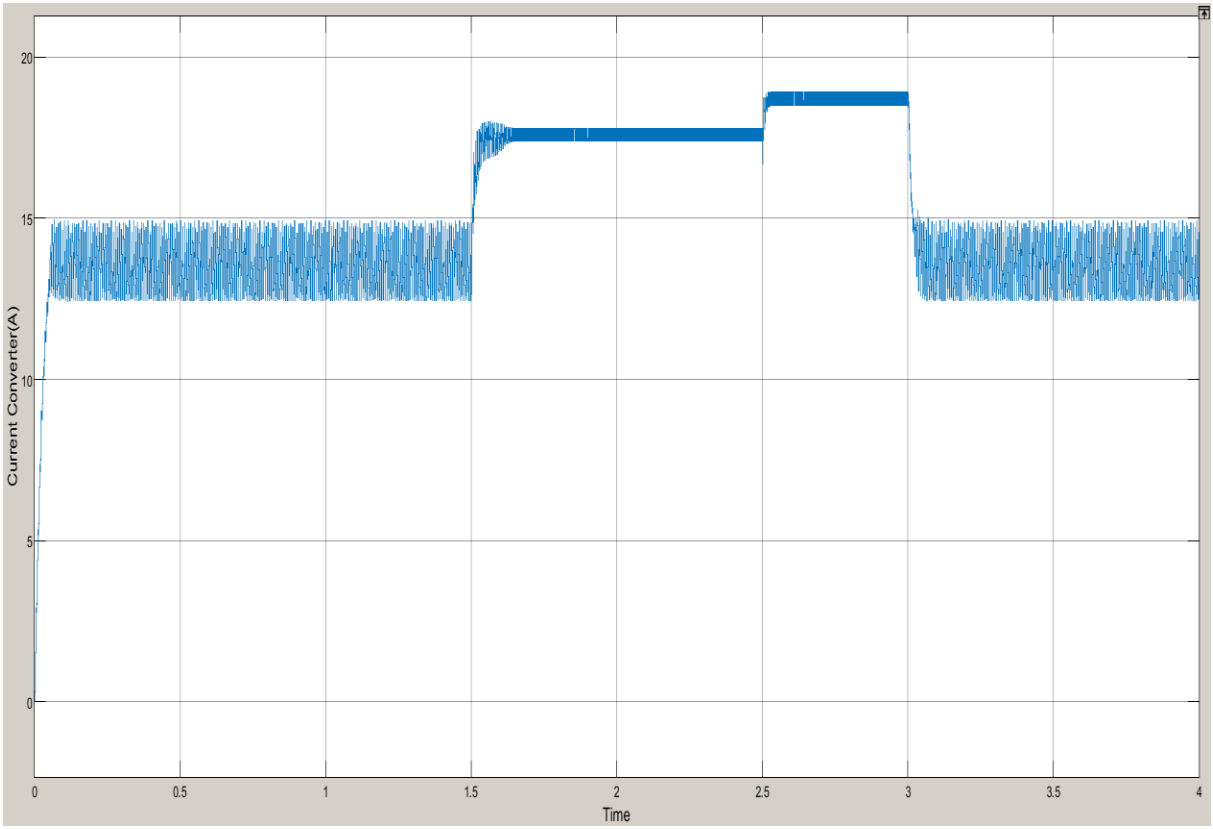


Figure (III.58): Current Converter(A)

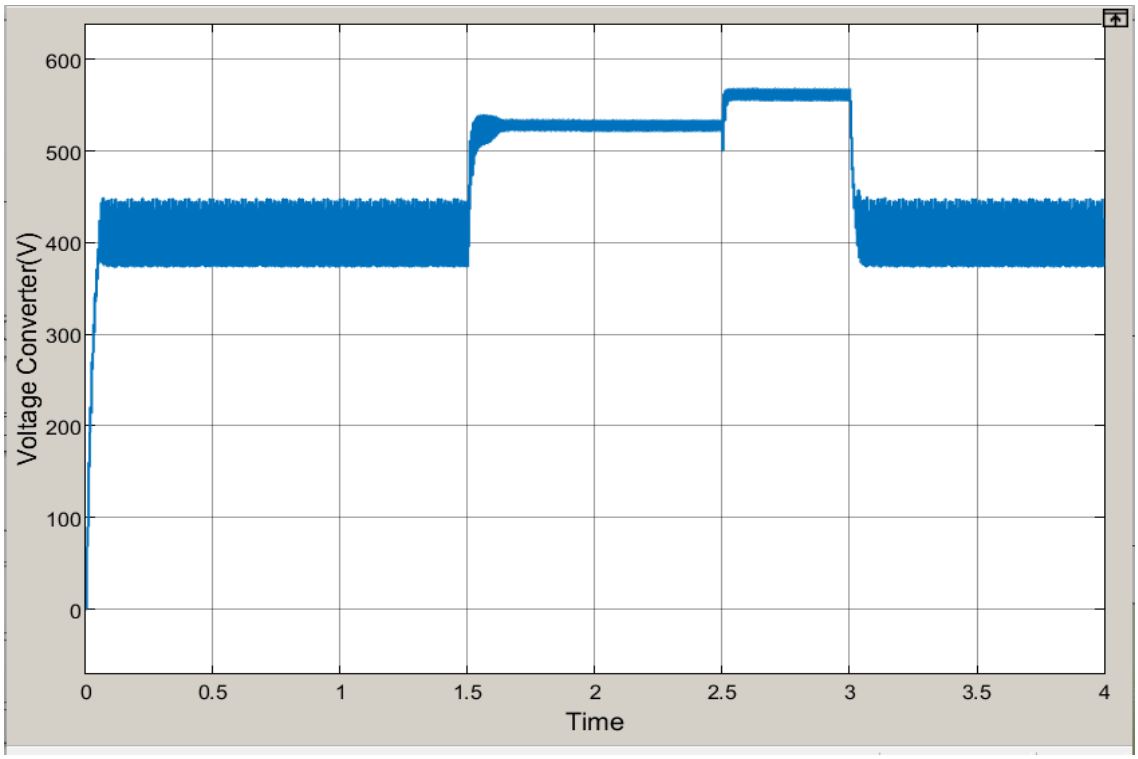


Figure (III.59): Voltage Converter(V6)

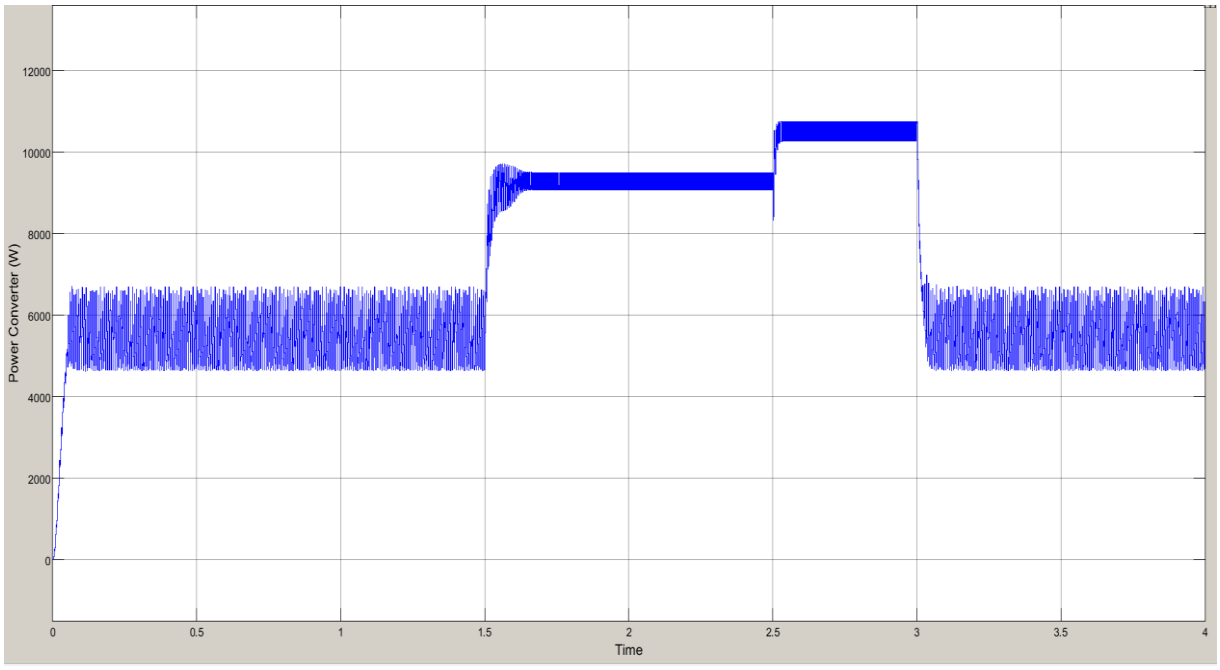


Figure (III.60): Power Converter(w)

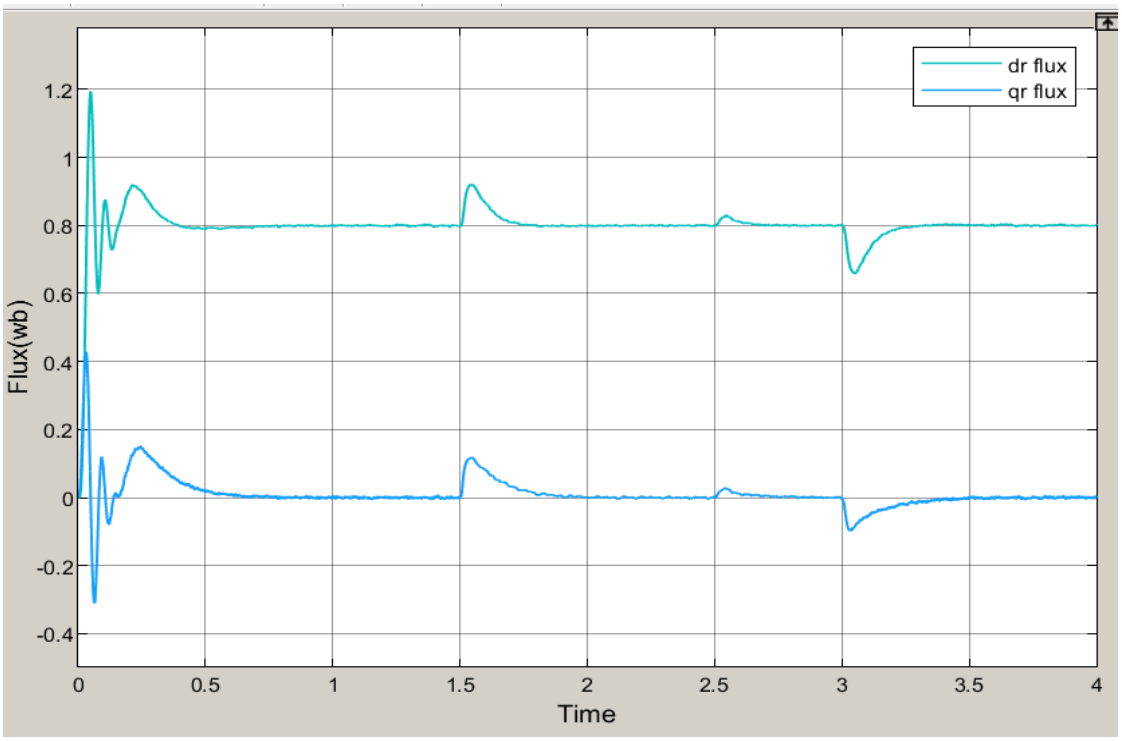


Figure( III.61): flux (wb)

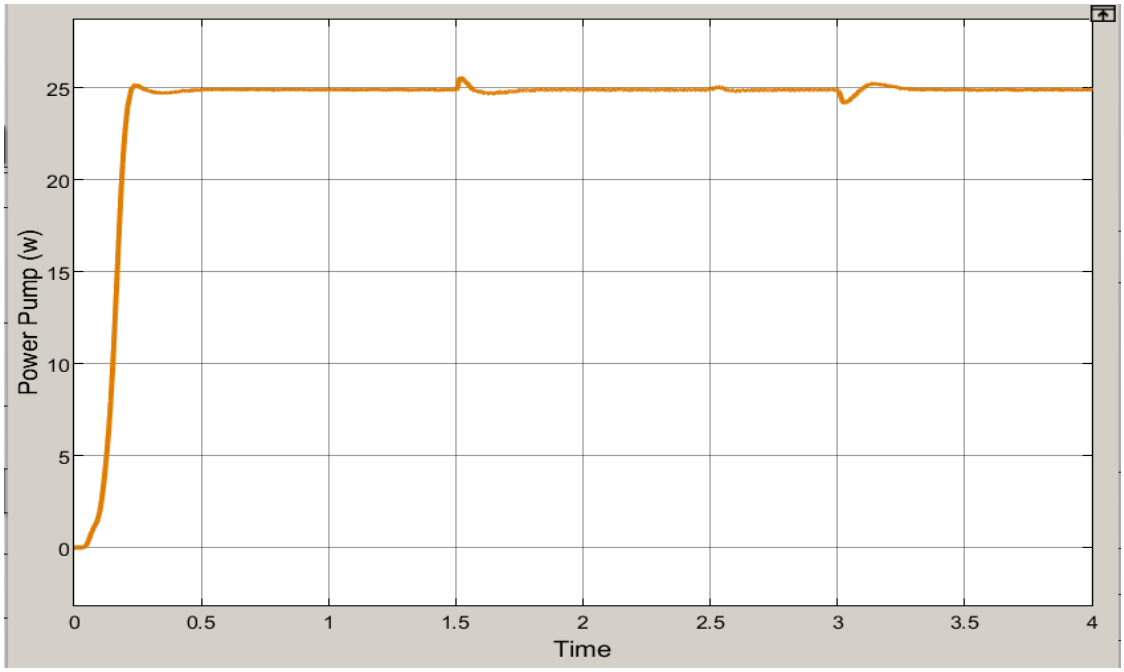


Figure(III.62):Power Pump (w)

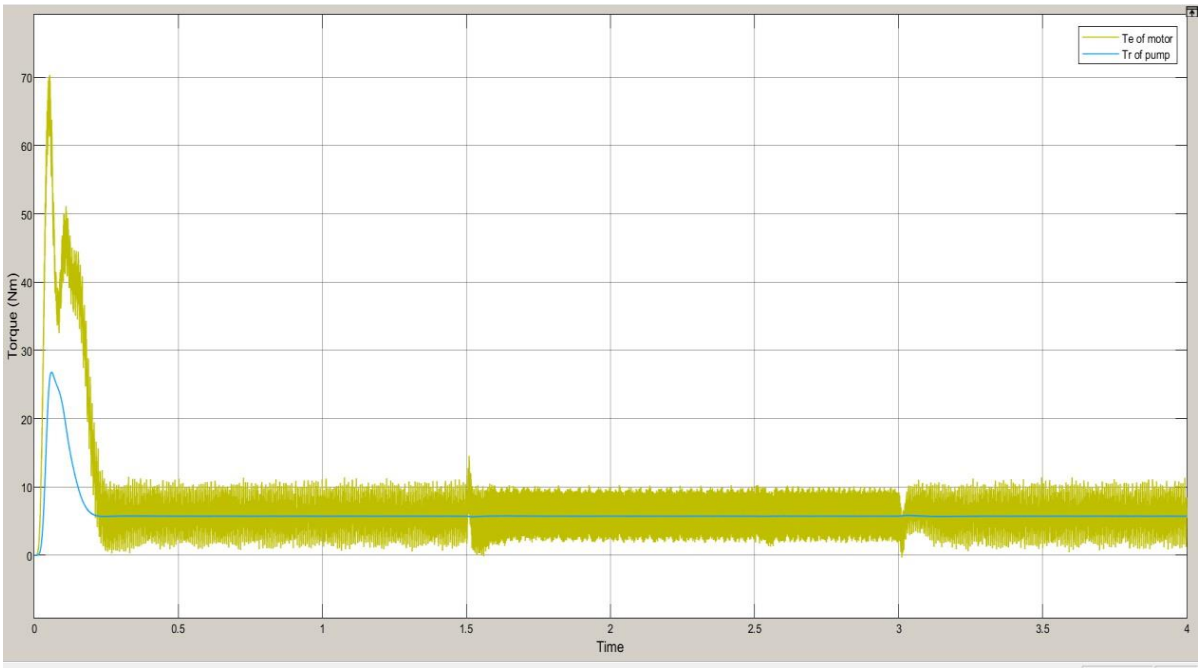


Figure(III.63):Torque (Nm)

- The results show that IFOC control provides fast dynamic response and good motor torque stability, while the MPPT algorithm ensures gradual and stable pump torque tracking. The observed electromagnetic torque ripples remain within acceptable limits, indicating efficient control performance. A slight disturbance of about 3 seconds due to a change in solar radiation
- however, the system quickly regains its stability. Overall, the combination of FOC and MPPT has proven to be highly effective in maintaining control performance and maximizing energy utilization.

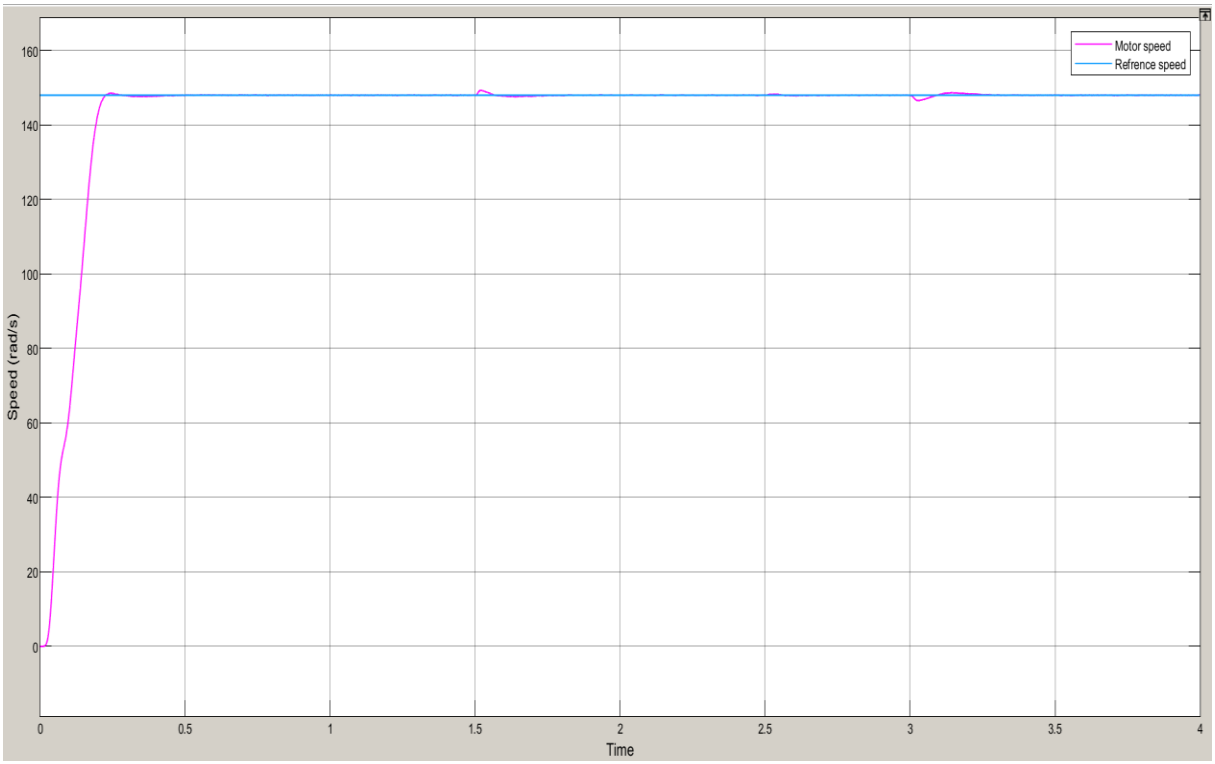


Figure(III.64):Speed(rad/s)

- After performing the simulation and implementing the Maximum Power Point Tracking (MPPT) algorithm based on the Incremental Conductance (INC) method, the system's behavior was evaluated under different solar irradiation levels. The results indicated improved stability in tracking the maximum power point, particularly at moderate to high irradiance levels such as 800 ($W/m^2$) and 1000 ($W/m^2$). Unlike the Perturb and Observe method, the INC algorithm demonstrated better performance in rapidly changing irradiation conditions by minimizing steady-state oscillations. Nevertheless, some minor fluctuations were still observed at low irradiance values around 500 ($W/m^2$), which could affect the precision of power extraction under such conditions. Overall, these findings confirm the INC method's robustness and suitability for dynamic environmental scenarios, though further optimization may be required to reduce residual oscillations for enhanced system stability.
    - The indirect field-oriented control (IFOC) contributes to optimal energy extraction while maintaining the stability of the magnetic flux. The minimal fluctuations observed indr.qr flux demonstrate the effective decoupling of torque and flux, as well as a fast and accurate dynamic response of the system.

### III.4 Analysis of PV Pumping System modeling in MATALAB\smiling

Incremental Conductance (IncCond). Both methods showed effective tracking of the maximum power point, enhancing the pump's efficiency. However, IncCond demonstrated better stability by reducing oscillations around the MPP compared to P&O.

At 500 W/m² of irradiance, the system operated efficiently under both algorithms. The motor speed closely followed the reference, indicating good dynamic response. A sudden increase in irradiance at $t = 1.5\ s$ caused a brief rise in motor speed and pump output, while a drop at $t = 3\ s$ led to a minor, short-lived disturbance. This highlights the system's ability to adapt quickly to climatic variations, especially with the help of robust MPPT control.

Overall, both algorithms proved effective, with Incremental Conductance offering better control quality and smoother system behavior.

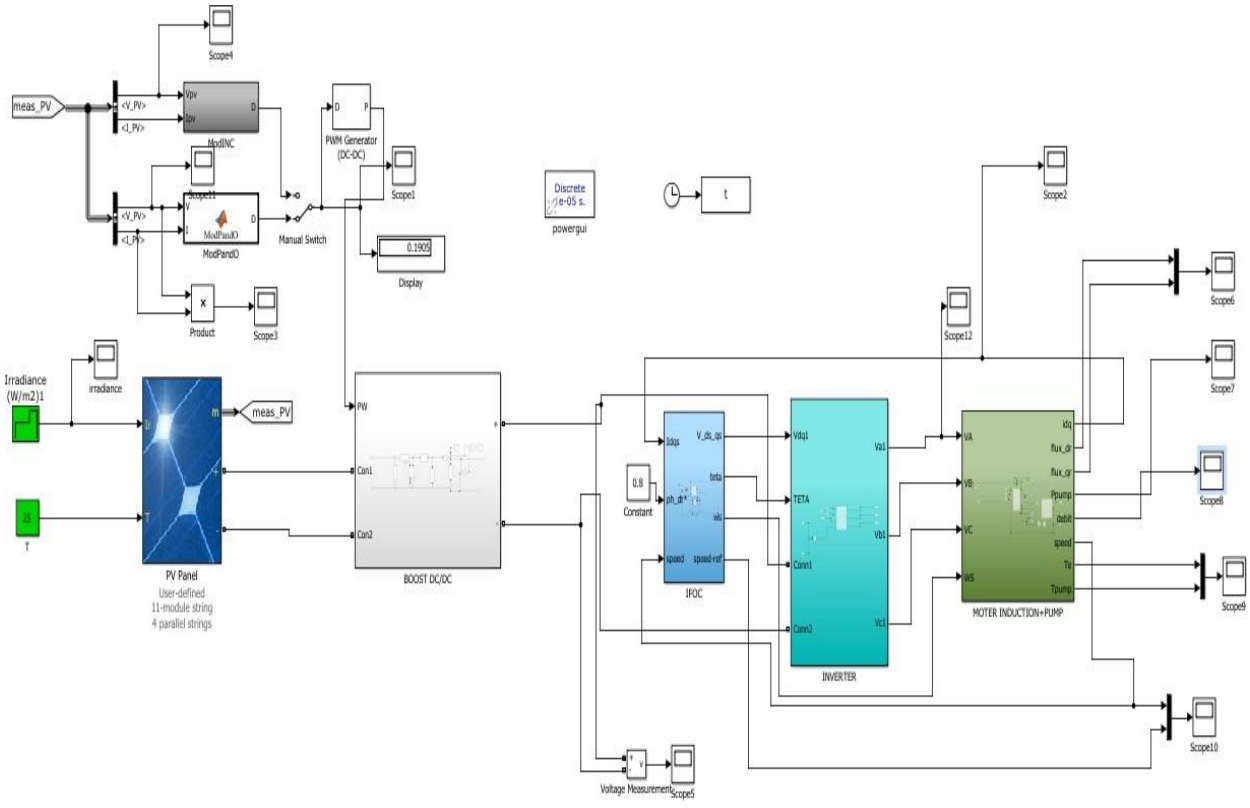


Figure(III.65):Simulation, and Performance Evaluation of a Photovoltaic Water pumping system

### III.5 Conclusion:

In conclusion, the simulation of the photovoltaic water pumping system confirmed the effectiveness of the proposed control strategies. Both MPPT methods, P&O and INC, successfully tracked the maximum power point, with the INC method showing better performance in terms of stability and response to sudden irradiance changes. The integration of IFOC for motor control contributed significantly to the smooth and efficient operation of the induction motor. Overall, the system demonstrated reliable behavior under various solar conditions, validating its potential for practical deployment in real-world water pumping applications.

# General Conclusion

## General Conclusion

This study aimed to analyze and improve the performance of a standalone photovoltaic (PV) water pumping system, with a particular focus on comparing Maximum Power Point Tracking (MPPT) algorithms and their impact on overall system efficiency. The work was organized into three main chapters, each yielding significant findings that contribute to a deeper understanding of how to design and operate such systems optimally.

In Chapter One, a comprehensive theoretical background on PV systems and water pumping technologies was presented. The basic principles of solar energy conversion were explained, along with a detailed description of PV system components and their functions. The chapter also reviewed common types of electric motors and hydraulic pumps used in water pumping applications, providing a solid foundational understanding of how these elements work together to achieve efficient operation. This background knowledge was essential for developing accurate mathematical models in the following chapter.

In Chapter Two, detailed mathematical models were developed for various system components, including the PV generator, DC-DC Boost converter, inverter, induction motor, and centrifugal pump. These models were built based on physical and electrical laws to simulate system behavior under realistic and variable operating conditions. This modeling enabled the prediction of component performance and identification of critical points within the system that could be optimized, representing a crucial step towards improved system efficiency.

Chapter Three involved simulating the system using MATLAB/Simulink to evaluate the influence of different MPPT algorithms on system performance. The Perturb and Observe (P&O) and Incremental Conductance (IncCond) algorithms were applied to control the Boost converter and compared in terms of response speed, stability, and energy efficiency. Results showed that IncCond provided superior tracking accuracy and faster stabilization, whereas P&O was simpler to implement but exhibited oscillations around the maximum power point. These results offered practical insight into selecting the most suitable algorithm for specific application requirements.

Through this study, several conclusions were drawn that contribute to the improved design and operation of PV water pumping systems, particularly in remote areas lacking reliable water and electrical infrastructure. Moreover, the outcomes of this work offer a valuable scientific reference for future research, especially in the integration of AI techniques or weather prediction methods to enhance system performance even further.

Recommendations and Future Work:

Based on the findings of this study, it is recommended to adopt the Incremental Conductance algorithm in PV water pumping systems that demand high accuracy and stability in MPPT performance, particularly in environments with frequent solar irradiance and temperature fluctuations. Accurate mathematical modeling of system components is also encouraged, as it directly impacts simulation reliability and the development of effective control strategies.

This work also opens up several potential directions for future research:

- Integrating artificial intelligence techniques, such as genetic algorithms or neural networks, into MPPT strategies to improve responsiveness and adaptability.

- Designing adaptive or fuzzy logic-based control systems to enhance performance under nonlinear or unpredictable operating conditions.

- Employing predictive control based on solar irradiance forecasting (using meteorological or satellite data) to improve energy management and reduce faults.

- Incorporating energy storage elements (e.g., batteries or supercapacitors) to ensure continuous water supply during cloudy periods.

- Developing a physical prototype to validate the proposed models and simulations in real-world conditions.

The work presented in this thesis represents a significant step toward developing sustainable PV-powered water pumping solutions. It lays the groundwork for future advancements in intelligent, efficient, and resilient systems that align with the goals of sustainable development and energy-water security in underserved regions.

# References

## References

[1] : Solar Energy Industries Association (SEIA), "Solar Energy Basics," *SEIA.org*, 2024.

[2] :NASA Solar System Exploration, "The Sun: Facts and Information," *NASA.gov*, 2024. Link

[3] : NASA Solar System Exploration, *The Sun: Facts and Information*, 2024.

[4] SIBOMANA Adrien ( Cacluc et dimensionnement d'une system solaire photovoltaique pour l'alimentation en electricite des habitante de la commune ntega : Cas de la Collin MAKOMBE) avril 2018 memoire de master

[5] European Commission. (2024). *Photovoltaic Geographical Information System (PVGIS)*. Retrieved from https://joint-research-centre.ec.europa.eu/photovoltaic-geographical-information-system-pvgis_en

[6] https://kartoweb.itc.nl/geometrics/Coordinate%20systems/coordsys.html

[7] M. BESSEM ABDELGHANI (Modulization and simulation of Pv pumping systems) master's thesis university of Annaba Baji Mokhtar 2018

[8] BOUDERBALA Hamza (Solar panel modeling and control) master's thesis BADJI MOKHTAR – ANNABA UNIVERSITY 2021/ 2022

[9] International Renewable Energy Agency (IRENA). (2022). *Renewable Energy: Solar Energy.* Abu Dhabi: IRENA. Available at: https://www.irena.org/solar

[10] International Energy Agency (IEA). (2022). *Renewable Energy Market Update: Outlook for 2022 and 2023*. Retrieved from IEA.org.

[11] National Renewable Energy Laboratory (NREL). (2022). *Best Research Cell Efficiency Chart*. Retrieved from NREL.gov.

[12] Green, M.A., Emery, K., Hishikawa, Y., Warta, W., & Zou, J. (2020). Solar Cell Efficiency Tables (Version 50). *Progress in Photovoltaics: Research and Applications*, 28(1), 3-15. DOI: 10.1002/pip.3237.

[13] Solar Energy Materials and Solar Cells, 231, 111167. DOI: 10.1016/j.solmat.2021.111167

[14] REN21. (2021). *Renewables 2021 Global Status Report*. Retrieved from REN21.net

[15] https://www.geeksforgeeks.org/photovoltaic-cell/?

[16] GeeksforGeeks. (2023). Types of Solar Cells. https://www.geeksforgeeks.org/types-of-solar-cells

[17] EnergySage. (2024). Types of Solar Panels: What's the Best Option in 2024? https://news.energysage.com/types-of-solar-panels/

[18] Solar Star Info. (2023). Different Types of Solar Cells & Their Applications. https://solarstarinfo.com/solar/types-of-solar-cells

[19]https://www.researchgate.net/figure/Caracteristique-resultante-dun-groupement-de-n-s-cellules-en-serie_fig7_327839184

[20] .KADDOUR Yacine .DERBAL Oussama« Modeling and simulation of a photovoltaic pumping system» master's thesis Center universitaire SALHI AHMED -Naâma- 2019/2020

[21] International Renewable Energy Agency (IRENA), "Solar Pumping for Sustainable Water Supply," IRENA, 2023.

[22] https://www.researchgate.net/figure/Global-solar-radiation-components-direct-diffuse-and-reflected-radiations_fig1_36205337

[23] DANOUNE Mohammed Bilal « Study of a renewable energy system based on green hydrogen» doctarant thesis Université Kasdi Merbah-Ouargla2021

[24] https://www.deegesolar.co.uk/different_types_of_solar_pv_systems

[25] https://jmhpower.com/hybrid-solar-system-vs-on-grid-solar-system/

[26] https://umangotsolar.com/off-grid-solar-power-systems/

[27] ADADA Mohamed-El Amine. And BOUDIEB Kamel. « Simulation of a photovoltaic pumping system»master's thesis Belhadj Bouchaib University Center, Ain-Temouchent 2019/2020

[28] https://www.maysunsolar.com/blog-what-are-the-main-components-of-solar-panels/

[29] researchgate.net/figure/and-P-V-characteristics-of-a-typical-solar-cell_fig4_320284529

[30] Ahmed Moubarak, Gaber El-Saady and El-Noby A. Ibrahim «BATTERY ENERGY STORAGE FOR VARIABLE SPEED PHOTOVOLTAIC WATER PUMPING SYSTEM» ARPN Journal of Engineering and Applied Sciences VOL. 13, NO. 23, DECEMBER 2018

[31] Bendjoudi et F. Lakhdari « Etude et simulation d'un système de pompage photovoltaïque avec batteries». Master's thesis university Bejaia 2014.

[32] SLIMANI Mohamed «Study of different techniques for controlling PWM inverters». Master's thesis École Nationale Polytechnique 2015

[33] DEKHIL Amar et SIBOUKEUR Abderrezzak« Study of a photovoltaic pumping systeme ». Master's thesis university UNIVERSITE KASDI MERBAH OUARGLA 2021/2022

|[34] D. Chinna Kullay Reddy1 , S. Satyanarayana2« Design of Hybrid Solar Wind Energy System in a Microgrid with MPPT Techniques». International Journal of Electrical and Computer Engineering (IJECE) Vol. 8 April 2018

[35] https://www.investopedia.com/terms/f/fuzzy-logic.asp

[36] NACER TAREK. « GENERATION OF PWM SIGNALS USING A DSP » Master's thesis SAAD DAHLEB UNIVERSITY IN BLIDA 2010/2011

[37] https://www.gibbonsgroup.co.uk/media/blog/5-golden-rules-of-centrifugal-pump-maintenance/

[38] Bouchareb Khalil et Touati Ayyoub « Modeling and simulation of a PV system adapted by MPPT control based on a sliding mode. » Master's thesis 8Mai 1945 University – Guelma 2021

[39] https://myelectrical.com/notes/entryid/251/induction-motor-equivalent-circuit

[40] J. A. Tapia (*Electromagnetic Modelling of High-Speed Induction Motors*)Master's thesis, University of Manchester, 2015

[41]https://www.researchgate.net/publication/325374997_Modeling_and_sizing_the_coil_in_boost_converters_dedicated_to_photovoltaic_sources/references

[42] B. Meliani, A. Meroufel, and H. Khouidmi (Fuzzy Gain Scheduling of PI Controller for Dual Star Induction Machine fed by a Matrix Converter) Journal of Electronic and Computer Engineering anuary 2012

[43] Mostafa Barzegar Kalashani, Murtaza Farsadi(New Structure for Photovoltaic System Applications with Maximum Power Point Tracking Ability) vol 4 decembre 2014

[44] : Bensalem, A. "Commande et optimisation d'un système de pompage photovoltaïque". Mémoire de Master, Université de Biskra.2018

[45] :Abid, M. "Étude et commande d'un système de pompage photovoltaïque". Mémoire de Master, Université de Batna 2 2020

[46] : Haddadi, A. "Modélisation et commande d'un système de pompage photovoltaïque". Mémoire de Master, Université de Tlemcen.2017

[47] : Touati, S. "Réalisation et commande d'un système PV avec suiveur MPPT". Mémoire de Master, Université de Bejaia.2020

[48] : Djouadi, Y. "Étude et réalisation d'un système MPPT pour application photovoltaïque". Mémoire de Master, Université de Boumerdes.2019

[49] Mechkar, M. "Commande d'un système PV pour pompage avec MPPT". Mémoire de Master, Université de M'sila. 2020

[50] : Bougherara, A."Commande d'un système PV avec algorithme MPPT basé sur l'INC". Mémoire de Master, Université de Batna 2. 2021

[51] : Aït Amara, Y. . "Étude et simulation d'un système photovoltaïque avec MPPT INC". Mémoire de Master, Université de Bejaia.2019

[52] Touil, F. "Commande d'un convertisseur DC-DC pour système PV avec INC". Mémoire de Master, Université de M'sila. 2018

[53] Tafsir Abdoulaye Gaye1, Biram Dieng1(Study and Optimization of a Photovoltaic Mill System Functioning on the Course of the Sun) Energy and Power Engineering, 2017,

[54] Adel A. Elbaset Hamdi Ali 2 Montaser Abd-El Sattar (A MODIFIED PERTURB AND OBSERVE ALGORITHM FOR MAXIMUM POWER POINT TRACKING OF PHOTOVOLTAIC SYSTEM USING BUCK-BOOST CONVERTER) Journal of Engineering Sciences vol 43 may 2015

[55] Iharka Sz¨ucs-Csillik and Dorina Poput¸a (THE ASTRO-BIBLIO-STUDENTS PROGRA) DIDACTICA MATHEMATICA, Vol. 00 · December 2015

[56]:https://www.monolithicpower.com/en/learning/mpscholar/electric-motors/ac motors/priciples-of-ac-motor-operation